TEXTILE RESEARCH JOURNAL

VOL. XXII, No. 3 March, 1952

Mechanics of Elastic Performance of Textile Materials

Part VIII: Graphical Analysis of Fabric Geometry*

E. V. Painter†

Fabric Research Laboratories, Inc., Boston, Massachusetts

Abstract

Graphs have been developed to simplify the study of fabric geometry. A simultaneous plot of the mathematical relations developed by Peirce aids in visualizing dimensional changes in fabrics and gives accurate values of the various parameters without lengthy calculations and interpolations from tables.

The use of the graphs is discussed as they apply to various types of weaves, fibers, and their dimensional changes.

Introduction

The modern developments in new fabric treatments and weaving of new fibers have not been aided as much as they should have been by a well-developed theory of the form and changes therein of fibrous structures. The cross-sectional swelling of a rayon fiber can be determined accurately in the laboratory, but by the time this fiber is twisted into a yarn, which is then woven into a complex geometric form, it is practically impossible to follow rigorously the chain of events which relate this simple change in the fiber to the dimensional changes observed in the fabric. The endless variety of fibers, twists, and weaves makes the job almost impossible of solution by empirical methods. The only alternative is the development of a theory of ideal behavior, so that each specific case may be reduced to a simple study of deviations from the ideal.

The brilliant mathematical analyses of Peirce [1, 2] have laid the groundwork for this theory of the ideal. However, considerable calculation and lengthy interpolations from tables are required to make use of his work. Peirce recognized this difficulty and suggested the use of graphs for particular relations. This idea has been carried a little further in the present study; one graph is presented herein

* Part of a study on the physical properties of fabrics as determined by the inherent properties of fibers and their geometrical form, conducted by The Fabric Research Laboratories under the sponsorship of the Office of The Quartermaster General.

Parts I and II of this series appeared in the February and December, 1948, issues, respectively, Part III in the January, 1950, Parts IV and V in the August, 1950, Part VI in the October, 1950, and Part VII in the May, 1951, issues.

† Present address: Johnson & Johnson, Chicago, Ill.

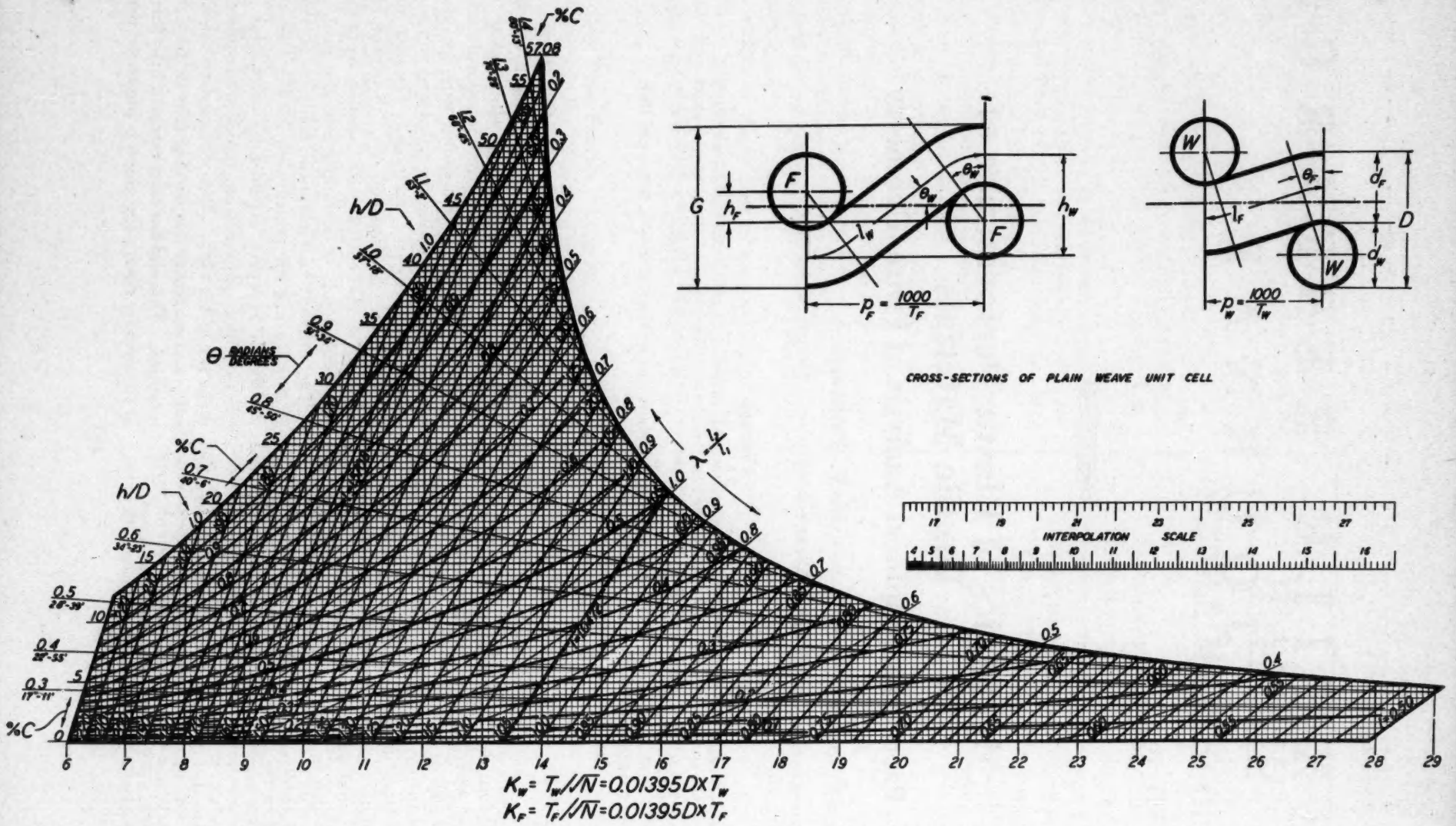

FIG. 1. *Main graph, depicting the geometrical relations of the plain weave.* (*Based on equations given by Peirce* [*1, 2*].)

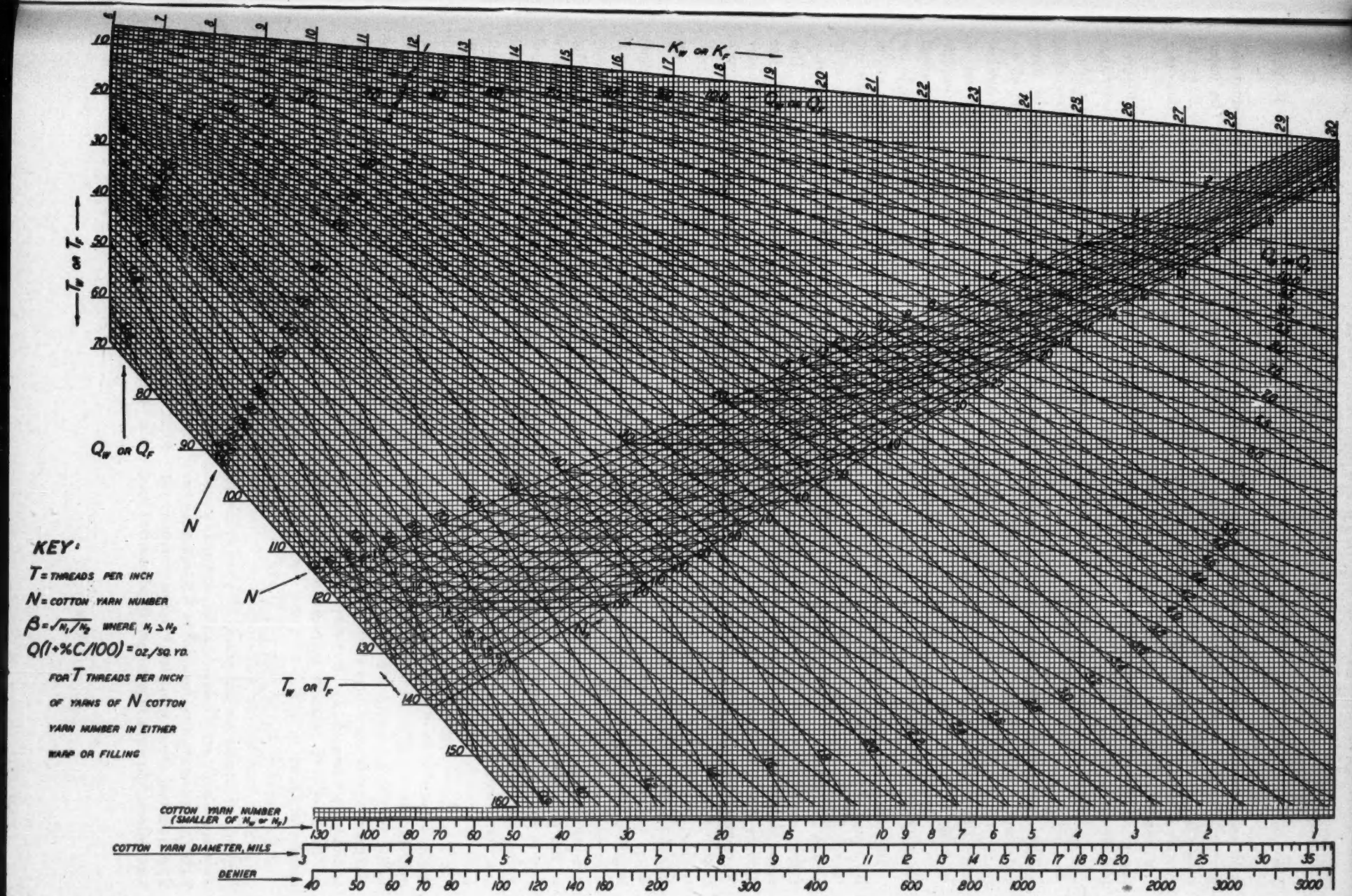

FIG. 2. *Auxiliary graph; reduced cover factor,* K, *from texture,* T, *and yarn number,* N.

which depicts all of the relations of the ideal plain-weave geometry, much in the manner of a psychrometric chart or Mollier diagram. The use of the graphs is described in the following section, while the details of derivation and method of construction are given in the Appendix. Peirce's nomenclature is used throughout.

Use of the Graphs

The main graph is shown in Figure 1, and the auxilliary graph in Figure 2. The main graph depicts the geometrical relations of the plain weave, while the auxilliary graph gives related information in terms of thread count and yarn number.

Description of the Main Graph

In Figure 1 any plain-weave fabric is fully defined by a pair of two related points which can be located on the graph to give numerical values for ten of the eleven variables (D is the eleventh) which define a fabric structure. This is made possible by the superposition of several sets of curves and lines on a background set of rectangular coordinates relating % crimp to reduced cover factor. From the location of one of the points on the graph, it is possible to read off directly the reduced cover factor for the filling yarns, K_f, and the following values for the warp yarns: the % crimp, $\%C_w$; the fractional length of yarn between two filling yarns, l_w/D; the fractional maximum amplitude, h_w/D; and the maximum angle of inclination, θ_w. The other point of the pair locates the value of the reduced cover factor for the warp yarns, K_w, and the following values for the filling yarns: the % crimp, $\%C_f$; the fractional length of yarn between two warp yarns, l_f/D; the fractional maximum amplitude, h_f/D; and the maximum angle of inclination, θ_f. Thus, it might be said that one point represents the geometry of the warp yarns *versus* the spacing of the filling yarns, K_f, while the other point represents the geometry of the filling yarns *versus* the spacing of the warp yarns, K_w. The two points are located on the graph in relation to one another by the simple fact that

$$h_w/D + h_f/D = 1.0. \qquad (1)$$

The set of curves on the graph (Figure 1) giving values of h/D are those curving upward to the right. The heavy line for $h/D = 0.5$ separates the upper part of the graph from the lower; one of the two points defining a fabric must lie above this line, and the other below it, except for the special case when both points are directly on it. The upper left boundary of the graph is the line $h/D = 1.0$; when one of the points is on this line, the other must be on the base line at $h/D = 0$.

The straight lines inclined to the right in Figure 1 give values for l/D. In depicting the interchange of crimp between warp and filling yarns of a fabric, the two points defining the fabric must move along these straight lines, one point up and the other down (keeping $h_w/D + h_f/D = 1.0$). One of the points must lie on or to the left of the line marked $l = 1.5708$, in order to allow the other set of yarns to straighten out completely, a complete straightening represented by the point being located on the base line. However, if both points lie to the right of the line $l = 1.5708$, then neither set of yarns can ever assume a straight-line configuration, and the minimum crimp possible in either set of yarns is governed by the condition in which they are jammed against the other set of yarns. This condition occurs where the top of the l/D line terminates at the "jam line," which is the upper right-hand boundary of the graph along which various values of λ have been laid out.

$$\lambda = l_2/l_1 \qquad (\text{where } l_2 < l_1) \qquad (2)$$

The ratio is always taken so that $\lambda < 1.0$, regardless of whether the length of yarn between crossovers, l, for warp or for filling must be placed in the numerator. The value of λ expresses the "squareness" of a fabric—*i.e.*, values of λ near 1.0 indicate square interstices, and the interstices become more and more oblong as λ decreases. The λ lines are laid on the graph in pairs, one line referring to the point for the warp yarns and the other line referring to the point for the filling yarns. Thus, if the point for the filling yarns lies at maximum crimp on the jam line (*e.g.*, point 8, Figure 3), then the point for the warp yarns *must* lie at minimum crimp at the intersection of the line and the l_w/D line (*e.g.*, point 12, Figure 3). The λ lines are especially helpful in the design of fabrics, since yarns do not slip along one another at the crossovers, and, hence, the setup in the fabric at the loom remains the same for the life of the fabric.

One more set of lines on the main graph remains to be discussed. The straight lines inclining upward to the left give values of θ, the angle of maximum inclination of a yarn to the plane of the fabric. The value of this angle is of little use in most

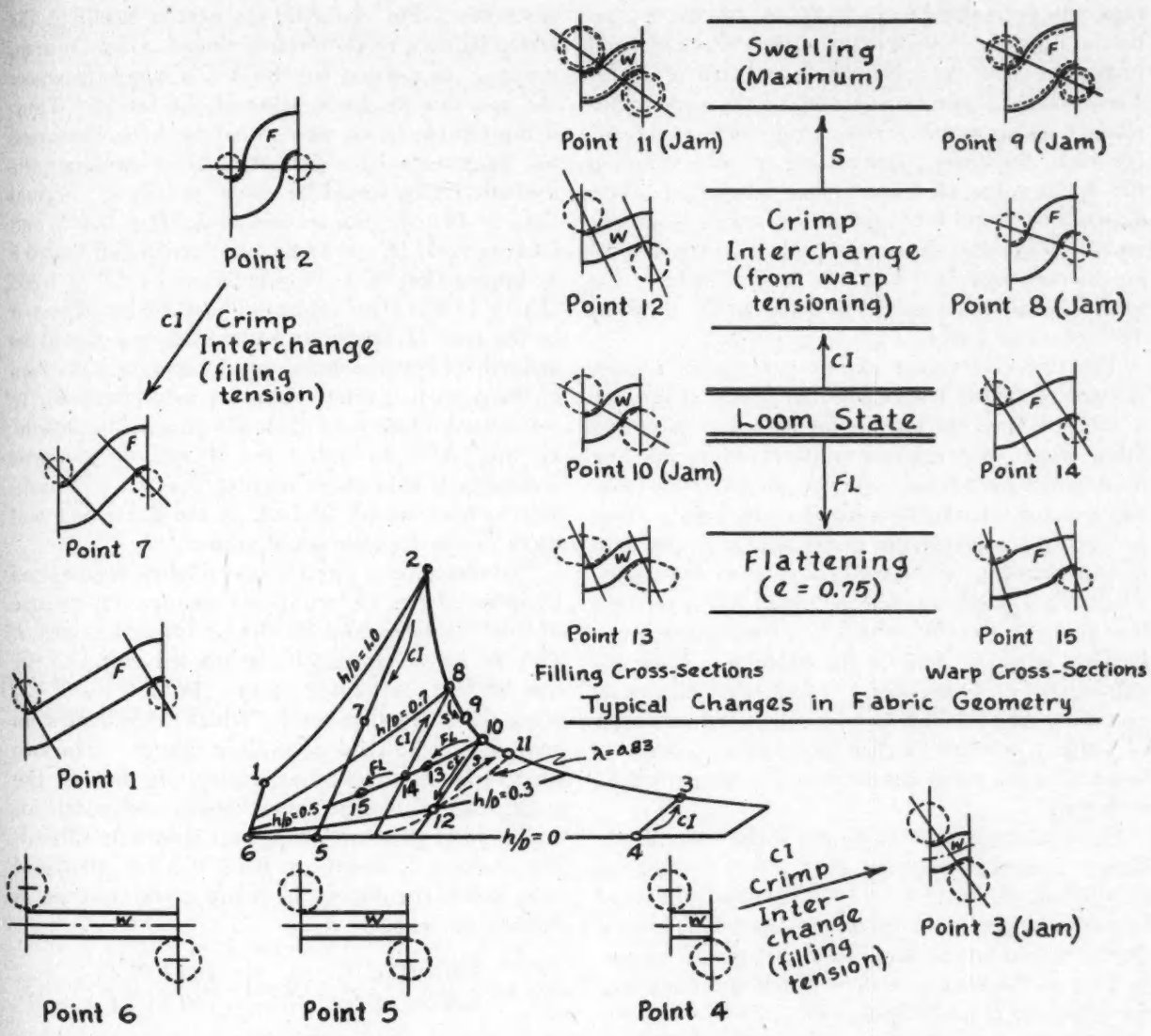

FIG. 3. *Geometry of various points on main graph.*

fabric-geometry problems, except where it might be used in the calculation of stress translations in tensile-strength computations. The angle θ is important in the basic theory of fabric geometry since it occurs in four of the seven simultaneous equations which link the eleven variables defining the plain weave.

Examples of Use of the Main Graph

There are three major changes in shape of the unit cell outlined by Peirce which cause concomitant changes in fabric dimensions: (1) crimp interchange, (2) yarn swelling, and (3) yarn flattening. The geometry of these various shapes is shown in Figure 3 in relation to the points on the main graph which depict them (points 8–15). In addition, Figure 3 shows the shapes of the unit cell at various other "limiting" points on the graph (points 1–7).

The assumptions and calculations necessary to construct the examples are given in Table I. A tight-weave fabric was chosen in order to demonstrate the use of the jam line in defining limiting values. For a fabric with neither yarn jammed, it is necessary to fix four of the eleven variables which define any plain-weave fabric; if one yarn is jammed, only three of the values are needed for definition of the fabric structure; if both yarns are jammed, only two values need be known. Actually, in the last

case, the geometry of the structure can be defined by the ratio $\lambda = l_2/l_1$, but the scale will not be fixed unless one other value is fixed, such as one of the l's. The variable D can be regarded as the scale factor which fixes linear fabric dimensions such as threads per inch, thickness, yarn diameter, etc. Finding the finite value of D and these attendant fabric dimensions is the function of the auxiliary graph, and the examples shown in Table I in terms of D are carried over into Table V to demonstrate the use of the auxiliary graph in defining the physical dimensions of a fabric.

The two l/D values chosen for the loom-state example in Table I were selected rather arbitrarily as follows: Since the loom-state fabric has minimum filling crimp, the warp point must be on the jam line for a tight-woven fabric, and the point $l_w/D = 1.047$ was selected since $h_w/D = 0.500$ at this point. This is a central point of the graph and it is useful to show a drawing of the configuration at this point. The $l_f/D = 1.265$ was selected since it hits the jam line at $h_f/D = 0.700$, which is a convenient intermediate point to show in the drawing. After the assumption of these initial values, the changes in geometry which follow can be calculated as shown in Table I without further assumptions except as to whether the yarns remain round or are permitted to flatten.

The diameters of yarns shown in the examples in Figure 3 were chosen so that $\beta = 1.5$—that is, $d_f = 1.5\, d_w$, or $\sqrt{N_w/N_f} = 1.5$. However, it should be pointed out that the fabric geometry and changes therein would be the same whatever β was chosen. As long as the sum $d_1 + d_2 = D$ remains constant, the geometry is unchanged.

In the examples of crimp interchange, swelling, and flattening in Table I, it can be seen that the basic assumption is that yarns do not slip at crossovers—that is, the values of l_w and l_f remain constant throughout all changes of geometry. This is one of the basic concepts of fabric dynamics.

In the example of flattening given in Table I, the assumption was made that the final state of crimp was determined by the h/D's remaining constant. As Peirce pointed out, it is always difficult to predict the state of crimp balance remaining in a fabric after a change in D (either flattening of yarns or partial, but not maximum, swelling; crimp balance is defined by λ for maximum swelling). Of course, reasonable assumptions as to state of crimp balance can be made once the cause of the change in D is known. For instance, for partial swelling, the crimp balance tends towards the so-called "normal crimps," as defined by the h/D's which intersect the jam line at the λ value of the fabric. Thus, if the sample fabric were dried back to the original loom-state yarn diameters after swelling, the normal crimps would be given as follows: normal $\%C_w = 10.7$ at intersection of $h_w/D = 0.415$ and $l_w/D = 1.047$ ($K_f = 14.8$); and normal $\%C_f = 16.8$ at intersection of $h_f/D = 0.585$ and $l_f/D = 1.265$ ($K_w = 12.9$). The crimp balance to be expected in the case of flattening by calendering would be defined, as Peirce pointed out, by equating the sum of warp yarn diameter plus its amplitude, h_w, to the sum of filling yarn diameter plus its amplitude, h_f: thus, $d_w + h_w = d_f + h_f$. If one set of yarns is sized or is held under tension, that set will probably remain round, and all of the flattening will occur in the opposite set of yarns.

The shrinking or stretching of a fabric is governed by three effects: (1) crimp interchange, (2) change in yarn diameter, and (3) change in yarn length, l. The last factor can usually be ignored except in the case of very extensible yarns. Both (1) and (2) often occur simultaneously, which complicates an analysis or prediction of a fabric change. The two effects can be studied separately by use of the graph; the changes in fabric length and width for each type of structure change are shown in Table I. The changes in length or width can be calculated from either the change in crimp or the change in threads per inch.

$$S_w = 1 - \frac{100 + (\%C_w)_o}{100 + (\%C_w)_s}; \quad S_f = 1 - \frac{100 + (\%C_f)_o}{100 + (\%C_f)_s}; \quad (3)$$

$$S_w = 1 - (T_f)_o/(T_f)_s; \qquad S_f = 1 - (T_w)_o/(T_w)_s; \quad (4)$$

where S_w = warpwise, or length, shrinkage; S_f = fillingwise, or width, shrinkage; $\%C_w$ = % crimp in warp yarns; $\%C_f$ = % crimp in filling yarns; T_w = warp threads per inch; T_f = filling threads per inch; o = original fabric structure; s = shrunk fabric structure.

If the calculated value of S_w is negative, then the fabric has stretched instead of shrunk. Calculations of shrinkages from crimp changes are given in Table I. Calculations using values of T in equation (4) give the same values for shrinkage as are obtained by using values of crimp; this method is useful in checking the accuracy with which $\%C$'s and K's are read from the graph. It should be

TABLE I. CALCULATIONS FOR TYPICAL CHANGES IN FABRIC GEOMETRY SHOWN IN FIGURE 3

Configuration	Points for warp yarn geometry	Points for filling yarn geometry
Loom state*	Point 10 (Jam)	Point 14
Assume:	$l_w/D = 1.047$	$l_f/D = 1.265$
Calculate:		$h_f/D = 1 - h_w/D = 0.500$
Read from graph:	$h_w/D = 0.500$ $\%C_w = 20.9$ $K_f = 16.07$	$\%C_f = 10.6$ $K_w = 12.20$
Calculate:	$\lambda = 1.047/1.265 = 0.83$	
Crimp interchange†	Point 12	Point 8 (Jam)
Calculate:	$h_w/D = 1 - h_f/D = 0.300$	
Read from graph:	$\%C_w = 5.0$ $K_f = 14.00$	$h_f/D = 0.700$ $\%C_f = 32.8$ $K_w = 14.65$
Calculate:	$S_w = 1 - \frac{120.9}{105.0}$ $= -15.1\%$ shrinkage $= 15.1\%$ stretch in length	$S_f = 1 - \frac{110.6}{132.8}$ $= 16.7\%$ shrinkage in width
Swelling (maximum)‡	Point 11 (Jam)	Point 9 (Jam)
Read from graph:	$l_w/D = 0.95$ $\%C_w = 16.80$ $h_w/D = 0.415$ $K_f = 17.17$	$l_f/D = 1.14$ $\%C_f = 25.8$ $h_f/D = 0.585$ $K_w = 15.37$
Calculate:	$S_w = 1 - \frac{105.0}{116.8}$ $= 10.5\%$ shrinkage in length	$S_w = 1 - \frac{132.8}{125.8}$ $= -5.6\%$ shrinkage $= 5.6\%$ stretch in width
	$\frac{(\text{new } D)}{(\text{old } D)} = \frac{(\text{old } l/D)}{(\text{new } l/D)}$; since l is constant.	
	$\therefore \frac{(\text{new } D)}{(\text{old } D)} = \frac{1.047}{0.95} = \frac{1.265}{1.14} = 1.105,$ or, each yarn swelled 10.5% in diameter.	
Flattening**	Point 13	Point 15
Calculate:	$(\text{new } l_w/D) = \frac{1.047}{0.75} = 1.396$	$(\text{new } l_f/D) = \frac{1.265}{0.75} = 1.687$
Read from graph:	$\%C_w = 8.0\%$ $K_f = 10.75$	$\%C_f = 5.0$ $K_w = 8.66$
Calculate:	$S_w = 1 - \frac{120.9}{108.0}$ $= -11.9\%$ shrinkage $= 11.9\%$ stretch in length	$S_f = 1 - \frac{110.6}{105.0}$ $= -5.6\%$ shrinkage $= 5.6\%$ stretch in width

* This configuration illustrates the loom state because crimp is minimum in filling. Assume round yarns.

† Assume warp tensioning to produce minimum crimp in warp, keeping yarns round. *Solution:* Keep l/D's constant; points move along l/D lines until filling hits jam line.

‡ Assume yarns remain round, swell equally to minimum density, or maximum D, at which both yarns jam against each other. *Solution:* Keep l's constant, increase D to give minimum possible l/D's as read from jam line at $\lambda = 0.83$.

** Assume yarn diameter which is vertical to cloth plane is reduced 25%—that is, flattening coefficient $e = 0.75$. *Solution:* Keep l's constant, decrease D so that new $D = 0.75$ (old D). Assume h/D's constant to determine new state of crimp balance.

pointed out that the change in K upon shrinking reflects a change in both T and D, and when T's for the shrunk cloth are calculated from K's for the shrunk cloth, the change in D must be taken into account by using the value of D for the shrunk cloth.

Locating D *on the Main Graph*

The geometrical analysis of any particular fabric consists merely of locating the two points representing that fabric on the main graph. In order to do this, it is necessary to obtain the $\%C$'s and K's for each set of yarns. The value of K is obtained from T (threads per inch) and the proper value of D (the sum of diameters, or amplitudes, in mils) by the expression $K_w = 0.01395\, DT_w$. However, flattening of yarns is usually present to an unknown degree, and the value of D cannot be calculated from the sum of the diameters of the individual yarns because these are obtained on the assumption that the yarns are round. The proper value of D_f for flattened yarns can be obtained from the main graph by the simple procedure shown in Table II and illustrated in Figure 4. The procedure is based on the use of Peirce's approximate equation for amplitude:

$$h_1 = \frac{136\sqrt{\%C_1}}{T_2}. \qquad (5)$$

The sum

$$h_1 + h_2 = D_f \qquad (6)$$

then gives an approximate value of D_f, allowing calculation of h/D's. These values of h/D can, however, be considered as precise values even though calculated from approximate h's if one assumes that h/D's are independent of D—that is, the error is distributed proportionately between the two values of h. Of course, if it is known that all of the flattening occurs in one set of yarns only, such as would occur with hard sized-warp yarns, all of the error can be proportioned to the soft yarns, thus changing the h/D values. In making such assumptions, one must use great care in determining proper values for % crimp, since extensible yarns, or stiff yarns with crimp set into them, will give slightly erroneous experimental results, and small variations in crimp have a rather large influence on the results. It will nearly always be possible to determine D_f in this manner, with a precision of about 1% or better, since K can easily be read to the nearest 0.1.

This procedure for obtaining the precise value of D_f is offered as something of an improvement over the method given by Peirce, using the following

TABLE II. EXAMPLE OF LOCATING PRECISE D_f

	W	×	F	
Threads/in., T	72	×	53	Given
Crimp, $\%C$	10.8		16.6	Given
$136\ \%C_1/T_2 = h_1$	8.8			Approximate
$136\ \%C_2/T_1 = h_2$			7.7	Approximate
$h_1 + h_2 = D_f$		16.5		Approximate
h/D_f	0.532		0.468	Approximate
Read from graph, as in Figure 4, K	15.7		11.6	
$K/0.01395\ T = D'_f$		15.7		Precise
$(15.7/16.5)\ h = h'$	8.35		7.35	Precise

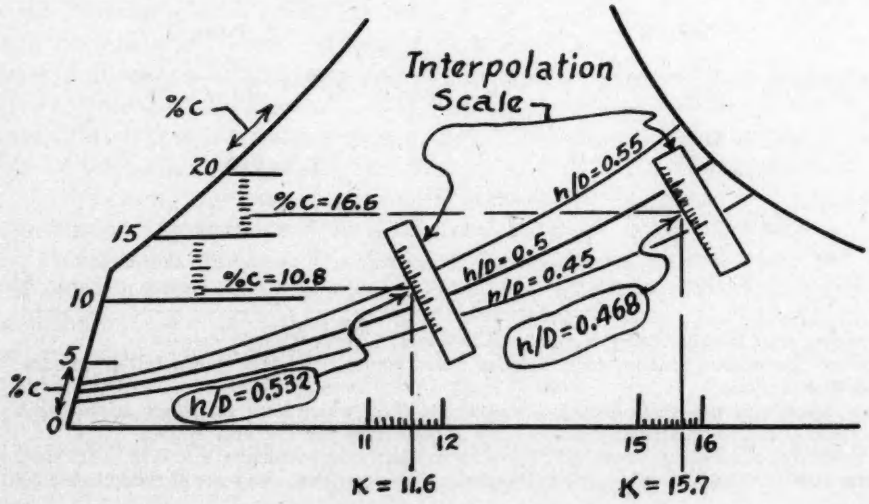

FIG. 4. *Location of* D_f.

equation:

$$D_f = \frac{p_2\,2C_1 + p_1\,2C_2}{1 + 0.20\,(C_1 + C_2) - (S_1 + S_2)}, \quad (7)$$

where $p = 1000/T$ = thread spacing, and S = correction factor to be read from a graph of $\%C$ *vs.* D/p. It is necessary to go through the above equation once without using the S's in order to get an approximate D with which to calculate one scale for the graph. Thus, a trial-and-error method is necessary. It is not simple in the present procedure to apportion all of the error to one set of yarns.

A further example of locating a fabric on the main graph is illustrated in Figure 5, which depicts the various fabric structure changes in an example given by Peirce. Various weights were hung on wet strips of fabric and Peirce then analyzed the structures after drying them under tension. The calculations for location of the loom-state sample are shown in Table III, and the values of K and $\%C$ for the various stretched samples are shown in Table IV. The lines for the average l/D values computed by Peirce are shown in Figure 5. It is interesting to note that the initial warp tension produced almost pure crimp interchange, as illustrated by movement of the points parallel to the constant l/D lines, while the initial filling tension produced almost pure flattening, as illustrated by movement of the points parallel to the constant h/D lines.

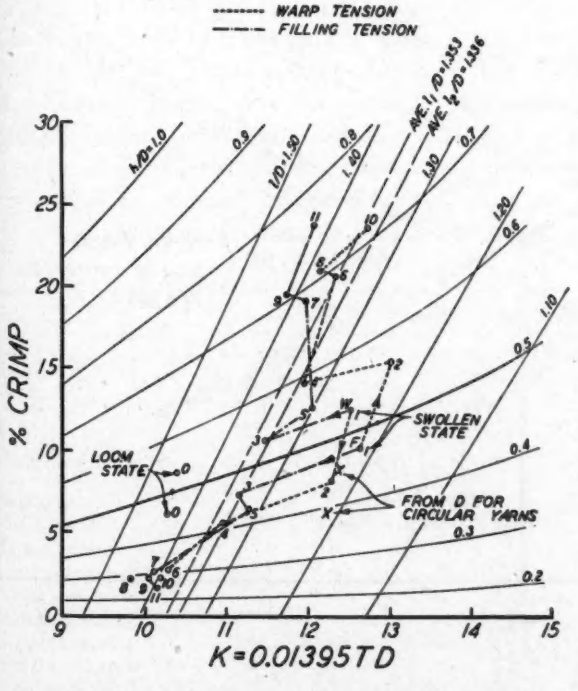

FIG. 5. *Dimensional changes in a canvas.*

Description of the Auxiliary Graph

The terms usually used to describe a fabric are texture, T (threads per inch), yarn number, N (or cotton count or denier), and weight, W (ounces per square yard). These terms are not available directly from the main graph, but they may be calculated by means of a few simple relations. These relations have been reduced to graphical form in Figure 2, the auxiliary graph. This has been

TABLE III. LOCATING PRECISE D_f FOR LOOM-STATE SAMPLE

	W	×	F	
Threads/in., T	32.4	×	32.8	Given
Crimp, $\%C$	8.7		6.2	Given
Yarn Nos., N_1, N_2	6.7		6.3	Given
$36/N_1 = d_1$	13.8 mils		14.4 mils	
Round-yarn sum, D		28.2 mils		
Reduced yarn No., N		6.5		
$136\ \%C_1/T_2 = h_1$	12.2 mils		10.4 mils	Approximate
$h_1 + h_2 = D_f$		22.6 mils		Approximate
h/D_f	0.540		0.460	Approximate
Read from graph, K	10.3		10.4	
$K/0.01395\ T = D'_f$		22.8 mils		Precise
$(22.8/22.6)\ h = h'$	12.3 mils		10.5 mils	Precise

Flattening coeff., $e = 22.8/28.2 = 0.81$
Thickness, $G = 13.8 + 12.3 = 26.1$ mils

TABLE IV. POINTS FOR GRAPH FROM PEIRCE'S DATA FOR "DIMENSIONAL CHANGES IN A CANVAS"

Cloth	Load* W	Load* F	D/p_1	D/p_2	K_1†	K_2†	$\%C_1$	$\%C_2$
0	Loom		.737	.747	10.29	10.41	8.7	6.2
1	Shrunk		.908	.898	12.65	12.51	12.5	10.3
2	.5		.934	.882	13.01	12.30	8.3	15.5
3		.5	.801	.824	11.17	11.48	10.8	7.4
4	1		.860	.787	11.98	10.97	5.6	14.1
5		1	.811	.865	11.30	12.06	13.6	6.5
6	2.5		.885	.739	12.33	10.30	2.8	20.7
7		2.5	.727	.860	10.13	11.99	19.3	2.7
8	5		.870	.705	12.12	9.84	2.3	21.0
9		5	.722	.840	10.08	11.71	19.6	2.3
10	10		.913	.734	12.72	10.22	2.4	23.6
11		10	.730	.866	10.18	12.08	23.8	1.7

* Load (lbs.) on 2 in. × 18 in. wet strip of fabric.
† $K = 13.95\ D/p$.

done despite the fact that the equations involved are quite simple; the graphical approach has the advantage over mere calculation of particular values in that limits are always clearly depicted.

It is apparent from the equations shown along the base of the main graph (Figure 1) that T is easily found from K if D is known, since

$$K_w = 0.01395\, DT_w. \tag{8}$$

It is developed in more detail in the following section that D can be stated in terms of N, the reduced yarn number, as follows:

$$D = 1/.01395\, N = (2)\,(35.85)/N. \tag{9}$$

Hence:

$$K_w = T_w/N. \tag{10}$$

In Figure 2 various sets of lines have been superposed on a background set of rectangular coordinates relating T, threads per inch (along the left side), to K, reduced cover factor (along the top). Various values of N, reduced yarn number, are given on the set of straight lines sloping downward to the right. Any point along any one of these N lines gives a particular value of T for that value of N and K. (These N lines should not be confused with the Q lines, which also curve down to the right. The Q lines give fabric weight in ounces per square yard; these are discussed later.)

K is called the reduced cover factor because N in equations (9) and (10) is the reduced yarn number of the fabric—*i.e.*, the cotton yarn number of the hypothetical yarn whose diameter is the average of the warp and filling yarn diameters. It is obvious that this average diameter is $D/2$ since D is the sum of warp and filling yarn diameters:

$$D = d_1 + d_2. \tag{11}$$

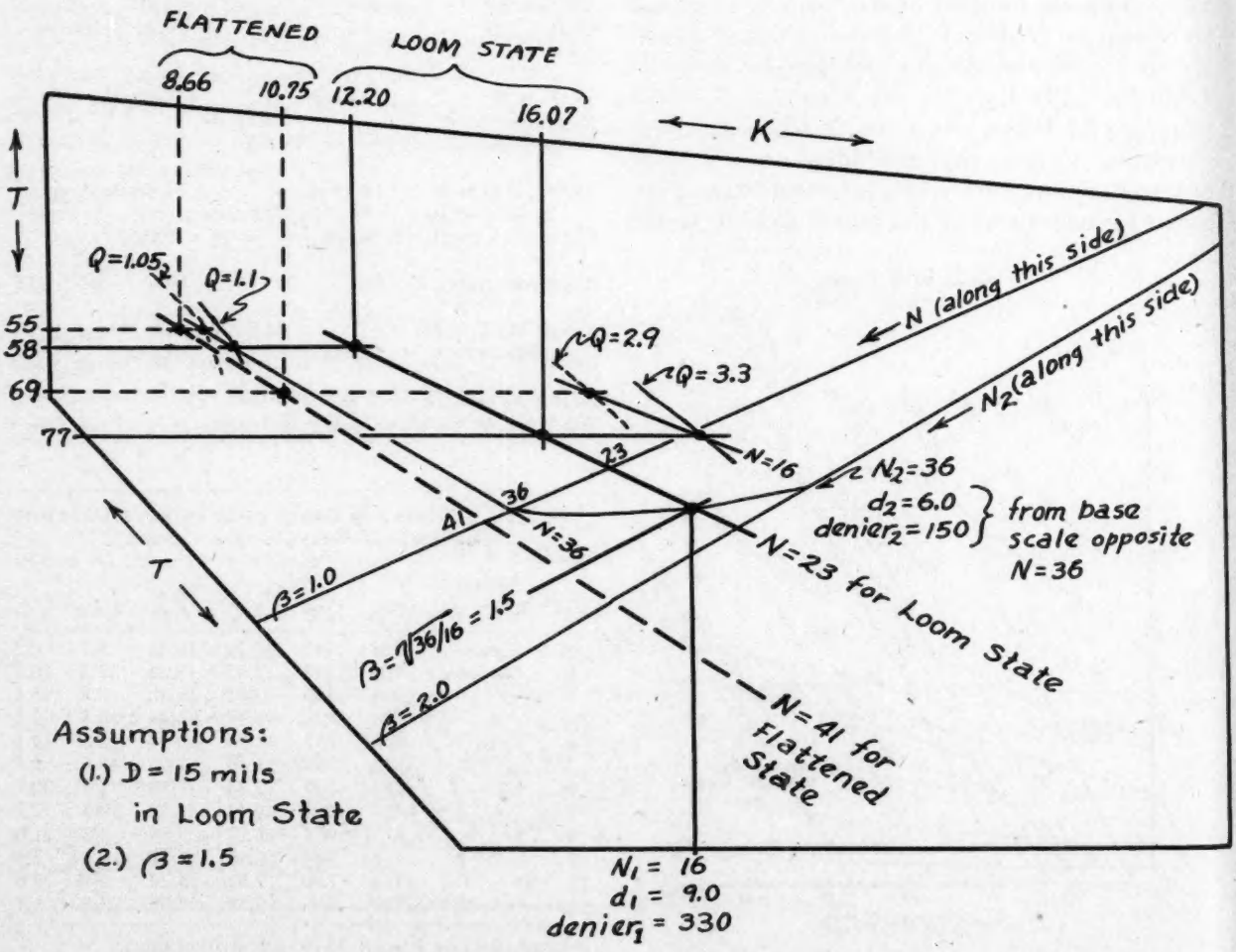

FIG. 6. *Example of use of auxiliary graph.*

If D is known from the main graph (obtained as described in the preceding section), the proper N line which relates K_w and T_w may be found quite simply by using the base scale in Figure 2 to locate the proper value of N opposite $D/2$.

The examples worked out previously in Table I are carried out in Figure 6 on the auxiliary graph by lifting just those portions necessary for illustration. In order to do this it was necessary to assign a value to D; the value of 15 mils was selected arbitrarily for the loom state. Reading the base scale in Figure 2, it can be seen that $N = 23$ lies opposite $D/2 = 15/2 = 7.5$ mils. The line $N = 23$ thus depicts the relation between K's and T's for the loom state. The flattened-state N value lies opposite $D_f/2 = (0.75)(15)/2 = 5.63$ mils, or $N = 41$. These lines are shown in Figure 6. It should be pointed out that if only crimps and threads per inch are known for a fabric, it is possible to define the fabric structure on the main graph and to locate the N line on the auxiliary graph. This N value, however, does not necessarily represent any kind of average of the warp and filling yarn numbers; it is merely the yarn number of a yarn with diameter equal to the average of the vertical diameters of the warp and filling yarns at the crossovers, and these latter are usually flattened.

It is also important to note that the diameter of the warp yarns alone, or of the filling yarns alone, can assume any value desired (*i.e.*, $\beta = \sqrt{N_2/N_1}$ is not fixed), and that only their sum, D, is necessary to determine the relation between T and K. It can be observed by a little study of the unit cell cross section shown in Figure 1 that one yarn—say, the warp—can be made smaller in diameter while the filling yarn is made larger (keeping D constant) without changing the essential geometry of the unit cell, the only change being the movement of the point of tangency of the two yarns along the radius line defined by θ, which, along with all the other values, remains constant.

The reduced yarn number, N, is separated graphically into its two real components, N_w and N_f, by means of the set of divergent straight lines of various values of β running downward to the left from the upper right-hand corner of the graph (Figure 6), in conjunction with the base scale across the bottom of the graph giving yarn number, diameter, and denier. This operation is shown in Figure 6 for the loom-state example. The flattened state can also be separated into N_w and N_f, but the values for N_w and N_f thus obtained are not real because they represent the yarn numbers of round yarns having the diameter to which the real yarns have been flattened. Further, it is obvious that if the flattening is not proportional in each yarn, the β value will change. The diameter scale can be used for trial-and-error solutions for actual cases. The equation which relates the scales for diameter and yarn number is

$$d_w = 35.85/\sqrt{N_w}. \qquad (12)$$

The assumptions about yarn density which are necessary for this equation are discussed in the next section.

Various other dimensions obtainable from the auxiliary graph are shown in Table V (except for the h's, which were calculated from the h/D's given previously).

The fabric thickness is always given by which-

TABLE V. FABRIC DIMENSIONS OBTAINED FROM AUXILIARY GRAPH

Fabric structure	Yarn diameters (mils) $W \times F$ d_w	d_f	Amplitudes (mils) $W \times F$ h_w	h_f	Fabric thickness (mils) G	Reduced yarn No. N	Threads per inch $W \times F$ T_w	T_f	Weight (oz./sq. yd.) ($N_w = 36$; $N_f = 16$) $W \times F$ $Q_1(1+C_1)$	$Q_2(1+C_2)$	Total fabric
Loom state (minimum $\%C_f$)	6.00	9.00	7.50	7.50	16.50	23.0	58.3	76.8	1.34	3.65	4.99
Warp tension (minimum $\%C_w$)	6.00	9.00	4.50	10.50	19.50	23.0	70.0	66.9	1.40	3.79	5.19
"Normal crimps"	6.00	9.00	6.20	8.80	17.80	23.0	61.5	70.5	1.30	3.52	4.82
Swollen state (maximum)	6.60	10.00	6.90	9.70	19.70	18.6	66.0	74.0	1.46	3.97	5.43
Flattened state ($e = 0.75$)	4.52	6.73	5.63	5.63	12.36	41.0	55.1	68.7	1.13	3.08	4.21

ever set of yarns gives the largest value of

$$G = h + d, \tag{13}$$

where G = thickness in mils.

The fabric weight is obtained by the sum of the weight in warp and filling yarns. As indicated in Figure 6, the Q values should always be read at the intersection of the T lines and the sloping N lines which represent the actual yarn number regardless of diameter. The equations which are thus represented graphically are as follows:

$$\begin{aligned} W_w &= Q_w\,(1 + \%C_w/100) \\ &= 0.686\,T_w\,(1 + \%C_w/100)/N_w \end{aligned} \tag{14}$$

$$\begin{aligned} W_f &= Q_f\,(1 + \%C_f/100) \\ &= 0.686\,T_f\,(1 + \%C_f/100)/N_f \end{aligned}$$

$$\text{Total fabric weight} = W_w + W_f,$$

where W = weight in oz./yd.^{2} and Q = value read from graph.

Use of Graphs for Fibers Other Than Cotton

It should be emphasized that determination of flattened D_f from observed plain-weave thread spacings and crimps by the process described in a previous section (p. 160) is valid for any type of flexible yarn, regardless of yarn density. The relations portrayed by the main graph are concerned with linear dimensions only. The yarn density is used to convert these linear dimensions to weights by relating yarn diameter and yarn number (or denier). This relation is as follows:

$$\begin{aligned} d_w &= 34.14/\sqrt{\phi_w \psi_w N_w} = 34.14/\sqrt{\rho_w N_w} \\ &= 0.468\sqrt{\text{denier}_w/\phi_w \psi_w} \\ &= 0.468\sqrt{\text{denier}_w/\rho_w} \\ &= 35.85/\sqrt{N_w} \text{ for cotton,} \end{aligned} \tag{15}$$

where ρ = yarn density = $\psi\phi$, ψ = fiber density, and ϕ = packing coefficient.

Cotton yarns were assumed by Peirce to have $\rho = 0.9$ g./cc., which for $\psi = 1.54$ g./cc. gives $\phi = 0.589$, or 41.1% voids.

When equation (15) is substituted in the summation equation (11) for D:

$$\begin{aligned} D &= 34.14/\sqrt{\rho_w N_w} + 34.14/\sqrt{\rho_f N_f} \\ &= (34.14)\,(1/\sqrt{N_w} + 1/\sqrt{N_f})/\sqrt{\rho} \\ &= (2)\,(34.14)/\sqrt{\rho N} = (2)\,(35.85)/\sqrt{N}, \end{aligned} \tag{16}$$

where $2/\sqrt{N} = 1/\sqrt{N_w} + 1/\sqrt{N_f}$, N = reduced yarn number as defined previously, and ρ = average yarn density.

The reduced cover factor, K, is actually defined in terms of T and N (equation (10)), and, hence, in order to express it in terms of D (equation (8)), it is necessary to make certain assumptions about the yarn density. The value assumed by Peirce for cotton yarns ($\rho = 0.9$, or, more precisely, $1/\sqrt{\rho} = \sqrt{v} = 1.0500$, where v is specific volume, cc./g.) was taken, which results in the constant 0.01395 used in equation (8). This assumption does not limit the use of the graph to cotton yarns and fabrics. The geometry of the fabric is the same, but the K values are in terms of cotton yarns which have the same diameter as whatever fabric or yarns of a given D are being considered. Thus, the proper name for the K used on the graph is "equivalent cotton plain-weave reduced cover factor." For example, a nylon fabric could have a reduced cover factor $K' = T/\sqrt{N}$, where N would be the cotton yarn number of the diameter-average yarn of warp and filling. This K' would not be usable in the main graph, since complete cover would not be given at $K' = 27.93$, but is given by $K = 27.93$. The proper K for the graph is obtained by inserting the actual D, in mils, in equation (8).

Fiber densities can be obtained from any textile handbook, but packing coefficients (or % voids in the yarn) must be determined by experiment for the particular yarns involved, or must be assumed on some rational basis. Peirce found that variations in packing density and fiber density tended to cancel out one another, and that therefore a standard yarn density of about 0.9 was a "reasonably good approximation for most textile materials." However, the entire shape of any woven structure is quite critically dependent upon the precise value of yarn density, and calculations of deviations from the simple ideal form, such as bowing, flattening, etc., require the use of the more precise value. It is unfortunate that handbooks do not list the % voids of different types of fibers in yarns of various twists.

Weave Density

In the concept of "weave density" outlined by Peirce, the swelling is allowed to continue until both sets of yarns jam each other and the structure is determined by λ, which is laid off along the jam line

on the main graph. Although λ is not exactly linear along the jam line, the use of the interpolation scale gives good approximations for intermediate values.

The weave density of any fabric is readily obtained from the graph by use of the λ values. The weave density is obtained from the square of the value of the actual l/D divided into the l/D value which terminates on the jam line at the particular value of λ pertaining to the fabric. The relation is derived as follows:

$$D = 68.28/\sqrt{N}. \tag{17}$$

Maximum D occurs when both threads jam. If N = constant, D_j at jam gives weave density, ρ_w:

$$(\rho_w = 68.28/ND_j^2) \div (\rho = 68.28/ND^2)$$
$$\therefore \quad \rho_w = \rho D^2/D_j^2. \tag{18}$$

But l is also constant; hence:

$$\rho_w = \rho(l/D_j)^2(D/l)^2 = 0.907(l/D_j)^2(D/l)^2, \tag{19}$$

where ρ_w = weave density, g./cc., or density to which both yarns must swell to jam fabric; ρ = actual density, g./cc., of yarns = 0.907; l/D is given; and $l/D_j = l/D$ line which intercepts jam line at λ value of fabric.

Example: Assume original fabric λ = 1.0, l_2/D = 1.45

$$\therefore \quad l_2/D_j = 1.047$$
$$\rho_w = (0.907)(1.047)^2/(1.45)^2 = 0.473 \text{ g./cc.}$$

Example: Assume original fabric λ = 0.8, l_2/D = 1.00

$$\therefore \quad l_2/D_j = 0.93; \quad l_1/D = 1.25 \quad (\therefore \ l_1/D_j = 1.16)$$
$$\rho_w = (0.907)(1.16)^2/(1.25)^2$$
$$= (0.907)(0.93)^2/(1.00)^2 = 0.782 \text{ g./cc.}$$

Use of Graphs for Weaves Other Than Plain Weave

As pointed out by Peirce, weaves other than plain weave contain the plain-weave unit cell at the yarn crossovers, and the graph for the plain weave can be used to depict these weaves by applying the proper correction factors to observed crimps and threads per inch. The correction factor is derived by adding the length of straight yarn in the float to the unit cell, and depends upon the type of weave and number of cross threads per float.

Basket (or Matt) Weaves.—The correction factor for basket weaves was given by Peirce, but is restated here in slightly more general terms to coincide with methods of calculation already presented herein. Primed quantities refer to the plain-weave equivalent:

$$T_w' = T_w/fR_w; \quad T_f' = T_f/fR_f \tag{20}$$
$$C_w' = C_w/R_f; \quad C_f' = C_f/R_w \tag{21}$$

where

$$R_w = \left[1 - \left(\frac{f-1}{f}\right)\left(\frac{X_w}{1000}\right)T_w\right],$$
$$R_f = \left[1 - \left(\frac{f-1}{f}\right)\left(\frac{X_f}{1000}\right)T_f\right],$$

f = number of cross threads per float, and X = center-to-center spacing, in mils, of threads not separated by cross yarns.

The quantity X may be measured with a magnifying micrometer in an actual fabric. It can often be assumed that $X = d$, the yarn diameter, which, in turn, may be calculated for a circular yarn by using equation (15). However, the factor R is fairly sensitive to changes in X, and thus a value should be used which gives a reasonable degree of flattening as calculated from the equivalent plain-weave D.

Twill Weaves.—Only approximate analyses can be made for twill weaves, since an underlying assumption of the plain weave is that the projection of the threads into the plane of the fabric is a straight line. In the twill weaves the yarns tend to bow to one side at the float, which increases the crimp over what it would have been had the yarn been straight. Twill weaves can thus be studied by calculating this increase in crimp. Factors to convert to plain-weave equivalents are quite simple when it is assumed that the thread spacings are the same at crossovers and floats:

$$T_w' = T_w; \quad T_f' = T_f. \tag{22}$$

The amount of straight yarn in the float to be added to the crossover length depends upon the symmetry of the twill, and the correction factor for symmetrical twills (2/3, 3/3 types) is given:

$$C = \frac{l - fp}{fp} = \frac{l' + (f-1)p - fp}{fp}$$
$$= \frac{l' - p}{fp} = C'/f \tag{23}$$
$$\therefore \quad C_w' = fC_w; \quad C_f' = fC_f.$$

For asymmetrical twills (2/1, 3/1 types) the correction factor is:

$$C = \frac{l - \left(\frac{f+1}{2}\right)p}{\left(\frac{f+1}{2}\right)p} = \frac{l' + \left(\frac{f-1}{2}\right)p - \left(\frac{f+1}{2}\right)p}{\left(\frac{f+1}{2}\right)p}$$

$$= \frac{l' - p}{\left(\frac{f+1}{2}\right)p} = \frac{C'}{\frac{f+1}{2}} \qquad (24)$$

$$\therefore \quad C_w' = \left(\frac{f+1}{2}\right)C_w; \quad C_f' = \left(\frac{f+1}{2}\right)C_f.$$

An equivalent plain-weave D can be calculated from these equations and used in equation (8) along with the equivalent plain-weave T's to obtain the two K values on the main graph which depict the plain-weave unit cell. If the observed twill crimps have been increased by bowing of the floats, this increase must be estimated and subtracted from the observed twill crimp before insertion in equations (23) or (24). The degree of flattening can then be obtained from the location of the plain-weave unit cell on the graph. Trial-and-error calculations will usually lead to reasonable values of bowing and flattening. This type of structure analysis must be accompanied by detailed microscope observations and a knowledge of the history of the fabric. For instance, the loom spacing of the warp in the reed has in some instances been used as a good estimate of the value of the plain-weave l for the filling yarns in a 3/1 twill.

Appendix

Basic Variables and Equations

Actually, the situation of eleven variables is not as bad as it sounds, since the group consists of five pairs in which one value is assigned to the warp yarns and the other to the filling yarns, plus the eleventh variable, D, the sum of diameters. The five variables are as follows: p, thread spacing, mils; l, thread length in unit cell, mils; h, thread amplitude, mils; C, fractional crimps ($100C = \%C$); θ, angle of inclination of thread, radians.

Peirce's analysis linked the eleven variables together with the following seven equations:

Projection parallel to cloth plane.—

$$h_1 = (l_1 - D\theta_1)\sin\theta_1 + D(1 - \cos\theta_1) \qquad (1)$$

$$h_2 = (l_2 - D\theta_2)\sin\theta_2 + D(1 - \cos\theta_2) \qquad (2)$$

Projection normal to cloth plane.—

$$p_2 = (l_1 - D\theta_1)\cos\theta_1 + D\sin\theta_1 \qquad (3)$$

$$p_1 = (l_2 - D\theta_2)\cos\theta_2 + D\sin\theta_2 \qquad (4)$$

Definition of crimp.—

$$C_1 = (l_1 - p_2)/p_2 \qquad (5)$$

$$C_2 = (l_2 - p_1)/p_1 \qquad (6)$$

Relation between paths of two sets of threads.—

$$D = h_1 + h_2 \qquad (7)$$

In his analysis, Peirce further simplified the situation of eleven variables by taking one of the variables, D, as a scale basis (or divisor) for three pairs of the other quantities: p, l, and h. However, no further simplification was possible, since no mathematical device could be found to eliminate and reduce the seven equations to one or two simple relations involving only thread spacings (p_1 and p_2), crimps (C_1 and C_2), and D. The best solution was the use of a table for p, h, and C for given intervals of l and θ, but even with the table it is necessary to perform lengthy interpolations for any particular value. Peirce presented one graph and a graphlike device, but the former did not give precise intermediate values and neither one gave limit structures.

Construction of the Main Graph

A composite graph has been developed which depicts precise values for all of the variables as well as limit structures by using $\%C$, crimp, *versus* T, threads per inch ($T = 1000/p$), as the basic coordinates, and superposing sets of lines for constant l/D, h/D, and θ. Actually, T is expressed in terms of K, the reduced cover factor, which will be explained later. The superposed lines are located as follows:

Constant l/D Lines

These lines are derived from the definition of crimp; the form of equation (5) may be rewritten in the following fashion:

$$C_1 = (l_1 - p_2)/p_2, \quad \text{or} \quad 1/p_2 = (1 + C_1)/l_1. \qquad (5)$$

Multiplying both sides by D:

$$(1 + C_1)D/l_1 = D/p_2 = T_2D/1000 = K_2/13.95, \qquad (8)$$

since, by definition, $T/1000 = p$, K = the reduced cover factor.

If D/l_1 = constant (which is true along constant l/D lines), then the first and last terms in equation (8) reduce to:

$$K_2 = a + bC_1, \tag{9}$$

in which a and b are constants. Thus, equation (9) shows that constant l_1/D lines are straight lines due to the linear relation between K_2, the reduced cover factor for one set of yarns, and C_1, the crimp in the other set of yarns. A similar situation exists between K_1 and C_2 for constant l_2/D lines. The subscripts are carried here to emphasize that the relation is between crimp in one set of yarns, "1," *versus* reduced cover factor (or threads per inch) in the other set of yarns, "2," or vice versa. Figure 1 shows these straight l/D lines on the $\%C_1$ *versus* K_2 graph.

Constant h/D Lines

The shape of constant h/D lines is that of approximate parabolas indicated by the approximate relation between $\%C_1$ and K_2 (or $\%C_2$ and K_1) derived by Peirce as follows:

Equations (1) and (3) were expanded to give:

$$h_1/D = 1.36\sqrt{C_1}(p_2/D) \tag{10}$$
$$= 136\sqrt{\%C_1}/T_2D = 1.897\sqrt{\%C_1}/K_2$$

(also a similar equation with reversed subscripts).

When h/D = constant:

$$K_2^2 = a\%C_1, \quad \text{or} \quad K_1^2 = a\%C_2, \tag{11}$$

in which a is an arbitrary constant, K is the reduced cover factor, and $\%C$ is the crimp.

Exact values of $\%C_1$ *versus* K_2 for plotting constant h/D lines were obtained by the use of Peirce's table ([1], Table II) relating values of h/D for various values of l/D and $(l - p)/D$. This was accomplished very easily by making an intermediate plot of h/D *versus* C for a family of constant l/D lines. It was then a simple matter to pick even values of h/D along these l/D lines and transfer them by means of the corresponding C value to the constant l/D lines on the $\%C_1$ *versus* K_2 graph. Smooth curves were then drawn through these points to give the constant h/D lines, as shown in Figure 2. The curves thus obtained give exact values of h/D.

Constant θ Lines

These are derived by substituting the definition of crimp, $l_1 = p_2(1 + C_1)$, and the definition of reduced cover factor, $13.95/K_2 = 1000/T_2D = p_2/D$, into equation (3) to give:

$$\%C_1 = (1 - \cos\theta_1)/\cos\theta_1 - (\sin\theta_1 - \theta_1\cos\theta_1)K_2/13.95\cos\theta_1. \tag{12}$$

When θ = constant, this reduces to

$$\%C_1 = a - bK_2, \tag{12a}$$

in which a and b are constants. These lines are shown in Figure 3.

Limit Structures

These are located as follows:

Jam Line: A thread is "jammed" when the straight portion $(l - D\theta) = 0$, as illustrated in Fig-

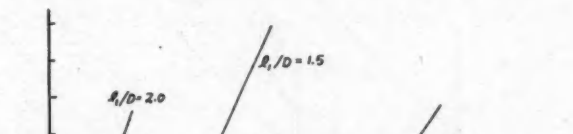

FIG. 1. *Constant l/D lines.*

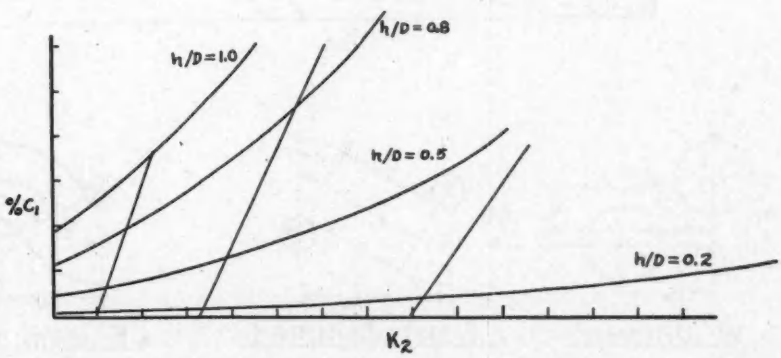

FIG. 2. *Constant h/D lines.*

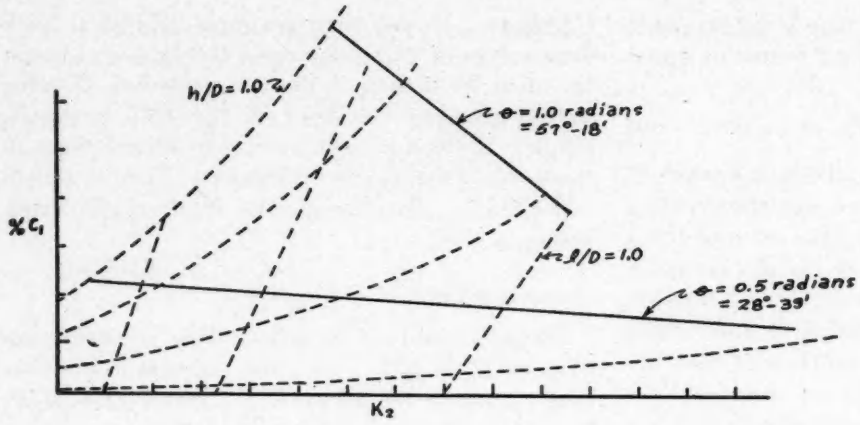

FIG. 3. *Constant θ lines.*

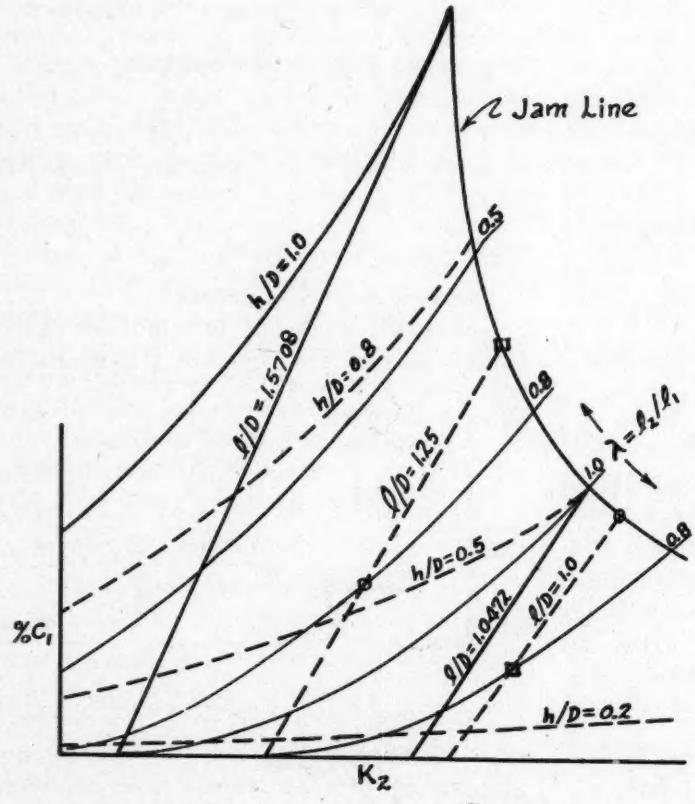

FIG. 4. *Jam line and crimp limits.*

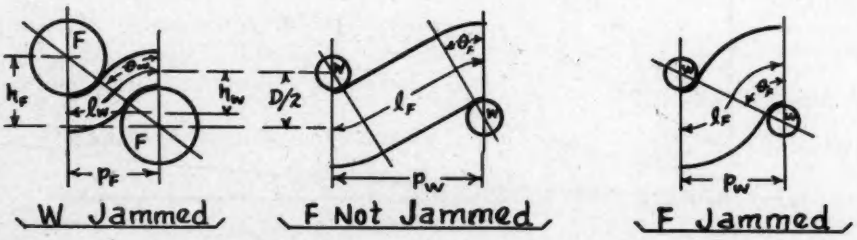

ure 4; it follows that:

$$\theta_1 = l_1/D. \quad (13)$$

Also, equation (3) reduces to

$$p_2/D = \sin(l_1/D) = 1000/T_2D = 13.95/K_2, \quad (14)$$

in which subscript "1" refers to warp, W, and subscript "2" refers to filling, F.

Using the first two parts of equation (14) and substituting in the definition of crimp (equation (5)):

$$C_1 = [(l_1/D) - \sin(l_1/D)]/\sin(l_1/D). \quad (15)$$

Substitution of the second and fourth parts of equation (14) gives the equation of the "jam line" in terms of $\%C_1$ and K_2 only:

$$13.95/K_2 = \sin[(1 + C_1)13.95/K_2]. \quad (16)$$

Even values of $\lambda = l_2/l_1$ are located along the jam line by selecting even values of λ and of l_2/D to give particular values of l_1/D, which are then inserted in equations (14) and (15) to give points for the graph in terms of $\%C_1$ and K_2 which define the jam line. The "unit cell structure" mentioned earlier is defined by λ and either one of the l/D's.

Minimum Crimps (in F When W Is Jammed): Since the straight portion $(l - D\theta)$ of the warp thread equals zero, equation (1) reduces to:

$$h_1/D = 1 - \cos\theta_1 = 1 - \cos(l_1/D). \quad (17)$$

Combining this equation with equation (7) gives

$$h_2/D = \cos(l_1/D). \quad (18)$$

The particular values of l_1/D used above, which go with the proper even values of λ and l_2/D, were then used in Peirce's table of h *vs.* l and $l - p$ to get precise values of C_2 to plot on the even-value lines of l_2/D. These points were then joined at equal values of λ to give the λ lines shown as solid lines curving down to the left in Figure 4. The l/D lines have been changed in Figure 4 from Figure 3 in order to show the ones which are related to limit points, such as $l/D = 1.5708$ and $l/D = 1.0472$.

Swollen Structure: Equations (19) and (20) show special cases of the swollen structure.

$$\theta_2 = l_2/D \quad (19)$$

$$\cos(l_1/D) + \cos(\lambda l_1/D) = 1 \quad (20)$$

Tightest Weave Containing Zero Crimp: Equations (21) and (22) show cases of the limit fabric which has zero crimp one way and maximum crimp the other—*i.e.*, the W-jammed, F-straight fabric whose points lie at the opposite ends of $l/D = 1.5708$. A fabric with both points on an l/D line less than 1.5708 cannot have zero crimp.

$$\theta_2 = 0 \quad (21)$$

$$\theta_1 = l_1/D = 90° = 1.5708 \text{ radians} \quad (22)$$

Acknowledgment

The writer wishes to express appreciation for the advice and frequent helpful discussions with Dr. M. M. Platt during the course of this work. Gratitude is also expressed to Mr. C. C. Chu for much of the tedious drafting work on the graphs and to Mrs. Janet Butler for help in calculating many long tables of figures. The Office of The Quartermaster General has been helpful in sponsoring the project under which this work was accomplished.

Literature Cited

1. Peirce, F. T., The Geometry of Cloth Structure, *J. Textile Inst.* **28**, T45–96 (1937).
2. Peirce, F. T., Geometrical Principles Applicable to the Design of Functional Fabrics, TEXTILE RESEARCH JOURNAL **17**, 123–47 (1947).

(Manuscript received October 29, 1951.)

Some Theoretical Aspects of Yarn and Fabric Density

R. M. Hoffman

Pioneering Research Division, Textile Fibers Department, E. I. du Pont de Nemours & Co., Inc., Wilmington, Delaware

Introduction

The bulk density of fabrics is a topic of current interest, and is associated with problems of loft, hand, covering power, and body comfort. The various textile fibers now in use range in density from 2.6 g./cc. for glass to 0.92 g./cc. for polyethylene. Fabrics, which can be considered to be mixtures of fibers and air, can vary through an even greater range of bulk density. Wool, with a fiber density of about 1.32 g./cc., can be woven into a fabric having a density of 0.30 g./cc. Such a fabric can be made which will be nearly opaque; it will possess good covering power in spite of its low density. In contrast, a chiffon fabric or a cotton gauze fabric will show large holes between the yarn interstices. The bulk density, obtained by dividing the weight of such a fabric by the product of its area and thickness, is, therefore, correspondingly low (0.20 g./cc., for example). No one should conclude from such data that cotton is a bulkier material than wool. This comparison does, however, raise a question as to the proper interpretation and use of fabric density data.

The air-filled space within the over-all boundaries of the fabric can occur: first, as *invisible* space trapped by the *fibers;* and, second, as *visible* space (*e.g.,* in chiffon) outlined by the *yarns.*

To a large degree, the air-filled spaces between the fibers govern the insulating and warmth properties of the fabric. On the other hand, the air-filled holes formed by the yarn interstices affect the porosity, air permeability, and summertime comfort of the fabric and reduce its opacity and covering power. In making warm fabric for overcoats, the aim is to get a maximum of the former and a minimum of the latter type of air space. In the case of woolen fabrics, fulling helps to bring about just such a result.

Because the functional properties of fabrics depend upon the amount and distribution of air in these two ways, it is important to characterize them quantitatively. Some methods which can be used are discussed below in three sections dealing with the density of fibers, yarns, and fabrics.

Fiber Density

A number of fiber densities are listed below in decreasing order:

Glass	2.60 g./cc.
Saran	1.68
Cellulose	1.52
Dacron polyester fiber	1.37
Silk	1.35
Vinyon	1.35
Cellulose acetate	1.33
Wool	1.32
Orlon acrylic fiber	1.18
Nylon	1.14
Polyethylene	0.92

Such information is a necessary but, at the same time, a very incomplete part of the bulk problem in terms of end-uses. It is obvious that a fluffy batting of glass fiber such as is used for thermal insulation will have an over-all density lower than that for a closely woven nylon twill fabric. Less obvious are the reasons behind the fact that Orlon staple can produce a bulkier (less dense) yarn and fabric than nylon in spite of the somewhat higher polymer density of Orlon. Some of the factors which equal and sometimes outweigh the importance of the polymer density are discussed below.

Yarn Density

From a wool fiber with a polymer density of about 1.32 g./cc., yarns with a variety of density values can be produced. With this polymer density, a yarn density of 0.40 g./cc. corresponds to 70% air space.

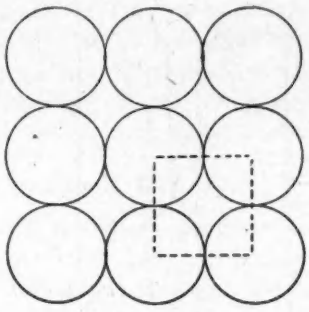

FIG. 1. *Rods arranged in cubic packing, with 22% air space.*

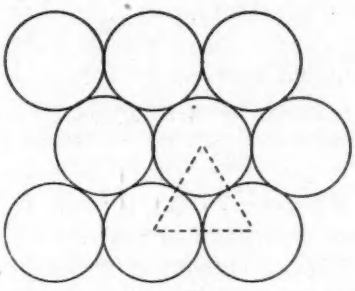

FIG. 2. *Rods arranged in hexagonal packing, with 9% air space.*

This can be calculated as follows:

$$\% \text{ air} = 100 \frac{\text{volume air}}{\text{volume yarn}}$$

$$= 100 \frac{\text{vol. yarn} - \text{vol. polymer}}{\text{vol. yarn}}$$

$$= 100 \left(1 - \frac{d_y}{d_p}\right) = 100 \left(1 - \frac{0.40}{1.32}\right) = 70\%,$$

where d_y = yarn density, and d_p = polymer density.

The amount of air space is dependent upon the way in which individual fibers can pack together. Packing is in turn affected by a number of variables, including fiber crimp, fiber stiffness and recovery behavior, yarn construction (plying and twist), and the shape, size, and size distribution of the fiber cross sections. Of these, the degree and permanence of the crimp are undoubtedly of major importance. The present discussion is limited to a theoretical treatment of the packing behavior of circular rods (fibers). While this one aspect is of perhaps lesser importance in the bulk problem, it does appear to be worthy of consideration. In a recent article [7], Schwarz treated a similar problem, particularly from the standpoint of obtaining the most compact or stable yarn structure. The problem of obtaining the least dense yarn, using mixtures of *dissimilar diameters,* is emphasized below.

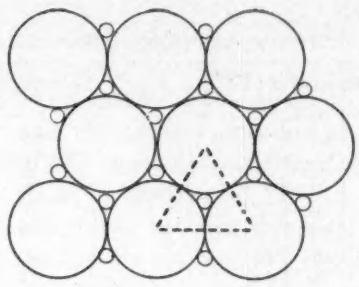

FIG. 3. *Rods arranged in "filled" hexagonal packing, with 5% air space.*

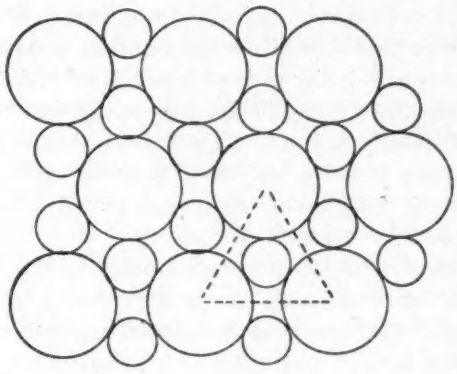

FIG. 4. *Rods arranged in opened hexagonal packing, with 20% air space. Denier ratio, 1/4. Number ratio, 2 small rods to 1 large rod.*

By analogy with the way in which sand fills the voids between the larger aggregates in concrete, it has often been assumed that the mixing together of large and small fibers would lead to denser yarns. It can be shown that this analogy is incorrect when applied to fibers unless the ratio of large and small deniers is of the order of 42 to 1.

Straight, parallel rods of uniform circular diameter can be packed together in a cubic arrangement (Figure 1) with an air space of 22% by volume. However, for rods that are free to move or shift about, the cubic arrangement is unstable and will revert to the denser hexagonal or close-packed type with only 9% air space (Figure 2).

The repeating unit in hexagonal packing consists of a triangle which can be drawn by connecting the centers of three adjacent and touching circles. In the center of this triangle there is room for an additional rod of smaller diameter (Figure 3). The insertion of such extra rods (two for each large rod)

TABLE I. HEXAGONAL PACKING PLUS EXTRA RODS

Denier ratio (S/L)	% Free space
1 to 42	5
1 to 25	10
1 to 11	16
1 to 6.3	19
1 to 4	20
1 to 2	19
1 to 1.78	16
1 to 1.4	14
1 to 1	9

would decrease the air space to 5%. This would require a diameter ratio of 1 to 0.155. Since the denier is proportional to the diameter squared, this amounts to a denier ratio of 1 to 0.024 (42 to 1).

If the extra rods in Figure 3 are not small enough to fit exactly but are slightly over-size, as shown in Figure 4, there will be a wedging apart of the large rods, with an accompanying gain in free space, as shown by the data in Table I.

With a 1 to 4 denier ratio mixed in the proportion of two small rods to one large rod, a free space of 20% is achieved for the closest possible *uniform* packing.

In addition to the ratio of deniers, another ratio is important—the ratio of the number of small to large rods. Not all of the types of packing which might be possible with different number ratios have been considered in the present study; however, certain uniform arrangements selected as being of possible interest are listed below.

Denier ratio (S/L)	Number ratio (S/L)	Weight ratio (S/L)	% Space
1 to 4	1 to 1	1 to 4	13
1 to 4	2 to 1	1 to 2	20
1 to 4	3 to 1	3 to 4	31
1 to 4	4 to 1	1 to 1	13
1 to 4	5 to 1	5 to 4	21

The mixture in which the denier ratio $S/L = 1/4$ and the number ratio $S/L = 3/1$ is especially interesting. It represents a "double optimum," with both the denier ratio and the number ratio being better than would be the case for a number of other choices. Furthermore, it has an advantage connected with the problem of disproportionation—*i.e.*, a given mixture, such as 3 to 1 in numbers, may not be uniformly mixed but may separate into localized areas of 2 to 1 and 4 to 1, etc. Even if this happens for the particular case under discussion, the other proportions are still fairly good and all show better

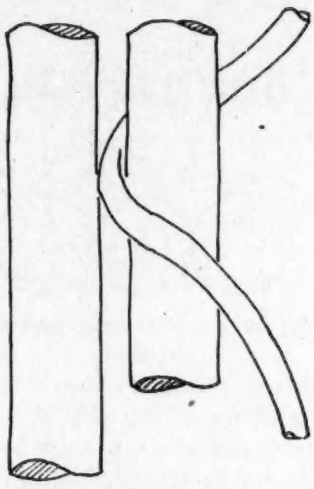

FIG. 5. *Illustration of the wedging-apart action of small fibers on large ones, with a resulting increase in bulk.*

than the 9% space which is characteristic of the close-packed hexagonal arrangement.

Another way of visualizing the beneficial wedging-apart action of small fibers on large ones is illustrated in Figure 5.

With actual yarn systems, in which the fibers are neither completely straight nor completely parallel, the *total* picture is quite different from the highly idealized approach as outlined. However, a *portion* of the total picture is similar. Close-packing may occur with fibers in localized areas of the yarns in fabrics, especially at the cross-over points (see Figure 6) where fiber-to-fiber pressure is the greatest. By raising the value for the tightest possible packing from 9% space to 20%–30% space, a fully equivalent gain should not be expected on the over-all yarn or fabric density. The density of a fabric is a summation or mixture of densities ranging from practically zero in the holes between cross-overs to nearly the polymer density for closely packed fibers. By using dissimilar fiber diameters, it should be possible to improve the bulk of the "worst" places by a considerable amount, and the over-all density by a lesser, but significant, amount. These conclusions are consistent with the belief that a *part* of the high bulk of ordinary wool yarns is due to the fact that the individual fibers vary in size through a range of approximately 2 to 20 denier.

Certain packing arrangements may possibly show reductions in interfiber friction and thereby improve the hand and wrinkle-resistance. This expectation is based on the probable influence of less fiber-to-

fiber contact as follows: in hexagonal packing each rod touches 6 others; in cubic packing each rod touches 4 others; in an "opened up" hexagonal packing, such as described above, the majority of the rods (the small ones) touch only 3 other filaments.

Fabric Density

Data on fabric densities, calculated in the usual way as already mentioned, are inadequate to describe and interpret differences between fabrics which do not have the same geometry. Nor is there any easy escape from this inadequacy by applying the oft-mentioned rule which prescribes that "the fibers should be compared in comparable fabrics." The increasing variety of textile fibers has so widened the ranges of physical properties, including those which affect the density of fabrics, that it becomes increasingly difficult to prepare a series of truly comparable fabrics that will embrace all the important fibers.

It is possible to prepare an Orlon fabric and a nylon fabric in which the yarn denier, crimp, weave pattern, thread count, and weight are all the same, and yet for which the yarn diameters and fabric thicknesses are different. This is true because Orlon produces a bulkier yarn than nylon in spite of its slightly greater polymer density. It is believed that such differences can be explained in terms of fiber cross-sectional shape, stiffness, resilience, and Cassie's tightness factor [1, 3], all of which contribute to holding the fibers apart.

Even in the case of a single material, it is often experimentally difficult to achieve a uniformly fixed warp and filling count in a series of fabrics by means of which could be studied the effect of some variable, such as twist, on density.

It is for these reasons that it is desirable to study and compare essentially different (non-comparable) fabrics with respect to density. This becomes possible to a large measure if one measures and calculates the following:

(1) The fabric weight, thickness, and apparent density.

(2) The light transmission of the fabric, using ultraviolet light to which most fibers are black.* This is used to calculate the effective width of the yarn.

(3) The density of the yarn as it resides in the fabric. This density may be quite different from that measured before weaving. During weaving and subsequent finishing, the material is subjected to tension and compressional stresses and other influences such as shrinkage conditions, etc., all of which may result in changes.

(4) The percent air between the *fibers*.

(5) The percent air between the *yarns*.

To these parameters can be added the density of the yarn before weaving. This total information can contribute much to an over-all understanding of the bulk density problem.

In order to obtain relatively simple mathematical relationships with which to calculate the yarn density after weaving, a few simplifying approximations are necessary. Based on fabric cross-section photographs, the over-and-under path of the yarn in plain-weave fabrics is found to be approximately a sine curve. In order to determine the volume of yarn present in a fabric, it is necessary to know the true yarn length—that is, the straightened-out length. If the amplitude and the period of a sine curve are measured, its length can be calculated by means of the equation:

$$S = \frac{2}{\pi}\sqrt{1+h^2}\int_0^{\pi/2}\sqrt{1-\left(\frac{h}{\sqrt{1+h^2}}\right)^2\sin^2\alpha}\,d\alpha,$$

using a table of values for elliptical integrals. For a sine curve which rises to a height h in a unit distance along the abscissa ($\alpha = 0$ to $\alpha = \pi/2$), S will be the length of the curve.

Because the use of this equation involves a rather laborious computation, it is interesting to note that the value for S is only slightly greater than the length of the hypotenuse, Z, of a right triangle with a height h and a base equal to unity. The tabulation below shows how closely the values of S and Z agree for sine curves of various degrees of amplitude which cover the range of crimp amplitudes encountered in actual fabrics.

h	S	$Z=\sqrt{h^2+1}$	$Z'=\sqrt{1.16h^2+1}$
0	1.00	1.00	1.00
.25	1.04	1.03	1.04
.50	1.14	1.12	1.14
.75	1.29	1.25	1.29
1.0	1.47	1.41	1.47

In the last column of the above tabulation, a correction factor of 1.16 has been added to the equation

*An instrument employing this principle has been designed and built in this laboratory by J. W. Ballou.

for Z. This modification gives values which even more closely approximate those from the much more laborious calculations necessary to obtain S and is therefore employed in the derivation given later. This approach is also much simpler than that used by Peirce [5] in his mathematical treatment of the uncrimped length of yarns in fabrics.

The accuracy of this approximation as applied to an actual fabric was checked as follows: Measurements on an enlarged photograph of a fabric cross section showed that the sinusoidal path of the yarn rose to a height of 0.35 unit over a base distance of 1 unit. This corresponds to a gross length of

$$\sqrt{1.16(.35)^2 + 1} = 1.07,$$

or 7% crimp. This value is considerably less than the average guess arrived at by visual estimation and with the fact in mind that a straight line is the shortest distance between two points. By the use of dividers, the actual length of the curved path was found to be 1.065 times longer than the straight-line path (a reasonably good check on the calculated value). As a second check, the pick count and thickness measurements from the actual fabric were used (described in more detail later) to calculate the length ratio, which in this case was 1.064; again the results were in good agreement. As a third but less direct check, the weight per unit area of the fabric and the sum of the count of ends and picks were used to calculate the ratio of the apparent denier after weaving (crimped) to the yarn denier before weaving (uncrimped); this was found to be 1.09. From this somewhat larger value it would appear that, in addition to the 7% crimp contraction, there was a small amount (2%) of real shrinkage which probably occurred during the finishing or boil-off of the fabric.

It has also been assumed that the yarns in fabrics may be deformed from a round to an elliptical cross-sectional shape. That this is a good assumption is indicated by Figure 6, which shows the edgewise views of several fabric samples. The equations based on this assumption of elliptical shape are also suitable for circular cross sections, in which case the elliptical axes a and b become equal.

The belief that yarns in fabrics generally possess circular cross sections is a misconception which is perpetuated by the scarcity of actual fabric cross-section photographs in textbooks on fabric design and structure. The majority of the textbooks on this subject use simplified drawings which are inaccurate on this point. A photograph showing the elliptical cross-sectional shape of yarns in fabrics

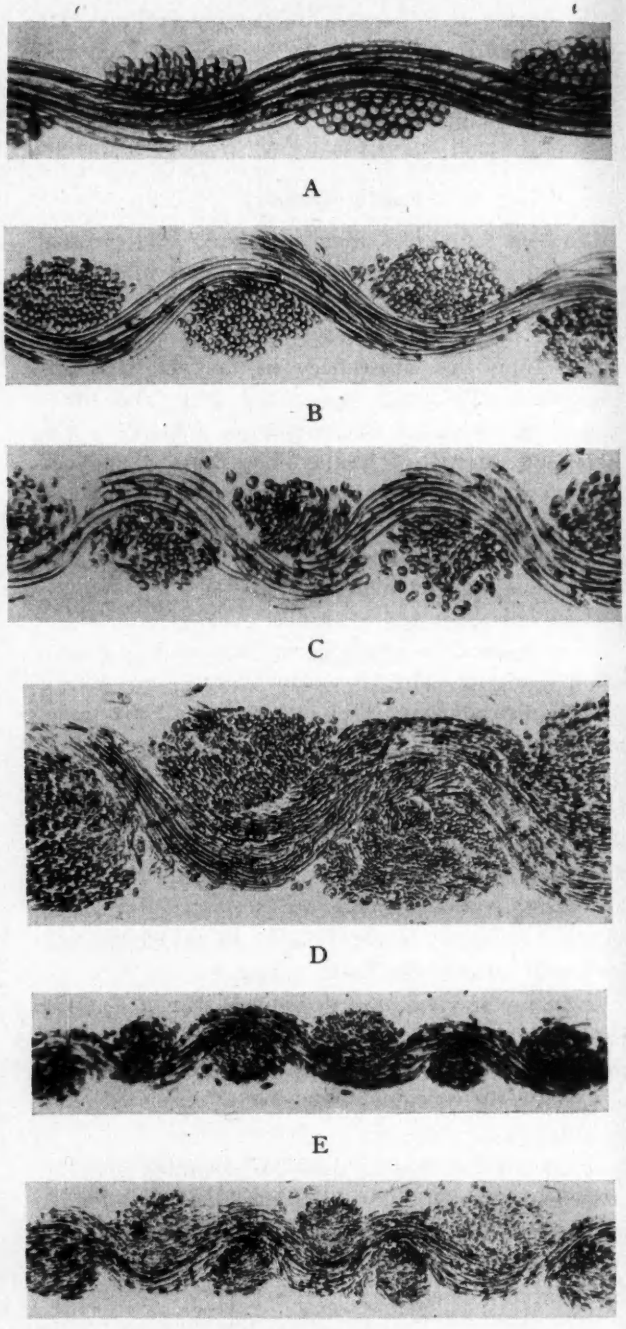

FIG. 6. *Cross-section photographs showing flattened or elliptical shape of yarns in various fabrics.* A—*Nylon.* B—*Dacron polyester fiber.* C—*Wool.* D—*Linen.* E—*Cotton.* F—*Cotton (higher twist than* E).

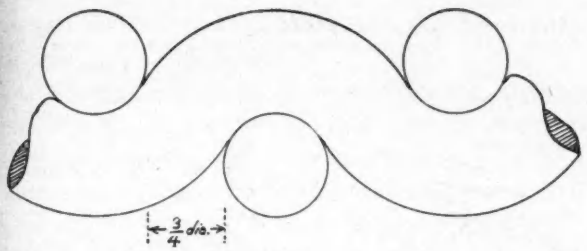

FIG. 7. *Illustration of tightest possible square weave with round yarns.*

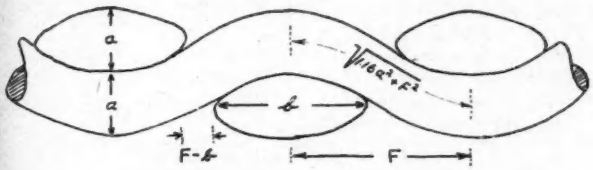

FIG. 8. *Illustration of more opaque square weave possible with flattened yarns.*

has been published in a textbook by Schwarz [6]. Commenting on the assumptions often made in fabric studies, Schwarz wrote, "These hypothetical conditions are often far from the actual facts. Yarns are assumed to be perfectly round and of a diameter corresponding to a formula the accuracy of which is very much in question." Peirce [5] in his studies of cloth geometry pointed out the importance of this change in shape as follows: "Most of the discrepancy between the mathematical assumptions and the actual form of real fabrics is due to flattening of the threads." Kober's [4] recent work on the density of fabrics is open to this same objection. Assuming a circular cross section, he calculated yarn diameters using the density of the yarn before weaving.

It is impossible to weave an opaque plain-weave fabric with perfectly round yarns and in a balanced construction (*i.e.*, equal crimp for warp and filling). The tightest plain weave theoretically possible would show by transmitted light square holes, each side equivalent in length to $\frac{3}{4}$ of a yarn diameter (Figure 7). For such a fabric or screen, the light transmission at normal incidence would be 18.4%. The ratio of the fabric density to the yarn density would be .54 to 1.

In contrast to round yarns, a yarn with an elliptical cross section possesses much more covering power and can produce a practically opaque plain-weave fabric when the yarn spacing approaches the yarn *width* in magnitude (Figure 8). Many fabrics in which this is the case can be found, and the

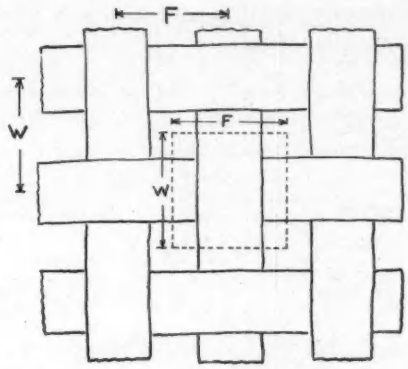

FIG. 9. *Plan view of unit cell (dotted lines) used in density calculations for plain-weave fabric.*

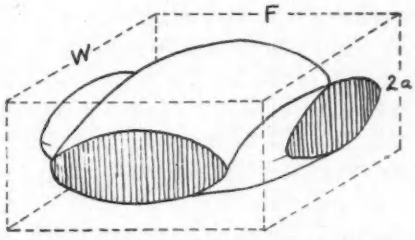

FIG. 10. *Isometric view of unit cell from Figure 9.*

flattened shape of yarns unravelled from them can be seen easily with a low-power magnifying glass.

The repeating unit cell used in deriving the relationship of yarn and fabric density is shown in dotted lines in Figure 9 and in isometric projection in Figure 10. The problem now is to find the relative volume of this cell and of the yarn within the cell. The derivation is as follows:

a = thickness of yarn = $\frac{1}{2}$ fabric thickness;

b = width of yarn;

$$b = \tfrac{1}{2}(W + F) - \tfrac{1}{2}\sqrt{(W + F)^2 - 4WF(1 - L)},$$

where W = center-to-center distance of warp ends,

F = center-to-center distance of filling ends,

L = fraction of light transmitted by fabric.

When $W = F$, then

$$\frac{b}{W} = \frac{b}{F} = (1 - \sqrt{L}) = C = \text{coverage factor},$$

$$\text{area of yarn cross section} = \frac{\pi ab}{4} = 0.785ab,$$

$$\text{length of filling yarn in cell} = \sqrt{1.16a^2 + W^2},$$

$$\text{length of warp yarn in cell} = \sqrt{1.16a^2 + F^2},$$

$$\text{total length of yarn in cell} = \sqrt{1.16a^2 + F^2} + \sqrt{1.16a^2 + W^2},$$

$$\text{volume of yarn in cell} = 0.785ab(\sqrt{1.16a^2 + F^2} + \sqrt{1.16a^2 + W^2}),$$

$$\text{volume of cell} = 2aWF.$$

Let d^* = density of yarn as it exists in fabric;
D = density of fabric.

Then

$$\frac{d^*}{D} = \frac{\text{volume of cell}}{\text{volume of yarn in cell}}$$

$$= \frac{2aWF}{0.785ab(\sqrt{1.16a^2 + W^2} + \sqrt{1.16a^2 + F^2})};$$

$$d^* = \frac{2.55D}{\frac{b}{F}\sqrt{1.16(a/W)^2 + 1} + \frac{b}{W}\sqrt{1.16(a/F)^2 + 1}}.$$

It is evident that the important parameters in this equation are simple ratios of yarn diameters (thickness and breadth) to yarn spacings (from filling and warp counts), which can be obtained by the procedure described, or, if desired, by the use of fabric cross-section photographs. In the case of a different degree of weave crimp in the warp and filling, it would be necessary to use the latter procedure.

The data in Table II illustrate the use of this equation. These data were taken from an experimental series used to study the effect of twist on density, using single-ply, continuous-filament yarn of 500 denier and a plain-weave fabric. The fiber was an experimental one of polyethylene terephthalate. The fiber cross sections were round.

When the densities were measured on these fabrics, it appeared that the higher-twist yarn had made the less dense fabric (.43 *vs.* .45 g./cc.). That such a conclusion might be misleading was indicated by the much more open appearance of the higher-twist fabric.

The analysis in Table II shows that the higher twist produced the following differences: (*a*) a slightly thicker fabric (.018 *vs.* .017 in.); (*b*) a more open weave (9.3% *vs.* 2.1% light transmission); (*c*) a more dense yarn (.74 *vs.* .59 g./cc.); (*d*) a less flattened yarn (1.9 *vs.* 2.6 for ratio b/a); (*e*) a less desirable fabric from the standpoint of air between fibers (27% *vs.* 43%).

It can also be concluded that fabric No. 1, produced from the lower-twist yarn, would be the warmer of the two fabrics—which is not evident from the measurement of fabric density alone.

By winding these yarns before weaving on a package under a constant tension of .04 g./denier and measuring the weight per unit volume, the following densities were obtained: 4Z yarn, .61 g./cc.; 12Z yarn, .53 g./cc.

In the case of the 4-turn yarn, the package density is almost exactly that found for the yarn in the fabric. The higher-twist yarn value does not agree as well. This, again, is believed to be a question of packing. In the case of high twist, the yarns tend to maintain their shape and identity in the package, and the resulting holes between yarns give rise to erroneously low density values. In the case of low twist, the yarns pack together more compactly, and the density values are less subject to this error. Therefore, one must use care in correlating package densities with yarn densities.

TABLE II

	Fabric No. 1	Fabric No. 2
Twist in yarn	4Z	12Z
Warp count	43	44
Filling count	38	37
Fabric thickness	.017 in.	.018 in.
Fabric density (D)	.45 g./cc.	.43 g./cc.
Light transmission	2.1%	9.3%
Thickness of yarn (a)	.0085 in.	.009 in.
Width of yarn (b)	.022 in.	.017 in.
Ratio b/a	2.60	1.89
Density of yarn in fabric (d^*)	.59 g./cc.	.74 g./cc.
Polymer density (d_p)	1.37 g./cc.	1.37 g./cc.
Percent total air in fabric, $100\ (1 - D/d_p)$	67%	69%
Percent air between yarns, $100\ (1 - D/d^*)$	24%	42%
Percent air between fibers (from difference of the above)	43%	27%

Four other fabric construction variables which affect the density of fabrics can be mentioned: (*a*) dissimilar twist in warp and filling; (*b*) face or cover; (*c*) weave pattern; and (*d*) surface nap.

When two highly twisted yarns which are both S or both Z cross each other at right angles, the touching filaments from the two yarns are inclined in the same direction and can intermesh or pack together slightly. If one yarn is S twist and the other Z twist, this packing is prevented because the filaments from the bottom yarn will be at right angles to those on the under surface of the top yarn at the point of contact.

The subject of obtaining "face" or cover in cloth was described in a recent article by Herring [2]. In a fabric without face, the warp and filling yarns are equally crimped. By a suitable loom adjustment, the warp can be made to take more of the crimp and to become more prominent on both surfaces of the cloth. The filling, on the other hand, is less crimped and more buried. Herring stated that such a fabric is fuller and more uniform in appearance, showing fewer reed marks. Such a fabric would also show an altered packing arrangement and would

require a modification of the density equations used above.

For more complicated weave patterns, such as twills and satins, a rigorous mathematical treatment becomes more complex. An approximate treatment, however, becomes even more simplified than for the case of plain weaves. This is because a satin weave introduces less interlacing of the yarns and, therefore, the crimped length of the threads is not much different than the uncrimped lengths. For round yarns of a diameter b spaced a distance W apart and stacked in two layers, one above the other at right angles but without over-and-under interlacing, the density relationship would be

$$\frac{d^*}{D} = \frac{\text{cell vol.}}{\text{yarn vol.}} = \frac{2bW^2}{.5\pi b^2 W} = \frac{1.27}{b/W} = \frac{1.27}{c},$$

where c = coverage $= 1 - \sqrt{L}$. For elliptical yarns having a thickness a and a width b, the derivation gives an identical result as follows:

$$\frac{d^*}{D} = \frac{2aW^2}{.5\pi abW} = \frac{1.27}{b/W} = \frac{1.27}{c}.$$

Thus, for both of the above cross-sectional shapes, it is the width or, more exactly, the width-to-spacing ratio or coverage factor which is important, and this can be determined simply by a light transmission measurement, L, on the fabric. It seems worthwhile to emphasize again that the yarn width cannot be safely calculated from a denier measurement except in the case of extremely high-twist yarns which remain circular in cross section.

In the case of real fabrics, the thickness enters the equation only to establish the actual or uncrimped length of yarn present, and this amounts to a second-order correction which can be approximated. If it is assumed that the yarn thickness is about half the width, then

$$d^* = \frac{1.27D}{C\sqrt{.29C^2 + 1}}.$$

Although this is derived for a balanced plain weave, it is a reasonably good approximation for many fabrics. This equation gives d^* values of 0.61 and 0.74 g./cc. in place of 0.59 and 0.74 g./cc., as already calculated for the yarns in the two fabrics above.

In the event that one wishes to compare the fabric densities of a number of fabrics which vary in openness of weave, it is convenient to adjust the data to a common basis. This is equivalent to an estimation of what the density values would have been if the fabrics had all been woven to the same degree of covering power. Choosing for the common basis the case in which $C = 1$ (zero light transmission), the above equation becomes

$$D_{C=1} = .895d^*.$$

Substituting for d^*,

$$D_{C=1} = \frac{1.14D}{C\sqrt{.29C^2 + 1}}.$$

Either of these two equations provides a useful number which can be called an adjusted or corrected fabric density. By means of them it is possible to estimate that fabrics No. 1 and No. 2 in Table II would have had densities of about .54 and .66 g./cc., respectively, if they had been woven in a manner such as to obtain the same (complete) coverage rather than the same warp and pick counts.

The presence of a surface nap on a fabric introduces a number of unsolved problems. As discussed previously [3], it it believed that a nap can influence the hand and the bulkiness of a fabric and that the commonly used pressure of 3 lbs. per sq. in. for thickness measurements is much too high to take this into account. It seems reasonable to expect that thermal insulating characteristics would be influenced by the presence of a nap between the surfaces of two fabrics used in combination, or between the fabric and the surface of the human body. This indicates that a third type of air space, in addition to the two mentioned at the start of this paper, may warrant consideration.

Concluding Remarks

The phenomena of imperfect packing of fibers in yarns and yarns in fabrics must be taken into account and placed on a quantitative basis in order to interpret density values. Certain of the theoretical aspects of this problem have been presented here. A simplified approach has been employed which approximates the conditions encountered in actual yarns and fabrics. Modification of the mathematical equations presented will be necessary in order to handle further complications, such as nonbalanced weaves, different diameter yarns in the warp and in the filling, and weave patterns other than the plain weave.

Acknowledgment

The author thanks C. J. Curtin for the fabric cross-section photographs, and J. W. Ballou, H. J. Kolb, H. F. Lauterbach, and D. W. Rahmes for substantial contributions to this work.

Literature Cited

1. Cassie, A. B. D., Physical Properties of Fibers and Textile Performance, *J. Textile Inst.* **37**, P154 (1946).
2. Herring, F. D., Warp Preparation and Weaving, *Textile Bull.* **77**, 77 (May 1951).
3. Hoffman, R. M., and Beste, L. F., Some Relations of Fiber Properties to Fabric Hand, TEXTILE RESEARCH JOURNAL **21**, 66 (1951).
4. Kober, P., Die Gewebedichte als Grundlage einer Gewebeordnung, *Melliand Textilber.* **32**, 513 (1951).
5. Peirce, F. T., Geometry of Cloth Structure, *J. Textile Inst.* **28**, T45 (1937).
6. Schwarz, E. R., "Textiles and the Microscope," 1st edition, New York, McGraw-Hill Book Company, 1934, pp. 2 and 243.
7. Schwarz, E. R., Certain Aspects of Yarn Structure, TEXTILE RESEARCH JOURNAL **21**, 125 (1951).

(Manuscript received October 19, 1951.)

Enzymic Degradation of Cellulose Fibers

Robert Blum and William H. Stahl

Pioneering Research Laboratories, U. S. Army Quartermaster Corps, Philadelphia, Pennsylvania

Introduction

It has long been known that when fungi degrade cotton, the tensile strength decreases at a rapid rate. Other properties (except a few noted under the microscope), however, change very little or not at all. Such observations have led to the conclusion that microbiological degradation of cotton is, to a very large extent, a localized process [3]. The fundamental question immediately follows: In which region or regions of the fiber does the destructive attack occur? An answer to this question would be of importance in clarifying the general problem of microbiological degradation of cotton, and would perhaps assist in finding better means of preventing or retarding such degradation. Accordingly, the work reported in this paper was undertaken in an attempt to supplement the existing knowledge in this field.

Much of the work published on this subject had been carried out with the living microorganisms acting on the cotton. In the experiments described below, the effects of a *cell-free extracellular cellulolytic enzyme solution* on the properties of cotton fiber and on two synthetic cellulose filaments were studied. A few comparative observations were also made on *fungus-degraded* cotton.

Experimental

Materials

A cell-free extracellular cellulase solution was prepared by the method of Saunders, Siu, and Genest [17] from the fungus *Myrothecium verrucaria* (QM 460), except that the following nutrient salt solution was used: NH_4NO_3, 3.00 g.; $MgSO_4 \cdot 7H_2O$, 2.22 g.; KH_2PO_4, 2.59 g.; K_2HPO_4, 2.21 g.; H_2O, 1l. The enzyme filtrate was preserved under toluene.

Cotton fibers in the form of sliver were purified by extracting with ethyl alcohol in a Soxhlet extractor for 8 hrs., and then with ethyl ether for 2 hrs. After drying at 50°C the fibers were refluxed in 1% sodium hydroxide under nitrogen for 7 hrs., and washed free of caustic with tap water, dilute hydrochloric acid, and distilled water. The material was finally dried at 50°C overnight.

Viscose rayon strands * known as "regular bright" and *cuprammonium (Bemberg) rayon* * known as "Grade No. 1" were extracted with alcohol and ether and dried at room temperature.

Specimens of fungal-degraded cotton duck, which were incubated for 14 days with *Alternaria* sp., *Fusarium diversisporum, Cladosporium herbarum, Curvularia lunata, Epicoccum* sp., or *Chaetomium globosum,*† were studied. These specimens had lost from 79%–92% of their original breaking strength.

Methods

Preparation of Samples.—Accurately weighed samples of each of the three materials (approximately 8 g. of cotton, 15 g. of viscose rayon, and 7 g. of Bemberg rayon) were incubated in closed flasks with 500 ml. of the enzyme solution at 40°C for varying time periods. A parallel series of samples as controls were incubated with the basic salt solution alone. At the end of each incubation period the samples were washed by decantation with about 15 portions of distilled water and partially dried at 50°C. Drying was completed in a vacuum oven at 50°C. A third series of flasks containing enzyme alone was allowed to remain at 40°C for varying time periods in order to estimate the rate of loss of enzyme activity.

In an early exploratory experiment, cotton samples were prepared as described above, except that they were incubated at 23°C for 27 days.

Before decantation, tests were made for bacterial and fungal contamination by inoculating tubes of peptone agar and potato dextrose agar with the solutions. The results were all negative.

Chemical and Physical Procedures.—The 1,4-β-polyglucosidase activity, reducing power, and pH of the enzyme solutions were determined before and after incubation. Activity was evaluated by measuring the change in the reducing power of hydroxyethyl cellulose (HEC). With but minor modifications, the method is that described by Reese, Siu, and Levinson [15] for determining *"C_x"* activity. The reducing powers of the solutions after digestion of the fiber samples were determined by Sumner's procedure [21]. pH was measured directly with a glass electrode.

Immediately after drying, the fiber samples were reweighed in order to determine the loss of weight as a result of degradation. Changes in load-elongation properties, degree of polymerization, and degree of crystallinity were determined. Comparative microscopic observations were also made.

Load-elongation properties were determined with the Sookne-Harris single-fiber tester [19]. For cotton, the gage length was 1.3 cm. and the rate of elongation was 0.033 in. per min. For viscose rayon, the gage length was 4.3 cm. and the rate of elongation 0.2 in. per min. All samples was conditioned at 70°F and 65% relative humidity for a minimum of 3 days before testing. Because the Bemberg rayon lost almost all of its strength very rapidly, it was not possible to separate filament samples for load-elongation determinations.

Degree of polymerization (D.P.) was determined by the cupriethylenediamine hydroxide (cuprien) viscosity procedure described in A.S.T.M. Designation D 539–40T, and as developed by Conrad and Tripp [6, 7]. Specific viscosity, η_{sp}, was converted to intrinsic viscosity, $[\eta]$, by the equation of Tripp and Conrad [22]: $[\eta] = a\eta_{sp}{}^{b} - c$. For a concentration of 0.50 g./ml., $a = 1.70$, $b = 0.694$, $c = 0.160$; for a concentration of 0.25 g./ml., $a = 3.27$, $b = 0.786$, $c = 0.137$. Degree of polymerization was calculated using Staudinger's equation, D.P. $= K[\eta]$, with K taken as 190.

Changes in degree of crystallinity (D.C.) of enzyme-degraded fibers were determined from x-ray diffraction intensity tracings.* The ground samples were pressed into thin discs (approximately 0.8 mm.) to give essentially random distribution of the particle axis, thus eliminating the effect of orientation from the tracings. Diffraction intensities in the equatorial radial direction were recorded with the aid of the x-ray spectrometer and recorder. Similar traces were made in each case from a quartz surface, which served the purpose of calibration.

Microscopic Methods.—The samples were prepared for microscopic investigation in various ways. Most of the observations were made on fibers swollen in cuprien solution. This reagent, because of its greater stability, was found superior to cuprammonium hydroxide. By varying the strength of the solution, the rate and degree of swelling could be

* These materials were kindly supplied by the American Viscose Corporation and American Bemberg Corp., respectively.

† These specimens were kindly supplied by Dr. E. T. Reese of the Mycology Section of the Pioneering Research Laboratories.

* The x-ray diagrams were kindly prepared and interpreted by Dr. C. M. Conrad of the Southern Regional Research Laboratory, U. S. Dept. of Agriculture.

easily controlled and the specimens could be observed throughout the entire swelling process.

Specimens were cut into short lengths and dispersed in a drop of water on a slide. The water was then removed with absorbent paper and cuprien added either before covering with a glass slip or by irrigation after covering. By comparative observations with whole cotton fibers, it was found that cutting did not alter the characteristics of the swollen fibers. Cuprien solutions were prepared by diluting the solution used for viscosity determinations (2 parts ethylene diamine to 1 part copper, being 1*M* in copper). Dilutions of from 2 to 4 parts of cuprien to 20 parts of water by volume were found useful. Cotton specimens were also examined after swelling in sodium hydroxide and staining with Congo red according to the procedure of Clegg [5].

Photographs * were taken of cross sections of viscose rayon samples which had been differentially stained by the technique of Morehead and Sisson [13] to show the skin and the core. Electron photomicrographs of surface replicas of the viscose rayon were also made.

Results

Enzyme Activity

It has been postulated that more than one specific enzyme is involved in the degradation of cellulose. Pringsheim suggested [14] that one enzyme breaks the long-chain cellulose molecules to short chains (cellobiose), and another enzyme then hydrolyzes cellobiose to glucose. Reese and coworkers [12, 15] presented evidence that at least two enzymes, C_1 and C_x, are involved in the breakdown of cellulose to cellobiose, with cellobiase hydrolyzing the latter compound to glucose. Hydrolysis of cellobiose may occur within the organism or extracellularly. In view of these considerations, it is possible that the measured activity against hydroxyethylcellulose is not a complete measure of the ability of the enzyme to degrade cellulose in the solid state. However, it is undoubtedly a good measure of the effective concentration of an important component of the cellulase system. The enzyme referred to in this paper is defined specifically by the method of preparation as described above, and its activity by the method of measurement.

The results of the activity determinations are summarized in Figure 1. For the enzyme solution alone: at 5°C (storage temperature) there was no measurable loss in activity; at 23°C there was a gradual loss of activity with time; at 40°C the rate of loss of activity was greater. In the presence of cotton at 40°C the enzyme solution lost activity at about the same rate as the solution alone. Thus, the presence of cotton fiber appears to have had no significant effect on the activity of the enzyme solution. Loss in activity in this case, therefore, was very probably a temperature-time deactivation effect only. The activity curve for viscose rayon suggests the possibility that in the presence of this filament the enzyme lost activity at a slightly more rapid rate than did the enzyme alone. The deviations in the experimental data do not permit a rigid conclusion on this point. In contrast, the enzyme solution in the presence of Bemberg rayon lost activity very rapidly. This loss could not have been a temperature-time effect alone.

pH

Measurements of the original enzyme solution and of the solutions after incubation gave a pH of 6.0 $\pm$ 0.1 in all cases.

Loss of Weight

Loss-of-weight measurements (Figure 2) showed a very low rate of loss for cotton (approximately 1% in 61 days), a somewhat faster rate for viscose rayon (2.1% in 39 days), and a very rapid rate (decreasing with time) for Bemberg rayon.

The loss of weight as calculated from the increase in reducing power of the solution gave consistently lower results than the direct measurements. Calculation of weight loss was based on the assumption that the portion of the cellulose which had been solubilized was changed completely to glucose. If the assumption were not true (*i.e.*, breakdown were not completely to glucose), the calculated weight loss would be less than the directly measured loss. It is indicated, therefore, that at least a certain portion of the soluble breakdown products was larger than glucose in size.

Degree of Polymerization

The degree of polymerization data are depicted graphically in Figure 3. The cotton and viscose rayon residues showed no significant change in D.P.

* These photographs (Figures 11 to 14 inclusive) were taken by Dr. F. F. Morehead of the American Viscose Corporation. They were kindly released for publication by that company.

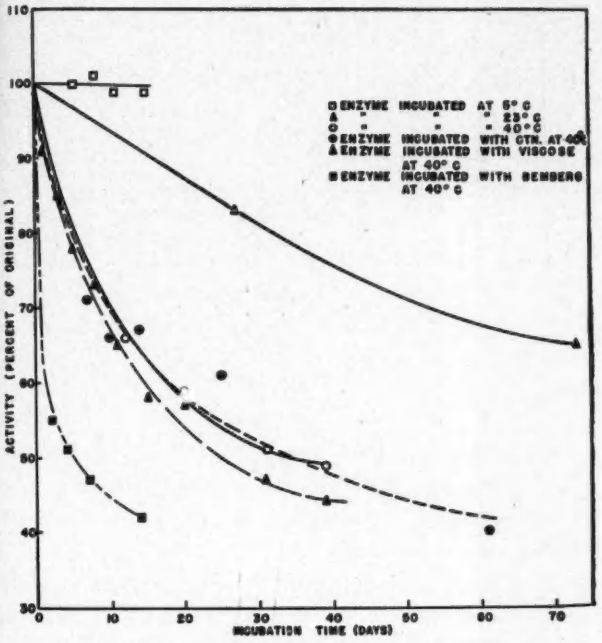
ACTIVITY (PERCENT OF ORIGINAL)
INCUBATION TIME (DAYS)
ENZYME INCUBATED AT 5° C
" " " 23° C
" " " 40° C
ENZYME INCUBATED WITH CTN. AT 40°
ENZYME INCUBATED WITH VISCOSE AT 40° C
ENZYME INCUBATED WITH BEMBERG AT 40° C

FIG. 1. *Change in activity of enzyme solution with incubation time.*

The small deviations are probably within the experimental error. Bemberg rayon, however, dropped very rapidly from a D.P. of 545 to a value of 141 in 3 days. Further changes with incubation time were insignificant.

Degree of Crystallinity

Interpretation of the x-ray data by Conrad indicated no essential changes in the degree of crystallinity of cotton digested for 3 and 61 days, as compared to the original cotton. There appeared to be a slight increase in crystalline diffraction over the control for viscose rayon digested for 11 and 39 days. Bemberg rayon samples which were digested for 2, 7, and 14 days showed a definite increase in crystalline diffraction over the control, but little or no differences in diffraction among the degraded samples.

Load-Elongation

The relationship between the loss of breaking strength (here defined as the load in grams at the break) and the elongation at break with incubation time is given in Figure 4. The control samples (incubated in salt solution alone) showed no significant deviation from the original samples and are therefore not included in the figure. The breaking-

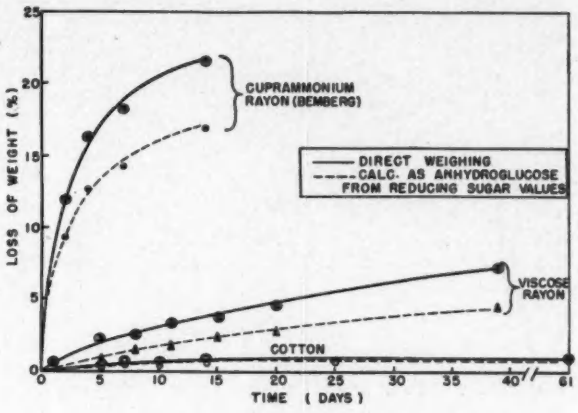

FIG. 2. *Loss of weight of cellulose fibers with incubation time.*

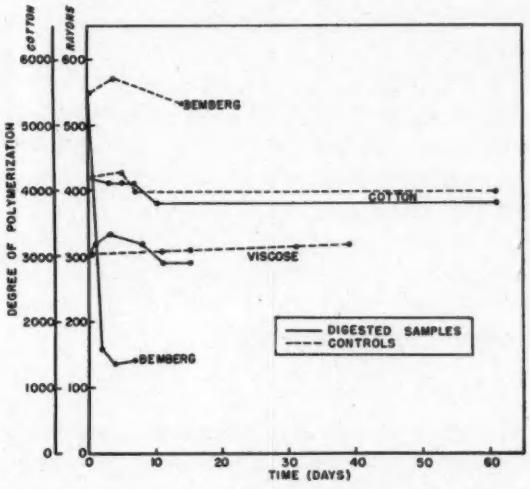

FIG. 3. *Change in degree of polymerization of cellulose fibers with incubation time.*

strength and elongation curves are similar, varying somewhat in magnitude. It appears, therefore, that enzymatic degradation affects these two properties in the same manner. For both viscose rayon and cotton, degradation (as measured by changes in these properties) proceeded at a very rapid and approximately equal rate during the first 3 days. Degradation of viscose rayon continued thereafter, but at a decreasing rate. Cotton in the presence of the enzyme solution at 40°C reached a maximum degradation of approximately 34% loss in breaking strength in about 3 to 5 days. At 23°C the extent to degradation of cotton (49% loss in breaking strength) was higher than at 40°C.

After 2 days of incubation with the enzyme solution, Bemberg rayon had apparently lost almost all

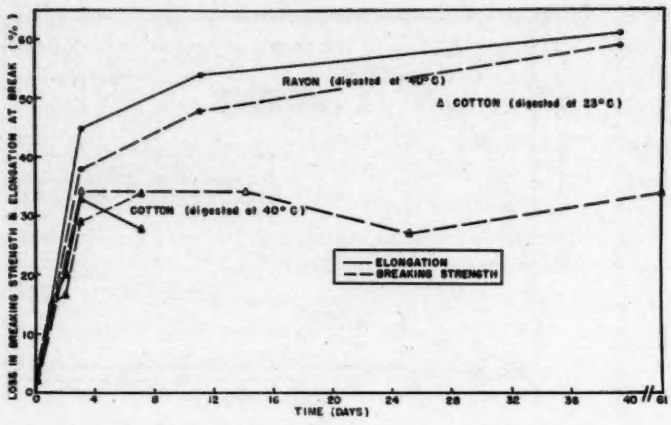

FIG. 4. *Change in tensile properties of cellulose fibers with incubation time.*

of its breaking strength. Only a very slight pull was required to break a strand of 74 filaments. They also crumbled readily under slight pressure.

Dye Absorption

When the fiber samples were prepared for microscopic observation by the Clegg procedure [5], it was noticed that degraded cotton and viscose were stained a much deeper red than the original materials. Both the degraded and undegraded Bemberg rayon stained very deeply and to approximately the same degree. The stained, degraded Bemberg samples had a slightly brown tinge.

Microscopic Observations

The observations of cotton fibers noted below are illustrated in essentials in Figures 5–10 inclusive.

The purified cotton as well as the salt control samples (Figure 5) swelled in cuprien in a manner reported many times in the literature (*e.g.,* Hock [10]). The spiral winding (the first layer of the secondary wall) was prominent, and appeared to restrict expansion generally over the entire fiber and also locally to cause ballooning. The type of ballooning caused by the formation of a narrow collar around the fiber by the primary wall or cuticle was observed, but was not very extensive as compared with unpurified fibers.

The enzyme-degraded samples differed in several respects from the original fibers. The spiral windings were not as prominent, and tended to disappear entirely in the more severely degraded samples (Figures 5–8 inclusive). In the early stages of degradation, expansion was still somewhat restricted but to a much lesser degree than in the original specimens (Figures 5 and 6). The fibers swelled much more evenly, mushrooming was less prominent, and ballooning appeared to only a very limited extent. In later stages, evidence of restriction to expansion disappeared completely.

The most striking result of degradation was the appearance of one or two prominent spiral lines which appeared as spiral fissures as swelling proceeded to its limit (Figures 6, 7, and 8). In the early stages of degradation (as measured by breaking-strength loss) faint lines began to appear which in a few instances could definitely be identified as fissures. They usually appeared as two distinct lines running parallel and close to each other in the highly swollen fibers. Close examination suggested that these parallel lines were simply the edges of a single fissure. In some cases the parallel lines appeared to be two distinct fissures. As degradation proceeded, the fissures became deeper and increased in extent (Figures 7 and 8). In highly degraded fibers (49% loss in breaking strength) the fissures in some cases extended to the lumen, and the fiber on swelling opened into a ribbon similar to an untwisted drinking straw (Figures 8 and 10). The fissures extended the entire length of all the fiber sections. Also in the highly degraded specimens shallower secondary notches could be seen on the surface of the fibers (Figure 7). These notches are very probably the same as those observed by Greathouse [9] in cotton fibers degraded by the fungus *M. verrucaria.*

Whenever both the spiral structure (winding) of the fiber and the spiral fissures could be observed (in the early stages of degradation) in a portion of a fiber, it was noted that the fissures and the spiral structure wound in opposite directions (*e.g.,* Z cuts appeared with S spirals). Then, too, it seemed that

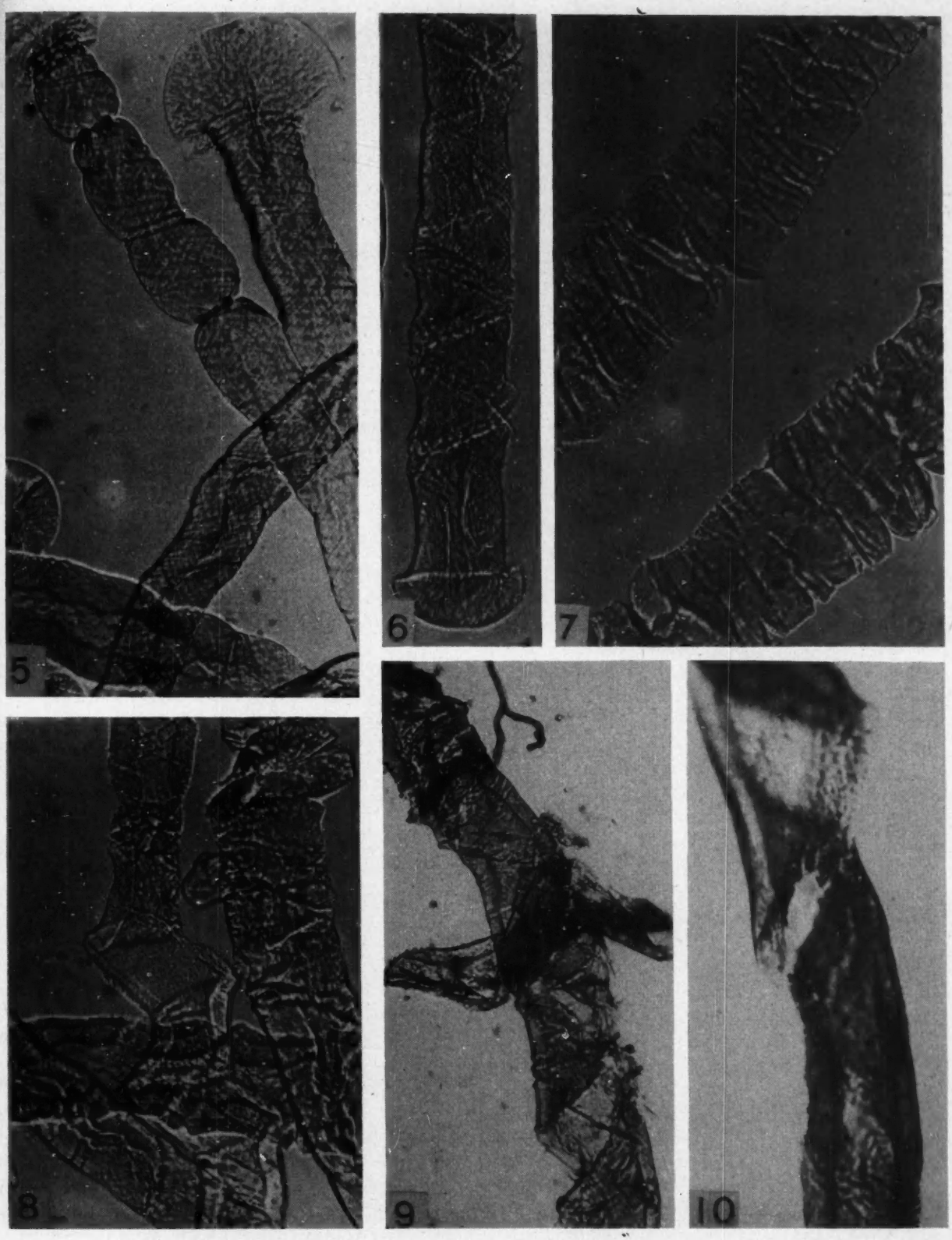

FIG. 5. *Cotton fiber swollen in cuprien after being incubated for 61 days in salt solution at 40°C.* FIG. 6. *Fibers swollen in cuprien after being incubated for 5 days in enzyme solution at 40°C.* FIGS. 7 and 8. *Fibers swollen in cuprien after being incubated in enzyme solution for 27 days at 23°C.* FIG. 9. *Fiber from cotton duck degraded by* Curvularia lunata, *swollen in 8% NaOH.* (*All of the above at 238 × magnification.*) FIG. 10. *Fiber prepared by the Clegg procedure after incubation in enzyme solution for 27 days at 23°C.* (*Magnification, 538 ×.*)

the spiral structure remained intact and passed over the fissures. It was also observed that the fissures would reverse their direction. Two types of reversals were found: either the fissure was continuous through the zone of reversal, or one fissure ended in the zone and another started alongside or shortly after the first. Anderson and Kerr [2] reported similar types of reversals of the first layer of the *secondary wall* in a histological study of normal cotton fiber. On any given portion of a fiber, one or two parallel fissures have been observed. More than two have not been noted.

All six samples of fungus-degraded duck which were examined were the same in appearance as the enzyme-degraded fibers. The above-noted visible evidence of damage varied in degree with the amount of growth in the neighborhood of the specimen. When growth was heavy, the specimens were similar in appearance to the fibers shown in Figures 7 and 8, except that the surface-notches were deeper and more extensive and there was a greater tendency to untwist into a ribbon along the spiral fissures. Figure 9 shows the spiral fissures and untwisting in a fiber degraded by *Curvularia lunata*. The secondary notches were not brought out by swelling in sodium hydroxide and therefore do not appear in this photograph. Most of the mycelial growth was on the outside of the fiber. In only a relatively few specimens was growth observed in the lumen.

Bright [4] demonstrated cracking of the cotton fibers as a result of fungal degradation. He did not mention the spiral nature of these cracks, although a photograph in his paper strongly suggests that they have a spiral form. Clegg [5] in a later paper noted splitting along "quick" spirals in some cases of damage by *fungi*. The spiral cracks or fissures appear very prominently in degraded cotton swollen in cuprien, but are rather obscure (even when the fibers are highly degraded) in fibers swollen in the reagents used by the above authors (compare Figures 7 and 10). It is perhaps for this reason that the spiral nature of the cracks received only cursory attention by them.

Optical studies revealed several notable differences between the original and the enzyme-treated viscose rayon.

Examination of cross sections showed that the undegraded filaments were stained by Congo red only very lightly in a shell around the fiber. The degraded specimens were stained heavily in the outer portion and chiefly on the high points of the ridges. Cross sections (Figure 12) of degraded viscose stained by Morehead's technique to bring out the skin showed regions (usually on the ridges) which were unstained. These unstained portions in some instances extended completely through the skin to the core. No such discontinuities were found in the undegraded fibers (Figure 11). Electron photomicrographs (Figures 13 and 14) of surface replicas showed an even appearance for the original fiber and a diffuse blotchy appearance for the surface of the degraded fiber. These observations indicated that the enzyme had caused irregular erosion of the surface of the fiber.

Swelling in cuprien showed further differences between degraded and undegraded samples (Figures 15–19 inclusive).

When *undegraded viscose* was treated with cuprien the filaments swelled evenly, approaching a cylindrical form, and the ridges tended to disappear. As swelling proceeded, a distinct transparent cylindrical sheath appeared around the filaments (Figure 15). When pressure was exerted this sheath broke into many long, fine fibrils (Figures 16 and 17). Under relatively high pressure, the main body of the filament tore longitudinally into coarse pieces, with no clearly defined structure (Figure 17).

On swelling in cuprien, the *enzyme-treated viscose* exhibited some characteristic differences from the original filaments: The sheath became less distinct and tended to disappear as the time of incubation increased. On crushing, the fibrils produced from the sheath became fewer and shorter and finally disappeared with the disappearance of the sheath. Also, as swelling proceeded, longitudinal spindle-shaped cracks appeared spontaneously in the degraded fibers (Figure 18). These cracks varied in extent and degree. Some specimens showed a few shallow cracks with varying lengths. Others split so extensively and deeply that the filament was broken generally into anastomosing fibrils varying greatly in diameter. There appeared to be a general tendency of the degraded filaments to break up into a network of fibrils. This tendency was especially noticeable on application of pressure. Under very light pressure the filaments broke into the network system described above (Figure 19). Under increased pressure there was a further breakdown into finer fibrils, and the fibrils tore transversely.

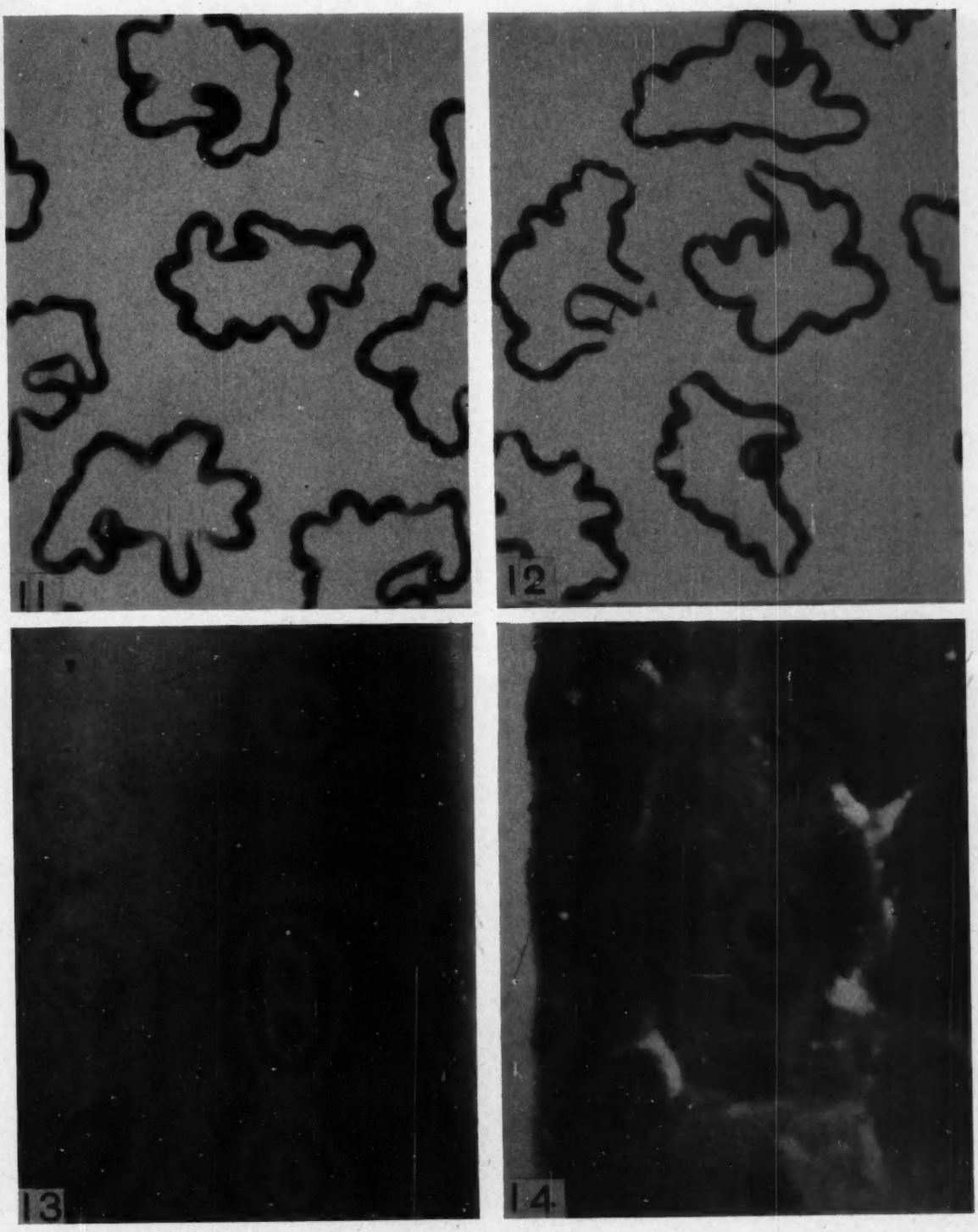

FIG. 11. *Cross sections of viscose rayon filaments incubated for 5 days at 40°C in salt solution and stained to show skin.* FIG. 12. *Same as Fig. 11, but incubated for 5 days at 40°C in enzyme solution. (Magnification, 1500 ×.)* FIG. 13. *Electron photomicrograph of surface replica of a portion of a viscose rayon filament that was incubated for 5 days at 40°C in salt solution.* FIG. 14. *Same as Fig. 13, but incubated 5 days at 40°C in enzyme solution. (Magnification, 25,000 ×.)*

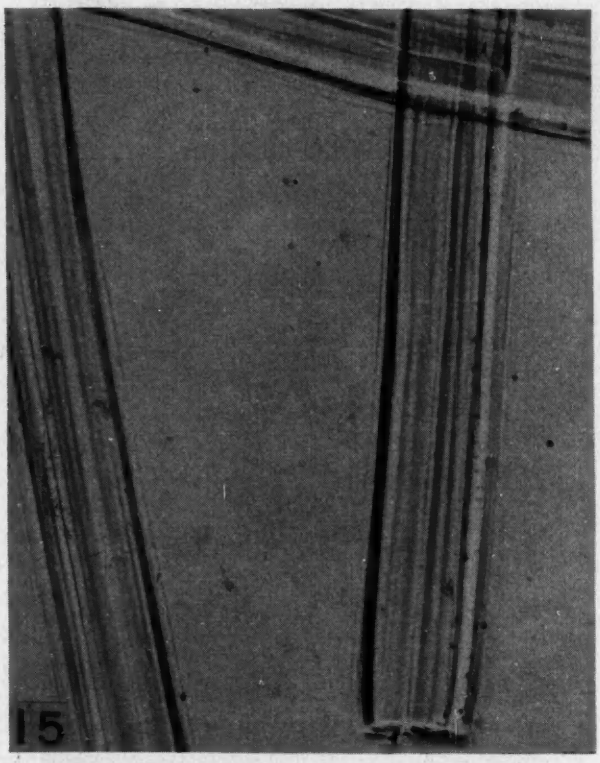

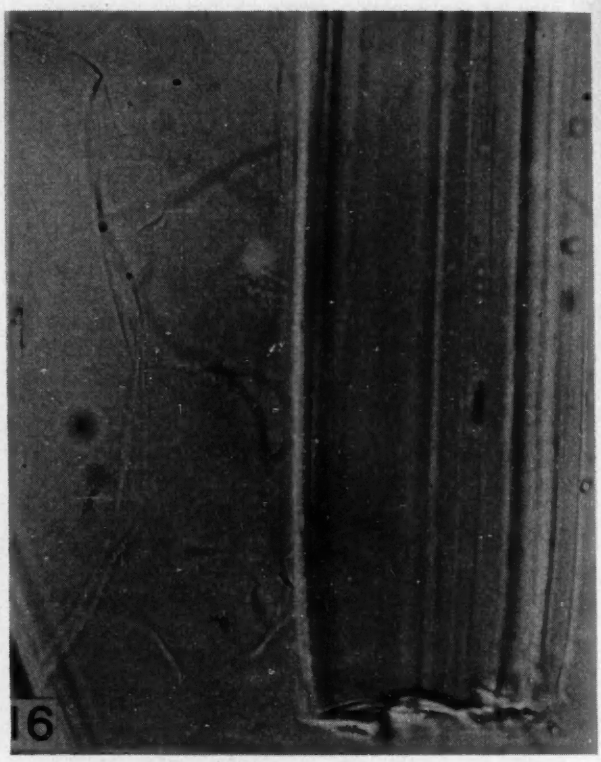

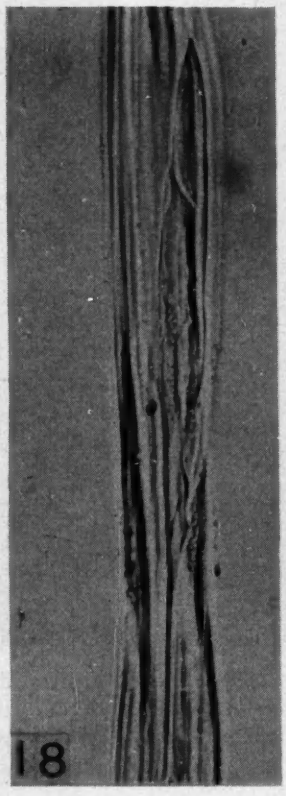

FIG. 15. *Viscose rayon filaments incubated in salt solution for 39 days at 40°C and swollen in cuprien. (Magnification, 240 ×.)* FIG. 16. *Same as Fig. 15, but very light pressure was applied after swelling. (Magnification, 510 ×.)* FIG. 17. *Same as Fig. 15, but heavy pressure was applied after swelling. (Magnification, 240 ×.)* FIG. 18. *Filaments incubated in enzyme solution for 39 days at 40°C and swollen in cuprien. (Magnification, 240 ×.) The spindle-shaped cracks appeared spontaneously as the filaments swelled.* FIG. 19. *Same as Fig. 18, but light pressure was applied. (Magnification, 240 ×.)*

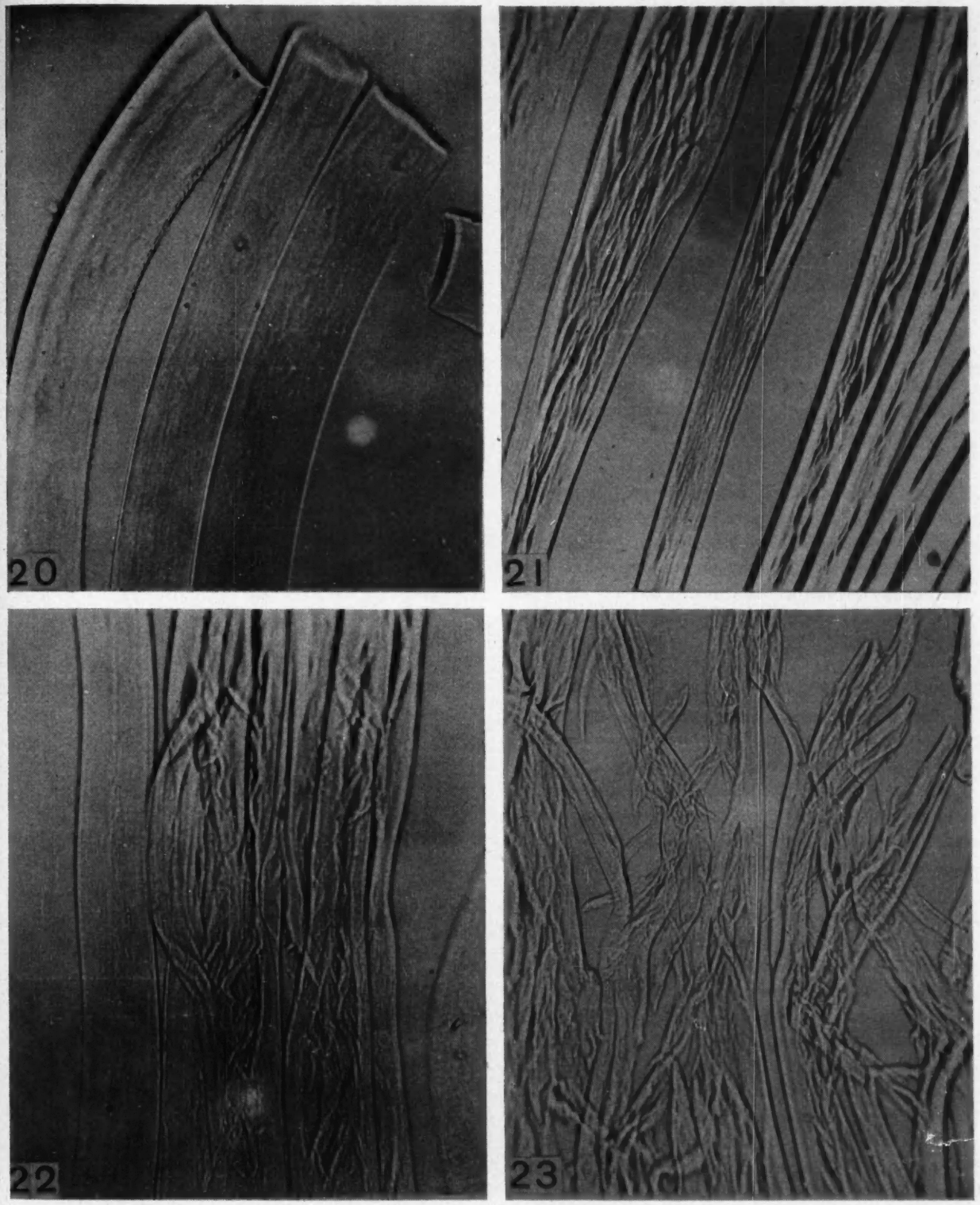

FIG. 20. *Original Bemberg rayon filaments swollen in cuprien.* FIG. 21. *Original filaments swollen in cuprien and subjected to heavy pressure after swelling.* FIG. 22. *Filaments incubated 14 days in enzyme solution at 40°C and swollen in cuprien. Very light pressure was applied.* FIG. 23. *Same as Fig. 22, except that moderate pressure was applied. (All of the above at 240 × magnification.)*

The appearance of the Bemberg rayon specimens is shown in Figures 20–23 inclusive.

Both the degraded and undegraded Bemberg rayon filaments swelled in a similar manner in cuprien (Figure 20). They expanded evenly, with a strong tendency to bend. In neither sample were cracks of any kind visible. A difference between the degraded and undegraded specimens became apparent when the filaments were put under pressure. On application of *relatively high* pressure, the *undegraded* filaments broke into a network of fine anastomosing fibrils (Figure 21) qualitatively similar to the network formed in degraded viscose. The *degraded* Bemberg rayon filament also broke into fibrils, but only a *very light* pressure was required to produce extensive splitting (Figure 22). Under heavier pressure the fibrils tore transversely (Figure 23).

Discussion

The experimental evidence suggests that degradation of the cellulose fibers by the enzyme solution was influenced to a very large extent by the nature of the fiber itself. Because of the differences in the characteristics of the three fibers studied, it is perhaps preferable to discuss the degradation of each separately.

Cotton

The breaking strength and elongation at the breaking point of the degraded cotton fiber decreased rapidly with time of incubation in the early stages. The loss in tensile properties may be the result of a surface degradation and a consequent removal of successive layers from the surface of the fiber, an attack within the fiber mass, or a combination of both processes.

That the surface of the fiber was degraded is indicated by several considerations. This process might, of course, be expected to occur (on any cellulose fiber) since the enzyme is in contact with the surface and the enzyme does degrade cellulose. Experimentally, the deeper staining of the enzyme-treated fibers with Congo red indicates stripping of the fiber surface. The Congo red test is commonly used to show surface damage to cotton fibers. Further evidences of surface degradation are the changes in swelling characteristics observed under the microscope. The visible spiral structure and the restrictions to swelling, presumably due to this structure, disappeared.

Although the surface of the fiber was undoubtedly stripped in the degradative process, it is very unlikely that this factor alone can be responsible for the large and rapid loss in breaking strength (approximately 30% in 3 days) in the early stages. The weight loss of the fiber during this time was at most less than 0.5%. Even if the entire change in weight were a result of loss from the fiber surface, the change in cross-sectional area would still be too small to account for the load-elongation change. The large loss in breaking strength can be ascribed to surface degradation only by assuming the highly improbable possibility that a great part of the tensile strength resides in a thin surface layer of the fiber. Therefore, internal degradation is a more probable factor.

Measurements of crystalline diffraction and degree of polymerization showed no significant changes in these properties and therefore gave no indication of internal degradation. The observation of spiral fissures is the only positive experimental evidence for internal degradation of cotton fibers. It appears, therefore, that in the early stages at least the degradative action of the enzyme was restricted to the fiber surface and to spiral planes of susceptibility within the fiber mass. Furthermore, it is reasonable to believe that the rapid loss in tensile properties was primarily a result of degradation along these planes. This postulate leads to the expectation that the rate of loss would remain high until the depth of degradation along the susceptible planes approached the lumen (at which time the fiber loses its distorted cylindrical form and becomes, in effect, a flat ribbon); the rate would then abruptly decrease to a magnitude reflecting any continuing degradation which may occur in less susceptible regions of the fiber. This expectation is in agreement with the fact that, under the experimental conditions, no further loss in tensile properties had been observed after 3–5 days of incubation.

The fact that the enzyme lost activity during the incubation period (see Figure 1) necessitates some modification of the above reasoning. In general, the velocity of a reaction catalyzed by an enzyme is a direct function of the enzyme activity (up to a limiting value). Therefore, if the enzyme had not lost activity during the incubation period, it would be expected that the rate of loss of tensile properties would not fall to zero, but would have some relatively small value reflecting continuing degradation. That this is likely is indicated by the observation

that cotton fibers incubated for 27 days at 20°C (at which temperature the rate of loss of enzyme activity is appreciably less than at 40°C) lost approximately 50% of their original breaking strength (Figure 4), while at 40°C over the same period of time the fibers lost an estimated (interpolated) 35% of their strength. Nevertheless, considering that loss of activity is a continuous function of time (Figure 1) at a given temperature, it is hardly likely that activity loss of itself would result in an abrupt decrease to zero of the rate of loss of tensile properties. Such an abrupt change must then be related to some fiber property. Therefore, one is again led to a postulate of regions of high and low susceptibility in the cotton fiber.

The postulated relationship between rapid tensile-properties loss and degradation along spiral lines of susceptibility is in accord also with the findings of Stanier [20] in his work with *Cytophaga hutchinsonii*. The degradative attack by this organism is apparently restricted to the cotton fiber surface. Stanier noted (and his photographs show) that swollen, degraded fibers are covered with spiral furrows. (These furrows, incidentally, are somewhat similar in appearance to the notches (Figure 7) observed in fibers highly degraded by the enzyme solution.) He did not describe, nor do his photographs indicate, the occurrence of internal spiral fissures. Furthermore, Stanier found that "Cotton fibers, even when heavily invested with *C. hutchinsonii*, retain to a considerable degree their original structural and tensile properties." Thus, it appears that in this case the degradative attack results in no production of spiral fissures and in only relatively small changes in tensile properties—an inverse manifestation of the suggested relationship between the two occurrences. Moreover, it should be noted that even though the surface is highly degraded, little of the tensile properties are lost. This observation provides evidence for the assumption made earlier that surface degradation alone cannot account for the large and rapid loss of tensile properties.

The discussion thus far has been concerned primarily with the effect of a *cell-free extracellular cellulase solution* on cotton fibers. Practically, the effect of the cellulose-degrading *organisms* themselves are of primary importance. The findings of other workers studying the effect of fungi, combined with a few observations made by the present authors, suggest that degradation of cotton by at least some fungi is fundamentally similar to degradation by the enzyme solution. Based on observations made by himself and many others, Greathouse [9] indicated that fungal degradation results in ". . . great loss in tensile strength with relatively small changes in chemical characteristics. . . ." Fleming and Thaysen [8], as well as many others, observed a decreased tendency of degraded fibers to balloon on swelling. Furthermore, as noted earlier, Clegg reported observing splitting along "quick" spirals in some cases of damage by fungi. The present authors have observed such splitting in *all* specimens degraded by six fungi. These effects caused by fungi are basically similar to the effects found to result from the action of the enzyme filtrates. Such a similarity is not surprising, since it is generally accepted that cellulolytic fungi elaborate an extracellular enzyme system which is primarily responsible for the degradation of cellulose.

It might be pointed out that because of the procedure for obtaining the enzyme filtrate used in these experiments, the filtrate undoubtedly is highly diluted and should therefore have a much lower cellulolytic activity than the enzyme system secreted directly on the fiber by the organisms. This condition perhaps accounts for the fact that while tensile-strength curves of fungal-degraded cotton given by Abrams [1] and Rogers, Wheeler, and Humfeld [16] show a definite decrease in loss rate well before this property is reduced to zero, it is neither as great in magnitude nor as abrupt as the change in rate of loss found for the enzyme-degraded cotton. The high enzyme concentration, then, would have the effect of increasing the rate of degradation in those regions of the fiber which are relatively resistant (as compared with the spiral planes of susceptibility) to enzyme action.

The spiral nature of the fissures and their reversals in direction naturally suggest a relationship to the spiral structure of the fiber. Anderson and Kerr [2] suggested that the spiral structures of the first few outer layers of the cotton fiber do not successively wind in the same direction, but that a template is soon established and thereafter successive internal layers all follow the same direction. Hock, Ramsey, and Harris [11] believe that the orientation of the fibrils immediately below the winding and of all subsequent layers are always in a direction opposite to that of the winding. Since the observed fissures in the degraded fibers have been

found to spiral in a direction opposite to that of the outer winding, it appears, in view of the findings of Hock *et al.*, that the fissures have the same direction of spiral as the internal layers of the fiber.

Viscose Rayon

Degradation of viscose rayon by the enzyme filtrate resulted in early rapid loss in tensile properties, an appreciable loss in weight, and extensive surface degradation. In this case surface degradation could conceivably account for an appreciable part of the tensile loss.

The relative ease with which the swollen, degraded filament was split into anastomasing fibrils suggests severe degradation between these fibrils. It is, therefore, not unreasonable to believe that interfibrillar degradation contributed in a large, if not major, measure to tensile-properties loss.

The negative results of the degree of polymerization and crystallinity measurements indicate that very little or no intrafibrillar degradation occurred.

The rather sharp decrease in the rate of tensile-properties loss again suggests that the degradative process resulting in such loss is a combination of two processes occurring at greatly different rates. The rapid rate process is perhaps degradation of the filament surface and of the interfibrillar cellulose. The slow rate process could be continuing degradation of the fibril surfaces.

Bemberg Rayon

Bemberg rayon incubated with the enzyme solution changed rapidly and radically in all measured properties within 3 days. Such changes clearly indicate that the degradative process in this material occurred rapidly throughout the entire filament mass. The ease with which the swollen, degraded filament was broken into fibrils suggests that the interfibrillar regions were degraded to a somewhat greater degree than were the intrafibrillar regions.

Of interest is the observed rapid abnormal loss of activity of the enzyme in contact with Bemberg rayon in contrast to the normal loss in the presence of cotton and viscose rayon. A few speculative thoughts on this subject are perhaps permissible. Such a loss may be a result of either inactivation or removal of the enzyme from solution by adsorption on the fiber surface. The former alternative does not appear very likely since no measurable abnormal activity loss was found in the presence of cotton and viscose rayon. The degree of adsorption would be a function of the surface area available to the enzyme. If adsorption is to account for the activity loss, then the results suggest that Bemberg rayon has a very much greater available surface area than does cotton or viscose rayon. Though both of the latter fibers have a fairly large external surface, it is apparently insufficient to absorb any measurable amount of enzyme. The large Bemberg surface area may be either external (the filament surface) or internal. The latter possibility is in accord with the observed very rapid change of tensile and other properties during the degradation process.

A concept of regions of high susceptibility was introduced, with no attempt made to define the nature of such regions. Some clarification of this concept is perhaps desirable. Regions of high susceptibility are identical with those regions which, on exposure of the fiber to the enzyme solution, showed a tendency to become weaker in the swollen state—*i.e.*, the observed spiral-fissure planes in cotton and the interfibrillar split planes in viscose and Bemberg rayons. Thus, the locations of these regions are defined experimentally; their nature, however, is not.

While the available factual information is insufficient at present to enable one to offer an incontestable explanation of such regions, two possibilities appear plausible:

The rate of degradation of a cellulose mass depends upon the number of active bonds (1-4-β-glucosidic linkages) accessible to the enzyme. Because of the large size of the enzyme molecule, it can be expected that not all of the internal bonds would be accessible, and that the number and location of the accessible bonds would be conditioned by the dimensions and distribution of the voids in the cellulose mass. The regions of high susceptibility then would be those regions containing spaces of such dimensions as to allow the enzyme to penetrate readily.

Localized variations in density related to the relative amounts and distribution of amorphous and crystalline cellulose may reasonably be expected to play an important role in determining the paths of rapid degradation. Many workers [18] have demonstrated that amorphous cellulose is degraded much more rapidly by enzyme than is an equal mass of crystalline cellulose. Furthermore, low-density

amorphous regions contain fewer linkages per unit volume than do the high-density crystalline regions. It follows, then, that the enzyme molecules can degrade the cellulose in a given volume more rapidly in amorphous regions than in crystalline regions. Therefore, if the distribution were such as to form lines of successive amorphous regions, paths of low density (and therefore high susceptibility) would result.

Accessibility and density have been presented separately as possible explanations for the observed regions of high susceptibility. They are not, however, mutually exclusive. It is conceivable that both are factors and that the relative importance of each is dependent upon the characteristics of the cellulose mass under consideration.

Summary

The early stage of degradation of cotton fiber by a cell-free enzyme solution prepared from a cellulolytic fungus was strongly characterized by a rapid loss of tensile strength. Neither at this stage nor at any later stages were there detectable changes in degree of polymerization or crystallinity. Microscopic observation of the swollen fibers revealed a gradual disappearance of the normal outer spiral winding and the appearance of spiral fissures which became more extensive and deeper with increasing incubation time.

The initial rapid loss of tensile properties is attributed to rapid degradation along spiral planes and a further slow loss to continuing attack on the exposed surfaces, resulting in general erosion and localized notching. Fungal degradation appears to occur in essentially the same manner as degradation by the enzyme solution.

Changes in the measured properties of enzyme-degraded viscose rayon were qualitatively similar to the changes of degraded cotton. Microscopic evidence suggested that rapid loss of tensile properties was caused by surface and interfibrillar degradation by the enzyme. Further slow loss in tensile properties may be ascribed to continued attack of the accessible external and interfibrillar surfaces.

Bemberg rayon was very rapidly and extensively degraded by the enzyme solution. Within 3 days the tensile properties dropped to negligible values, degree of polymerization decreased to approximately 30% of that of the original material, and the degree of crystallinity increased. During the course of degradation the rate of weight loss was very high initially and then decreased rapidly when 20%–25% of the cellulose had been solubilized. The relative ease with which the swollen, degraded filaments were broken into fibrils indicated that the degree of degradation was greater between than within the fibrils.

Acknowledgment

The authors wish to express their gratitude to Drs. R. G. H. Siu, G. R. Mandels, and E. T. Reese of the Pioneering Research Laboratories, and Drs. W. A. Sisson and O. A. Battista of American Viscose Corporation for their many helpful discussions and criticisms of the data obtained. Sincere thanks are offered to Mr. A. S. Wrigley of the Microscopy Section of the Pioneering Research Laboratories for the many photomicrographs, Mr. B. McQue of the Analytical Section for the fluidity determinations, and Mr. G. Winston of the Textile Laboratories for the statistical analysis of the tensile-properties data.

Literature Cited

1. Abrams, E., TEXTILE RESEARCH JOURNAL **20**, 71 (1950).
2. Anderson, D. B., and Kerr, T., *Ind. Eng. Chem.* **30**, 48 (1938).
3. Barghoorn, E. S., Textile Series Report No. 24, Microbiological Series No. 4, Office of The Quartermaster General, June 1946.
4. Bright, T. B., *J. Textile Inst.* **17**, T396 (1926).
5. Clegg, G. C., *J. Textile Inst.* **31**, T49 (1940).
6. Conrad, C. M., *Ind. Eng. Chem., Anal. Ed.* **13**, 526 (1941).
7. Conrad, C. M., and Tripp, V. W., TEXTILE RESEARCH JOURNAL **16**, 275 (1946).
8. Fleming, N., and Thaysen, A. C., *Biochem. J.* **15**, 407 (1921).
9. Greathouse, G. A., TEXTILE RESEARCH JOURNAL **20**, 227 (1950).
10. Hock, C. W., TEXTILE RESEARCH JOURNAL **20**, 141 (1950).
11. Hock, C. W., Ramsay, R. C., and Harris, M., TEXTILE RESEARCH JOURNAL **11**, 200 (1941).
12. Levinson, H. S., Mandels, G. R., and Reese, E. T., *Arch. Biochem. Biophys.* **31**, 351 (1951).
13. Morehead, F. F., and Sisson, W. A., TEXTILE RESEARCH JOURNAL **15**, 443 (1945).
14. Pringsheim, H., *Z. physiol. Chem.* **78**, 266 (1912).
15. Reese, E. T., Siu, R. G. H., and Levinson, H. S., *J. Bact.* **59**, 485 (1950).
16. Rogers, R. E., Wheeler, H. G., and Humfeld, H., *U. S. Dept. Agr., Tech. Bull.* 726 (1940).
17. Saunders, P. R., Siu, R. G. H., and Genest, R. N., *J. Biol. Chem.* **174**, 687 (1948).

18. Siu, R. G. H., "Microbiological Decomposition of Cellulose," New York, Reinhold Publishing Corp., 1951, p. 366.
19. Sookne, A., in "A.S.T.M. Standards" (Textile Materials), Philadelphia, 1948, p. 498.
20. Stanier, R. Y., *Bact. Rev.* **6**, 143 (1942).
21. Sumner, J. B., and Somers, G. F., "Laboratory Experiments in Biological Chemistry," New York, Academic Press, 1944.
22. Tripp, V. W., and Conrad, C. M., Personal communication.

(Manuscript received December 14, 1951.)

A Method of Repetitive Longitudinal Sectioning of Cords and Fabrics for Microscopic Examination*

S. Jack Davis†

Research Division, Callaway Mills Company, LaGrange, Georgia

Abstract

A new device and technique for making repetitive longitudinal microscopic sections of discrete and predetermined thickness from cords and fabrics is presented. The device provides for mounting fabric, which is embedded in resin, and elevating it by calibrated increments to a selected distance above the level of a cutting surface which guides a razor blade in cutting a section for microscopic examination. The technique involved is simple and rapid and should be acquired easily by those who are familar with the Hardy method of cross-sectioning fibers.

Examples illustrating the possibilities of such a technique in determining cover factor at various levels in fabrics, of determining the degree and character of penetration of various additives, and of the mechanism of particle retention in fabric filtration are given.

CORDS AND FABRICS have usually been considered in their macroscopic characteristics, cords being treated as flexible cylinders and fabrics as continuous planes of uniform thickness, equivalent to the gage. Although such concepts are often adequate in view of the simplifying assumptions necessary for an idealized geometrical analysis of such structures, the logical conclusions from such postulations all too often have been examined only by macroscopic means, where the results may be but the integral of possibly contradictory localized effects, or, in other words, may be only statistical in nature.

In the course of a fundamental study of filtration through fabrics, it was of interest to examine microscopic segments throughout the thickness of the fabric for an understanding of the mechanism of particle retention. The apparatus and method reported herein were developed for this purpose, and served to establish tangibly the locus of filtered particles.

Simple and rapid methods have been available for obtaining cross sections of textile fibers for microscopic examination as the result of the work of Hardy [4] and others [2, 5, 6, 7]. Bailey [1] described a method of sectioning cords and fabrics longitudinally, using a razor blade and cutting the sections manually while viewing the sample under the stereoscopic microscope.

Bailey's method is tedious and does not afford reliable repetitive sectioning of cords or fabric segments. For the present work it was imperative that

* Paper presented before The Fiber Society, Washington, D. C., Sept. 14, 1950.

† Present address: Chemstrand Corp., Decatur, Ala.

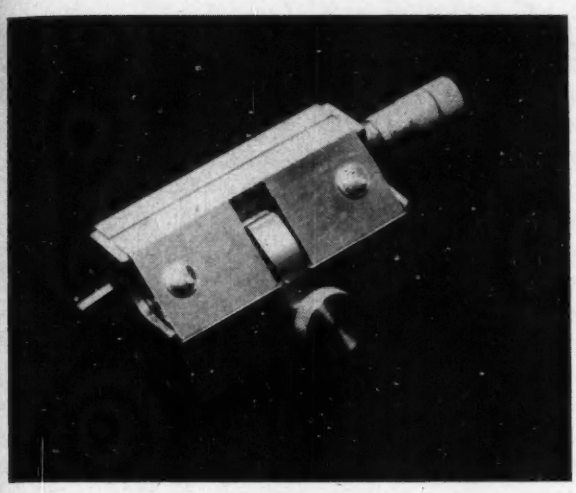

FIG. 1. *Longitudinal-sectioning device shown assembled (½ actual size).*

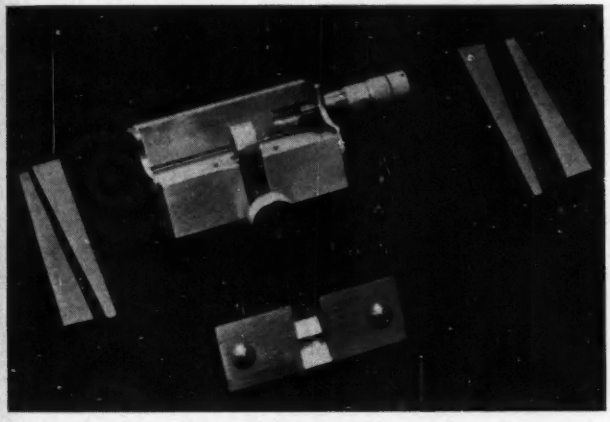

FIG. 2. *Longitudinal-sectioning device shown disassembled.*

a simple and rapid method which could be handled by any laboratory technician should supplant the intricate method of the artisan.

Apparatus and Method

The longitudinal-sectioning device* which was developed in this laboratory for the purpose of making repetitive longitudinal sections of discrete and predetermined thickness from cord or fabric has been described in detail in a patent [3].

Figure 1 shows the device assembled; Figure 2 shows it disassembled. The upper surface of the removable section of the apparatus (shown at bottom of Figure 2) is ground to the exact plane of the ground upper surface of the main block. When the removable section is clamped in position a space is formed between the section and the main body of the instrument. Within this slot is a movable spacer plate, the upper edge of which is ground to form a surface which is exactly parallel to the two upper surfaces described above.

The spacer plate is comprised of two inclined-plane wedges, the lower of which may be moved horizontally by the micrometer propelling screw shown by the knurled knob on the right. By turning the micrometer control, the horizontal movement of the lower wedge results in a vertical thrust on the upper member of the wedge assembly, which is minimized by the inclined-plane structure and permits of very small definite increments of movement in the vertical direction of the upper wedge. The upper surface of the spacer plate is knurled in order to facilitate the adhesion of the cord or fabric which is to be sectioned.

A cord or fabric section is repeatedly immersed in a resin solution (or emulsion) until the sample is completely embedded in resin. For the greater part of the work conducted in this laboratory, a commercially available nitrocellulose lacquer* was employed which is quite satisfactory for practically all samples where the cord or fabric additives are not soluble in an organic solvent. In cases where a solvent-soluble impregnant is to be examined, formulations of gum arabic, glycerol, and formaldehyde in aqueous solution may be used, although the sensitivity of such formulations to humidity is an inconvenience.

After the sample is properly embedded in resin and cut by scissors to approximately the width of the slot, it is then adhesively affixed to the spacer bar in the slot of the instrument, usually by the use of the same resin solution used for embedding. Ordinary care is required to be sure that the sample is properly situated in planar fashion on this spacer bar.

The spacer bar with the sample attached is lowered in the slot where the lower spacer bar has been shifted entirely to the (right) side after reverse turning of the micrometer control. The sample thus rests below the cutting edges of the device. The entire device may then be mounted on the stage of the stereoscopic microscope, where the sample may be

* The Callatome (trademark registration applied for) may be obtained from R. H. Bouligny Company, P. O. Box 2115, Charlotte, N. C.

* Neg-O-Lac, manufactured by the Photo-Chemical Laboratories, Washington, D. C. This preparation was recommended to the author by Mr. T. L. W. Bailey.

FIG. 3. *Cutting operation.*

raised by rotating the micrometer until the resin surface appears at about the same plane as the plane of the cutting surfaces. A short cut is then made, using the razor blade with a diagonal stroke, to remove the upper level of the resin surface. The sample is raised again through a short distance, and the sectioning of the resin film is repeated. This is continued until it is observed through the microscope that the upper surface of the fabric is just at the level of the cutting surface of the device.

At this point, the sample is raised above the level of the cutting surfaces a predetermined distance, which is known by calibration of the micrometer control. The average thickness of sample cut on the device, using the proper technique, is of the order of 5 μ to 10 μ. The device may then be removed from the stage, and a light coating of embedding resin is brushed on the projecting "stub" of fabric, which, after drying, forms a film on and between the cutting surfaces containing the fabric "stub." The device may be returned to the stage of the stereoscopic microscope, where the technician may cut the film containing the fabric projection with one or more diagonal strokes of the razor blade, the direction of which is defined by the cutting surfaces. It is not necessary to cut the specimen under the steroscopic microscope, however; Figure 3 shows the cutting operation in process without using the microscope.

The film containing the cord or fabric section is removed from the razor blade, and is transferred to the microscope slide and processed by the usual techniques. The entire method described above is, of course, similar to the Hardy technique for obtaining fiber cross sections, and may be acquired easily by those who are familar with the Hardy method.

Results

Illustrations of the results, which may be obtained with comparative ease, are presented here in several series of photographs. Each series represents selected views of sections from a specific locality of the fabric; the sections vary only in their distance from the fabric surfaces.

Since the specimen mounted in the sectioning device, or a section cut from it, is very large in area when compared to the field of a high-power microscope, it is necessary to establish reference points in order to assure viewing exactly the same field. How-

FIG. 4 (left) *and* FIGS. 5–8 (opposite page). *Views of selected planes through the thickness of a vacuum-cleaner filter-bag fabric (magnification, approximately 50 ×).*

FIG. 6

FIG. 5

FIG. 9

FIG. 12

FIG. 10

FIG. 13

FIGS. 9–13. *Views of selected planes through the thickness of a vinyl-coated drill fabric (magnification, approximately 33 ×).*

FIG. 11

ever, the photomicrographs presented herein were prepared for illustrative purposes only, and no effort was made to assure that a single microscopic field was involved in each series.

Furthermore, it would have been unduly wasteful of effort, materials, and space to present *each successive microscopic section* actually cut in the illustrations of this paper. Consequently, only selected views are presented for each series.

Repetitive Longitudinal Sections of Cords

No serious study involving longitudinal sections of cords has been made in this laboratory, although

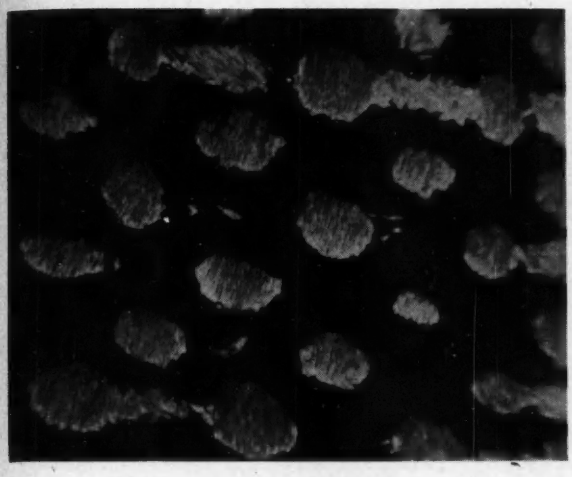

FIG. 14

FIG. 15

FIG. 16

FIG. 17

FIGS. 14–17. *Views of selected planes through the thickness of a vinyl-coated sheeting fabric (magnification, approximately 33 ×).*

one series of sections similar to that reported by Bailey [1] has been made for illustrative purposes.

Repetitive Longitudinal Sections of Vacuum-Cleaner Filter-Bag Fabric

Figures 4–8, inclusive, constitute a series of views through the thickness of an ordinary vacuum-cleaner filter-bag fabric in one location. The fabric had been soiled in regular use before the sample was taken. The dirt particles are evident in Figure 4, which is the second plane cut, and in Figure 5, which is the fourth plane. Figure 6, showing the sixth plane, is approximately at the center of the fabric; there is little evidence of soil at this point, and the cover factor is large. Figure 7 shows the eighth plane of the vacuum-cleaner bag fabric, and corresponds roughly, in opposite position, to the plane shown in Figure 5. On this opposite side of the fabric, however, there is no evidence of dirt-particle accumulation. Figure 8 is the tenth plane, which is approximately the opposite edge of the fabric. No dirt particles are evident, and the cover factor has diminished markedly.

This series of figures illustrates the geometrical relationship of fibers in several locations through the fabric thickness, and also illustrates the manner in which foreign particles are retained in air filtration.

FIG. 18

FIG. 19

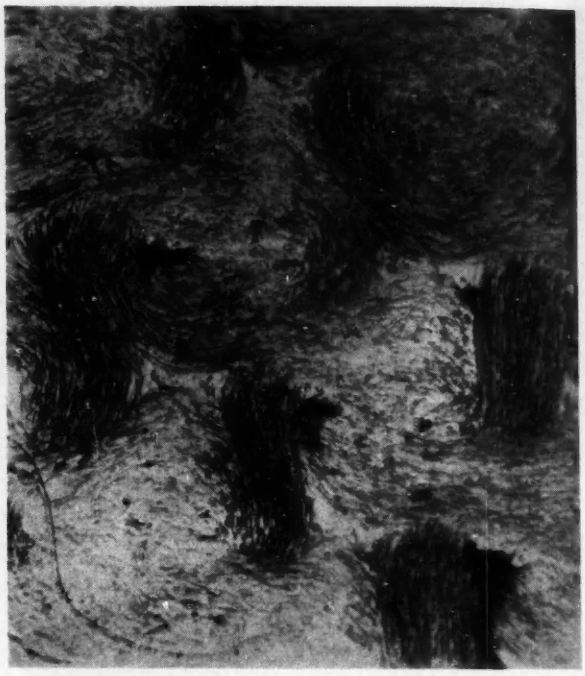

FIG. 20

FIGS. 18–20. *Views of selected planes through the thickness of a pyroxylin-coated sateen fabric (magnification, approximately 50 ×).*

Repetitive Longitudinal Sections of Coated Fabrics

It is industrially important to know the depth and manner of penetration of resinous materials used as coatings on fabrics. Several studies of this nature have been made in this laboratory, and three series of repetitive longitudinal sections have been selected to illustrate varying resin penetration, quality, and effects of fabric construction.

Vinyl-Coated 1.85-yd. Drill.—Figures 9–13, inclusive, are successive views of selected planes through the thickness of this coated fabric. Figure 9 shows the plane of fabric virtually at the fabric-coating interface, and shows only the scattered presence of fiber at this point. Minor imperfections in the resin film are evident.

Figure 10 shows the third plane of fabric, in which the geometrical arrangement of the fibers is more evident and the resin completely fills the interstices. More imperfections in the plastic film are seen at this point.

Figure 11 shows the fourth planar section of the fabric; the fiber cover factor has increased, and there still is evidence of thorough resin penetration at this level.

Figure 12 shows the fifth planar section, which is located near the center of the fabric. Penetration of

resin is far less complete at this point, since unfilled fabric interstices are evident. It is apparent that this drill fabric construction, even at the center of the fabric, does not have a high cover factor.

Figure 13 shows the sixth plane of the fabric, which is beyond the center of the fabric thickness toward the uncoated side. Very little resin is seen at this point, and the space between fiber groups is larger than in Figure 12.

This series of figures shows the degree of penetration of resin coating to extend through approximately half the thickness of a fabric of relatively low cover factor.

Vinyl-Coated 2.10-yd. Sheeting.—Figures 14–17, inclusive, illustrate the penetration of a similar resin coating in a fabric of different construction. Figure 14 shows the eighth plane cut; the plastic film was unusually thick. The regular spacing of fiber "islands" is characteristic of the construction; the film character is good.

Figures 15 and 16 are the ninth and tenth planes, respectively, cut in this series. Penetration of plastic is good. The effect of fabric construction on cover factor at various levels is illustrated.

Figure 17 is the eleventh plane cut, and is approximately at the center of the fabric. Penetration to this point is good, and it is observed that the cover factor is high, but not equal to unity.

Pyroxylin-Coated 1.12-yd. Sateen.—Figures 18–20, inclusive, are concerned with an entirely different resin as well as a different fabric type. Figure 18 shows the fourth plane cut; it may be seen that resin penetration is adequate, but resin film characteristics are poor. This is indicated by the numerous voids, showing resin-film discontinuity in the space between fibrous sections.

Figure 19 is the fifth plane cut, and the discontinuous nature of the resin is again evident.

Figure 20 is the sixth plane cut, which is at the approximate center of the fabric; there is a very small amount of resin penetration at this point. The very high cover factor of the sateen construction, approaching unity, is illustrated in this figure.

This series thus shows a poor resin film with adequate penetration into a sateen fabric. The penetration of resin beyond the fabric center is practically impossible for reasons which are evident from Figure 20.

Other Uses

Although the present method is qualitative in nature, quantitative estimations of cover factor at any level in a fabric may be made by either making a photomicrograph or making a camera lucida drawing of the section. The area involved may be determined by a planimeter. This is an especially useful method of estimating the ratio of impregnant to fiber at any level in the fabric.

Acknowledgment

It is a pleasure to acknowledge the suggestions and labor of many associates in the Research Division of Callaway Mills Company. Special thanks and credit for the photomicrographs in this paper are due Mrs. Richard Yates, Microscopist.

Literature Cited

1. Bailey, T. L. W., Jr., TEXTILE RESEARCH JOURNAL **17**, 655–63 (1947).
2. Bailey, T. L. W., Jr., and Rollins, M. L., TEXTILE RESEARCH JOURNAL **15**, 1–6 (1945).
3. Davis, S. J., and Colvin, J. J., U. S. Patent 2,556,681 (June 12, 1951) (assigned to Callaway Mills Company).
4. Hardy, J. I., TEXTILE RESEARCH **3**, 381–7 (1933).
5. Herzog, A., *Melliand Textilber.* **19**, 405–7 (1938); *J. Textile Inst.* **29**, A618 (1938).
6. Preston, J. M., *J. Textile Inst.* **27**, T216–18 (1936).
7. Schwarz, E. R., TEXTILE RESEARCH **6**, 270–2 (1936).

(Manuscript received January 7, 1952.)

Colorimetric Determination of the pH of Cotton Fiber

Walter A. Pons, Jr., and Carroll L. Hoffpauir

Southern Regional Research Laboratory, New Orleans, Louisiana*

THE MEASUREMENT of pH provides a relative estimation of the deterioration of cotton resulting from field weathering under humid conditions that may prevail between opening of the bolls and picking. These are the same conditions that contribute to the development of a high free fatty acid content in cottonseed before picking. Weathered cotton exhibits a decrease in organic acid content and an increase in pH [7, 8]. These changes are brought about by the use of organic acids as nutrients by microorganisms, leaving the potassium of the salts of the organic acids in the fiber as the carbonate. Rain may leach some of the organic and inorganic salts, with the result that the alkalinity determined on the ash of a unit quantity of the cotton may be reduced [8]. In addition, it has been demonstrated that the growth of microorganisms may alter the physical properties of the fiber, particularly the breaking strength and surface properties [2, 3].

Current methods for determining pH in cotton fiber employ an aqueous extraction of the fiber, followed by either an electrometric or colorimetric determination of the pH of the extract. Representative procedures are described by McCall *et al.* [8], Marsh *et al.* [7], and Hall and Elting [3]. Wakeham and Skau [9] demonstrated that the pH of an aqueous extract of cotton fabric is a function of the amount of water used for the extraction. These authors determined the pH of successive dilutions of an aqueous extract of the fabric, followed by extrapolation to zero dilution in order to define the pH in terms of the amount of water present in the fabric equilibrated to the standard atmosphere of 65% R.H. and 75°F. Although precise, this method does not satisfy the requirements for routine use where speed and simplicity are essential. The purpose of this paper is to present a colorimetric method by which indicator solutions are applied directly to the fiber. This approach should minimize the dilution effect and thereby achieve a close estimation of the actual pH of the fiber.

* One of the laboratories of the Bureau of Agricultural and Industrial Chemistry, Agricultural Research Administration, U. S. Department of Agriculture.

Basis of the Method

Sulfonphthalein indicators were chosen since they offer an easily distinguishable gradation of color with changing pH, and since neutralization of the sulfonic acid groups permits their use in poorly buffered systems [6]. Aqueous solutions of indicators were not employed due to the difficulty of wetting raw cotton. Early attempts to use neutralized sulfonphthalein indicators in essentially nonaqueous solutions of acetone and alcohols were unsuccessful, probably due to the insolubility of the noncellulosic constituents of the fiber in the organic solvents. It was found that solutions of these indicators in aqueous alcohols were more satisfactory; however, with the higher concentrations of alcohol the color change was less sensitive. A solution of the indicator in aqueous isopropyl alcohol (25% alcohol by volume) proved most satisfactory. This concentration was sufficient for immediate wetting of the cotton, and the indicator color change was practically instantaneous. The variation in color with pH was sharp and easily distinguishable. The color was more brilliant than that usually obtained with these indicators in aqueous solutions. This phenomenon has been attributed by Kolthoff [6] to the elimination of the dichromatism of the sulfonphthalein indicators in alcoholic solutions.

An indicator concentration of 0.005% was found to be optimum; higher concentrations gave colors which were too intense for accurate color matching. A ratio of 0.15 g. of sample to 1 ml. of indicator solution was used to obtain a uniform color distribution while keeping the dilution effect at a minimum.

The color standards were prepared with the same amounts of cotton and indicator solution as used for unknowns. Buffered cottons were utilized to prepare standards of known pH in order that the composition and physical nature of the color standards would approximate that of the unknowns. In addition, the buffered cottons are stable, and serve as the source material from which a set of color standards can be prepared quickly.

Small cylindrical glass vials, 19 mm. in diameter and 51 mm. in height, fitted with polyethylene clo-

sures were used as containers for both color standards and unknowns. The color standards were kept in a covered box constructed to hold them in parallel rows so that an unknown could be compared quickly with the appropriate standard. The box serves to protect the standards from undue exposure to light. The color standards are stable over a period of at least 6 months.

Reagents

(*1*) *Isopropyl alcohol, 98%, reagent grade.*—If appreciably acid, redistill over sodium hydroxide.

(*2*) *Isopropyl alcohol, 25% by volume.*—Dilute 98% isopropyl alcohol with distilled water to obtain a solution containing 25% alcohol by volume.

(*3*) *Stock indicator solutions, 0.05%.—Weigh* 0.100 g. of the solid indicators listed below, dissolve in 50 ml. of 98% isopropyl alcohol, add the indicated volumes of 0.1*N* sodium hydroxide, and dilute to 200 ml. with distilled water. Store in Pyrex glass bottles and protect from the light.

Chlorphenol red	—2.35 ml. of 0.1*N* NaOH
Bromcresol purple	—1.85 ml. of 0.1*N* NaOH
Bromthymol blue	—1.60 ml. of 0.1*N* NaOH
Phenol red	—2.85 ml. of 0.1*N* NaOH
m-Cresol purple	—2.65 ml. of 0.1*N* NaOH
Thymol blue	—2.15 ml. of 0.1*N* NaOH

(*4*) *Diluted indicator solutions, 0.005%.*—Dilute the neutralized stock indicator solutions in the ratio 1:10 with 25% isopropyl alcohol. Store in Pyrex glass bottles and protect from the light.

(*5*) *Long-range indicator, 0.005%.*—Prepare by mixing the following volumes of neutralized dilute (0.005%) indicator solutions: 2 volumes of *m*-cresol purple, 2 volumes of bromthymol blue, and 1 volume of thymol blue.

(*6*) *Stock buffer solutions* for the preparation of buffer mixtures of known pH.

(*a*) Monobasic potassium phosphate (KH_2PO_4), 0.1*M*, 13.62 g. per liter. Prepare from A.C.S. grade KH_2PO_4 which has been recrystallized from hot water and dried at 110°C.

(*b*) Sodium tetraborate ($Na_2B_4O_7 \cdot 10H_2O$), 0.05*M*, 19.10 g. per liter. Prepare from A.C.S. grade sodium tetraborate which has been recrystallized twice from water (below 50°C) and stored over a solution saturated with respect to both sucrose and sodium chloride.

(*c*) Succinic acid, reagent grade, 0.05*M*, 5.91 g. per liter.

(*7*) *Buffer mixtures of known pH value.*—Prepare mixtures of 0.05*M* borax with 0.05*M* succinic acid and of 0.05*M* borax with 0.1*M* potassium phosphate covering the pH range from 5.0 to 9.2 in 0.2 pH units, as directed by Kolthoff [5, 6]. If preferred, commercial buffer preparations covering similar pH ranges can be used.

(*8*) *Purified cotton.*—U.S.P. absorbent cotton or standard cotton cellulose prepared by recognized procedures [1, 4] is satisfactory.

Preparation of Standards

(*1*) *Buffered cottons.*—Soak about 10 g. of purified cotton in 100 ml. of the appropriate buffer mixture (pH 5.0–9.2 in 0.2 pH units) overnight in stoppered Pyrex glass containers. Remove the cottons, wring out gently by hand, and air-dry. Do not oven-dry as this leads to a crusting of the buffer salts on the surface of the cotton. The pH of the buffer solutions, after soaking of the cotton, should be checked electrometrically, and the pH values obtained assigned to the buffered cottons. No change in the pH of the buffer solutions was observed on soaking the cotton overnight. The actual pH values obtained were found to be in good agreement with those published by Kolthoff [5] for these buffer mixtures. Store the air-dry buffered cottons in tightly capped glass bottles.

(*2*) *Color standards.*—The useful pH range for each indicator is outlined in Table I. For each color standard required, transfer 0.15 g. of the appropriate buffered cotton to a clear glass vial, 19 mm. × 51 mm., containing 1 ml. of the appropriate dilute

TABLE I. INDICATOR RANGES FOR PREPARATION OF COLOR STANDARDS *

Indicator	pH range of buffered cotton	Best pH range for use†
Long range‡	5.0–9.0 in 0.4 pH units	—
Chlorphenol red	5.2–6.6 in 0.2 pH units	5.6–6.4
Bromcresol purple	5.2–6.8 in 0.2 pH units	5.8–6.6
Bromthymol blue	6.2–7.6 in 0.2 pH units	6.4–7.6
Phenol red	6.4–8.0 in 0.2 pH units	6.8–7.8
m-Cresol purple	7.6–8.8 in 0.2 pH units	7.8–8.5
Thymol blue	8.2–9.2 in 0.2 pH units	8.4–9.0

* 0.15 g. of buffered cotton and 1 ml. of 0.005% indicator solution.

† These ranges have been found to be most satisfactory for visual color matching. Color matching at the low and high parts of the range is difficult.

‡ Prepared by mixing dilute (0.005%) indicator solutions as follows: *m*-cresol purple, 2 volumes; bromthymol blue, 2 volumes; thymol blue, 1 volume.

(0.005%) indicator solution. Mix with a glass stirring rod and tamp the cotton firmly to the bottom of the vial. Cap the vial and seal with paraffin or other suitable material. After preparation, the standards are stable for at least 6 months. When not in use they should be protected from the light.

Procedure for Unknowns

Weigh 0.15 g. of sample, which should be hand-picked in small tufts to insure a representative sample free of foreign material. Transfer the sample to a clean glass vial (of the same size used for the color standards) containing 1 ml. of the long-range indicator. Mix with a glass stirring rod and tamp firmly to the bottom of the vial. Cap the vial and compare with the long-range color standards to obtain the approximate pH of the cotton sample.

Select the proper short-range indicator and repeat the procedure outlined above using 1 ml. of the appropriate indicator solution. In most cases report the pH as the closest color match with the standards. However, in some cases an estimation between standards can be made. Thus, if an unknown is judged to be between standards pH 6.4 and 6.6, report the pH as 6.5.

Adequate and reproducible illumination is required for the best results in color matching. Either bright daylight or illumination from a fluorescent daylight lamp is satisfactory.

Precision of the Method

In order to establish the precision of the colorimetric method, the pH of 85 samples of cotton fiber was determined by the proposed colorimetric method and by an electrometric method adapted from the work of Wakeham and Skau [9]. This method consists of the extraction of 0.5 g. of ground cotton (20-mesh) with 3 ml. of hot distilled water, followed by an electrometric determination of the pH of the cooled extract. The extract is returned to the sample, and measured volumes of distilled water are added, the pH being determined after each dilution. In this manner the pH's of 3, 4, 5, 6, 7, and 8 ml. of extract are obtained, and the values are then plotted against dilution. Extrapolation of the curve to zero dilution gives the pH of the cotton.

The results obtained for these samples by the two methods were examined statistically. The correlation coefficient was 0.96, showing that the results by the two methods are in good agreement. The average of the differences between the two methods was 0.13 pH unit, with a standard deviation of differences of 0.17 pH unit.

The average pH values obtained by the electrometric method for several of the dilutions were calculated. For zero dilution the average value was pH 6.56; for 3 ml. dilution, pH 6.72; for 5 ml. dilution, pH 6.85; and for 7 ml. dilution, pH 6.93. The average value for the colorimetric method, pH 6.65, falls between the zero and 3 ml. dilutions. These values indicate that the colorimetric method gives a close estimation of the actual pH of the cotton fiber. A pH determination can be made in approximately 2 min. For large numbers of samples considerable saving of time, as compared to present methods for the determination of pH in cotton fiber, can be realized.

Summary

A colorimetric method for the determination of the pH of cotton fiber is described. The method involves the direct application of neutralized sulfonphthalein indicators, dissolved in 25% isopropyl alcohol, to the fiber. The pH is determined by reference to color standards prepared from buffered cottons containing the same relative amounts of cotton and indicator solution.

The pH values obtained for 85 samples of cotton fiber by the colorimetric method and by an electrometric method were statistically analyzed to establish the precision of the method. A correlation coefficient of 0.96 and a standard deviation of differences of 0.17 pH unit were obtained. The results indicate that the colorimetric method gives a close approximation of the actual pH of cotton fiber.

Literature Cited

1. Corey, A. B., and Gray, H. LeB., *Ind. Eng. Chem.* **16**, 853–4, 1130 (1924).
2. Elting, J. P., *Science* **113**, 297–300 (1951).
3. Hall, L. T., and Elting, J. P., TEXTILE RESEARCH JOURNAL **21**, 580–90 (1951).
4. Hibbert *et al.*, *Ind. Eng. Chem.* **15**, 748–51 (1923).
5. Kolthoff, I. M., *J. Biol. Chem.* **63**, 135–41 (1925).
6. Kolthoff, I. M., "Acid Base Indicators" (translated by C. Rosenblum), New York, Macmillan, 1937.
7. Marsh, P. B., Guthrie, L. R., and Butler, M. L., TEXTILE RESEARCH JOURNAL **21**, 565–79 (1951).
8. McCall, E. R., Cirino, V. O., Stark, S. M., Jr., and Guthrie, J. D., *Science* **108**, 360–1 (1948).
9. Wakeham, H. R., and Skau, E. L., *Ind. Eng. Chem., Anal. Ed.* **15**, 616–18 (1943).

(Manuscript received February 5, 1952.)

INDUSTRIAL SECTION

Practical Application of Servomechanism Techniques to a Process-Control Problem*

S. P. Higgins, Jr.,† and G. W. McKnight‡

Industrial Division, Minneapolis-Honeywell Regulator Company, Philadelphia, Pennsylvania

Abstract

This paper demonstrates the application of servomechanism techniques to the solution of a problem in automatic control of industrial processes. A typical problem in this field—namely, a flow system—is analyzed by servo techniques. Predictions of system behavior by this method are correlated with the results obtained from the actual system tests.

PROCESS CONTROL, since its inception, has been aimed toward the most efficient use of process facilities to produce a uniform product of high quality. As processes and their associated control problems become more complex, the need becomes apparent for systematic analysis, with the problem expressed in terms of numbers, to supplement practical experience. The so-called "servo techniques" seem to offer a powerful tool for expressing process-control problems in terms of numbers.

The present paper attempts to show the usefulness of the servo methods for predicting system behavior on an actual process. Previous papers have presented data derived from these methods on hypothetical processes and have shown predicted results, but little data appears to be available in the literature showing *test* results on a physical system for comparative purposes. The present paper attempts to show that even simple servo methods provide useful information for process instrumentation.

* Paper presented Sept. 12, 1951, at the Instrument Society of America conference in Houston, Texas.

† Development Engineer.

‡ Application Engineer.

Origin of Servo Techniques

The search for a mathematical approach to process design and control application is not a new one. In the early stages, attempts were made to write differential equations for process and instruments to effectively define their operation. The complexity of equations and the difficulties experienced in assigning numbers to the coefficients were sufficient to make the methods impractical. Methods based on empirical formulas, such as the transient or step-change method [2], were more practical and did receive some acceptance, although the size of the required disturbances to the process and the degree of accuracy attained led many to use intuition, good judgment, and experience rather than any formalized approach to solve the problems.

During the last war, great progress was made in predicting the performance of combinations of devices for antiaircraft artillery use. The methods were taken from many fields, including feed-back amplifier and electrical filter circuit design. Collectively these have become known as the "servomechanism techniques." Since the factors involved in ef-

fectively laying a gun are in many ways very similar to those of process control, it is only logical that the servo theory should be applied to process analysis.

As occurs in the positional servo devices for anti-aircraft artillery, the limitations of many physical components used in the process industries—such as pumps, heat exchangers, controllers, valves, measuring and transmitting devices—have combined effects on the quality and quantity of the end-product. Naturally, for the most efficient operation of a plant, each of the above components should be correctly specified for the job. Thus, the process and its instrumentation must be considered jointly during the plant-design stages rather than separately as in the old practice of designing the process and later adding the instruments. Naturally, compromises may have to be made, since important factors other than the ultimate in performance must also be considered.

The experience of Brown and Campbell with the application of servo techniques to system design prompted them to propose the need for men trained in these many phases of process control and instrumentation to be called "system engineers" [1]. Before system engineering is feasible, however, methods of analyzing the various components of the system and of predicting their combined behavior must be made available on a practical basis.

As a vehicle for crossing the boundary between the process and instrumentation phases, servo techniques seem to offer many advantages. Most people, however, when confronted with the term "servo techniques," think immediately of involved terminology and mathematicians equipped with computers. Such is not necessarily the case. This can best be proved by examining the techniques themselves.

What Servo Techniques Are

Each component or process to be tested is essentially an energy-transferring or -modulating device —that is, if a change is made in the input of the device, at some later time there will be a related change in its output. Obviously, the nature of the input signal, the device construction, and especially the relative ability of the device to transfer energy will determine the amount by which the output lags or leads the input as well as the degree of amplification obtained from the device. This energy-transferring characteristic is known in the servo field as the "transfer function" of the device. (In the case of an energy-modulating device, such as a controller, the transfer function is a measure of the regulating ability of the device).

One of the most practical ways of determining the transfer function of a device or process is to observe its response to a sinusoidally varying disturbance. This is commonly known as the "frequency-response method." If the system under test is linear, the output response must also be sinusoidal with time—that is, the frequency of the response sinusoid must be identical with the frequency of the disturbing sinusoid.

It is realized that most systems are not linear. Nonlinearities, due to valve characteristics, hysteresis, friction, and other losses, exist in all processes. However, if the band of operation is kept within a relatively narrow range, the system will usually be sufficiently linear to permit the successful application of servo methods for predicting system behavior within this range.

Use of Frequency-Response Plots

If the sinusoidal disturbance is introduced, as mentioned above, the dynamic characteristics of the component under test will determine the ratio of the magnitudes of the output to the input signal and will cause them to be displaced timewise. If the frequency of the disturbing signal is changed, a new magnitude ratio and a different amount of phase shift will occur after the transient has died out. The transfer function and, hence, the dynamic performance of the unit are determined by measuring the ratio of output amplitude to input amplitude and by

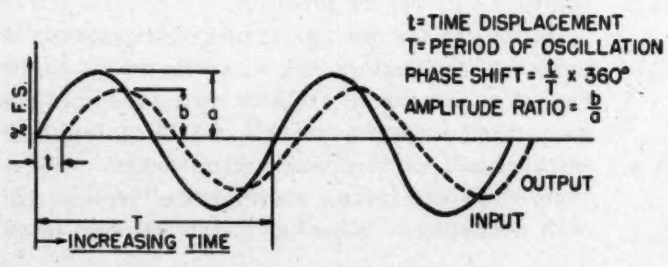

FIG. 1. *Output response of a passive network to a sinusoidal input disturbance.*

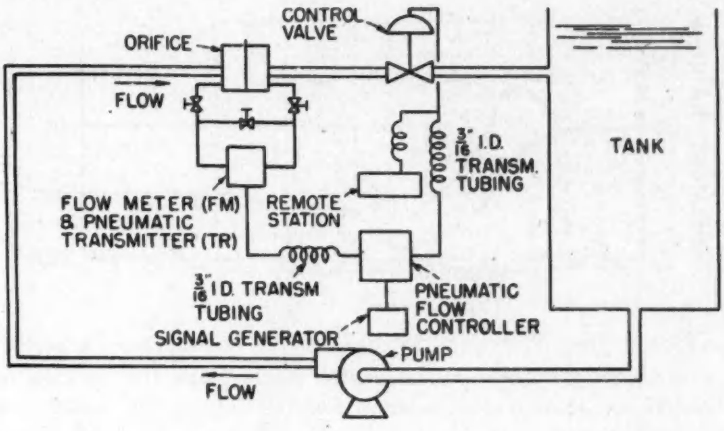

FIG. 2. *Flow loop.*

measuring the phase shift between the curves over a range of input frequencies. This is shown diagrammatically in Figure 1 for one value of input frequency.

If sinusoidal disturbances are introduced into a process or component at different frequencies (such as by loading a valve in a process), a series of amplitude ratios and phase-shift angles will be determined. If plots are made of amplitude ratio and phase lag against frequency of disturbance, the resultant curves establish the dynamic characteristics for the component or system under test. These plots are known as "frequency-response plots."

Although the frequency-response plots themselves give valuable information, as is shown later, some correlation to system performance, such as the response of a system to a change in controller set point, must exist so that the data will have practical utility. Various methods are available for making this correlation, one of which is used in the analysis to be described. It is of interest to note that the transfer-function plots themselves indicate the method to be chosen as well as the probable accuracy associated with the correlation.

Obviously, the above is an oversimplified outline of the techniques, and does not indicate some of the physical difficulties involved. One difficult problem is the design of a signal generator and recorder capable of producing an undistorted sinusoid over a wide range of frequencies, with pneumatic, electrical, and motion outputs. This has been accomplished, and information concerning it will be published at a future date. Similarly, the necessity for evaluating the frequency data in terms of the previous process and control experience cannot be discounted, and this problem will be discussed later in the paper.

Description of Control Loop Selected

In order to facilitate testing, it was desired to have available a simple process-control system having sufficient physical significance to be associated with actual processes. Experience indicated that a flow-control system could be constructed in the laboratory to meet the above requirements. This flow-control loop is shown schematically in Figure 2.

A centrifugal pump is used to pump water around and back into the sump tank. The flow is measured by conventional orifice methods. The length of connecting tubing between the meter, controller, and control valve can be varied, along with the appropriate side tubing lengths, so as to show the response for a process-mounted controller as well as for a controller mounted in the control house. In addition, flowmeters of the mercury and dry type are tested

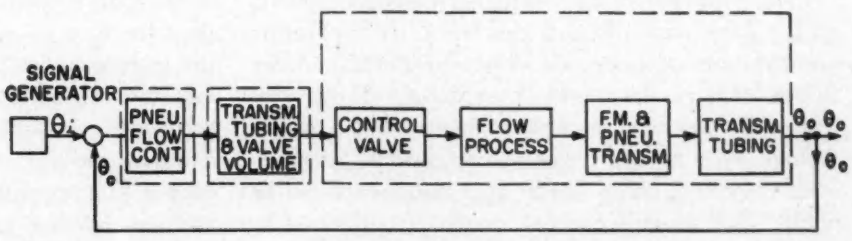

FIG. 3. *Block diagram of flow-control loop.*

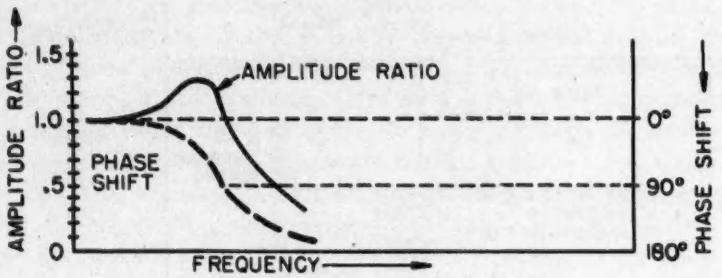

FIG. 4. *Frequency response of a simple system.*

with the controller in the locations mentioned above. The signal generator is the device which loads the system or system components with a sinusoidally varying disturbance.

The various elements of the system of Figure 2 may be represented as a series of blocks, as shown in the block diagram of Figure 3. The signal generator is an analytical tool only, and forms no part of the automatic flow-control system. The breaking up of the system into the parts indicated by the blocks is done so that the parts may be isolated as needed for analysis and design. The ultimate objective is to identify or tag each block in such a way that we can determine what the design of each of the blocks should be for optimum performance of the system as a whole. This, in the language of the servomechanism engineer, is a method offering the means for analysis of the elements for blocks that exist or for synthesis of those yet to be designed.

It may be more convenient, in certain cases, to have the block represent two or more components in the system, such as the valve and process. The individual transfer function for the process could then be obtained if the valve transfer function (*i.e.*, the response in valve position to valve pressure) were known. The blocks drawn with dash lines in Figure 3 show one instance where the transfer function across a group of components might be studied, rather than the individual transfer functions of the components themselves.

Application of Method to Ideal System

Before the use of the frequency-response method on the flow-control loop is described, its application to a hypothetical example will be considered in order to see what results might be expected. If the system under test acts, in certain respects, like a simple system, such as the common two-capacity process-control system, many useful approximations can be made. For example, such a system, if subjected to a sudden set point change, might have a damped oscillatory response, as evidenced by over- and underpeaking, with each successive peak being smaller in magnitude than the preceding peak. An example of this type of recovery is the well-known *quarter-amplitude recovery curve*. Such a system, if subjected to sinusoidally varying set point changes would have a closed-loop frequency response, as shown in Figure 4.

Note the amplitude peak and the rapid change of phase at the resonant frequency (Figure 4). If the frequency response of the system under test resembles the response of the simple system in the region of resonance, some simple methods can be applied to approximate system transient response from the system frequency response. From the relative height of the amplitude peak and the frequency at which it occurs (the resonant frequency), the transient response can be approximated by the use of Figures 5 and 6.

Figure 5 shows the damping factor, ζ, as a function of the amplitude ratio. With the damping ratio established, Figure 6 shows the transient response in terms of the damping ratio and the natural frequency. As shown in the diagram, the natural frequency is related to the resonant frequency by the following equations:

$$\omega_N = \frac{\omega_R}{\sqrt{1 - 2\zeta^2}} \qquad (1a)$$

$$\omega_R = 2\pi f_R \qquad (1b)$$

where ω_N = natural frequency (radians/min.), ω_R = resonant frequency (radians/min.), and f_R = resonant frequency (cycles/min.). Thus, the height of the resonance peak indicates the degree of damping, and the resonant frequency indicates the time for recovery. A high peak, showing a relatively low damping ratio, would indicate that the transient response to a set point change would have large over- and undershoots, as indicated for the smaller valves

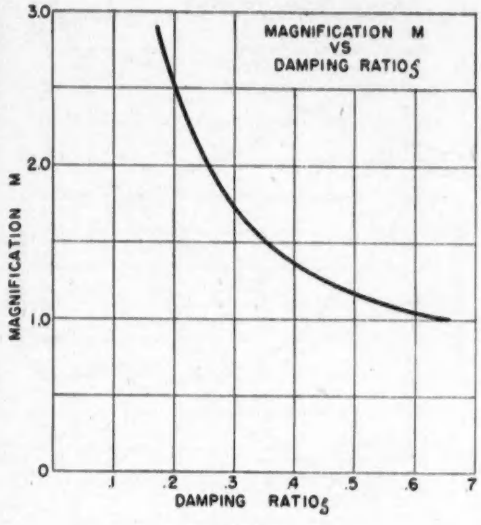

FIG. 5

of ζ on Figure 6. A system having high resonant frequency would require a shorter time for recovery than one having a low resonant frequency. The abcissa of the curve of Figure 6 is expressed as $\omega_N t$.

Thus, the curve is easily dimensionalized with respect to time by observing the value of $\omega_N t$ for the point in question. Time is given by the following expression:

$$\text{Actual time} = \frac{\omega_N t \text{ (from Figure 6)}}{\omega_N} \qquad (2)$$

The closed-loop frequency response may be measured, or it may be derived from the frequency response of the components used to make up the closed loop. If, for example, A, B, and C are components for which we know the transfer functions, the overall open-loop transfer functions can be determined by multiplying the amplitude ratios and adding the phase angles. Thus, the open-loop frequency response for one frequency is as follows:

$$M_S = M_A \times M_B \times M_C \qquad (3a)$$

$$P_S = P_A + P_B + P_C \qquad (3b)$$

where M = amplitude ratio, and P = phase lag.

With the amplitude ratio and the phase lag established for a number of these frequencies, the open-loop transfer function of the system comprised of the components is, in effect, predicted. The conversion from the open-loop frequency response of the system to the closed-loop frequency response is easily accomplished graphically or by charts, which will not be discussed here.

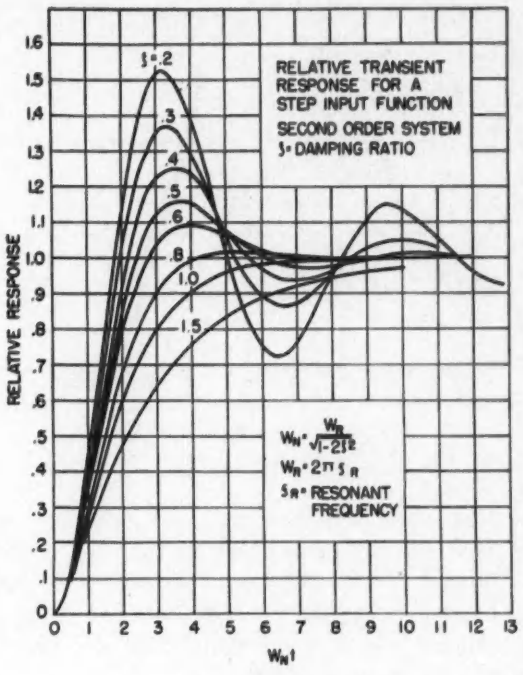

FIG. 6

Thus, it has been shown that the closed-loop frequency response which is representative of the system transient response can be measured on an existing system or computed from the component responses.

Description of Test Procedure

In order to test the validity of the assumptions, four different flow-control systems, as described in Table I, were examined using the methods described above.

Thus, the test data will be presented for a typical flow-control problem showing the relative effect of controller location as well as a comparison of wet and dry meter operation.

The flowmeters were mounted at the orifice using conventional manifolds. The final control element

TABLE I. FLOW-CONTROL SYSTEMS

System	Type of flowmeter	Transmitter to: Controller*	Transmitter to: Remote-set*	Controller to: Valve*	Controller to: Remote-set*
A	Mercury meter	150 ft.	150 ft.	150 ft.	5 ft.
B	Mercury meter	30 ft.	150 ft.	5 ft.	150 ft.
C	Dry transmitter	150 ft.	150 ft.	150 ft.	5 ft.
D	Dry transmitter	30 ft.	150 ft.	5 ft.	150 ft.

* All connecting tubing was $\frac{3}{16}$-in. inside diameter tubing.

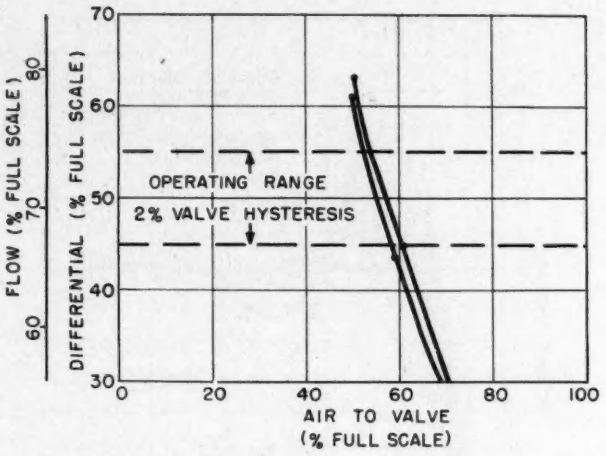

FIG. 7. *Control-valve characteristics.*

was a standard control valve. No valve positioner was used; the hysteresis curve for the valve is shown in Figure 7. Transient plots (response to a sudden step change in set point) were obtained using two conventional two-pen pneumatic receivers with 30-sec. and 6-min. chart drives.

For simplicity, controller adjustments were made for each system on the basis of transient response to set point changes. No attempt was made to obtain optimum settings for each case, so that the systems cannot be compared directly from the data. This was done since the purpose of the present paper is to show the practical applicability of the approach rather than to provide detailed system information.

Both the set point and the transmitted flow signals were recorded, following a sudden (10% of full-scale) change in set-point pressure. After these transient tests, the controller was subjected to a sinusoidally varying set-point pressure covering approximately 20% double amplitude. The flow signal at the controller was then recorded, and plots were made to show the amplitude and phase of this signal referred to the set-point signal.

This plot established the closed-loop frequency response for the system under test. The correlation of transient response by the graphical methods previously described to the closed-loop frequency response was checked at this time.

Having established the correlation between the over-all system frequency and transient responses, the components contained in the closed loop were individually tested for their response to sinusoidal forcing signals of small amplitude and at the level at which they operated for the closed-loop frequency-response tests. The data thus obtained consisted again of amplitude ratio and phase angle between the component output signal and the sinusoidal input at several frequencies. In this case, all inputs and outputs were in the form of pneumatic pressure signals.

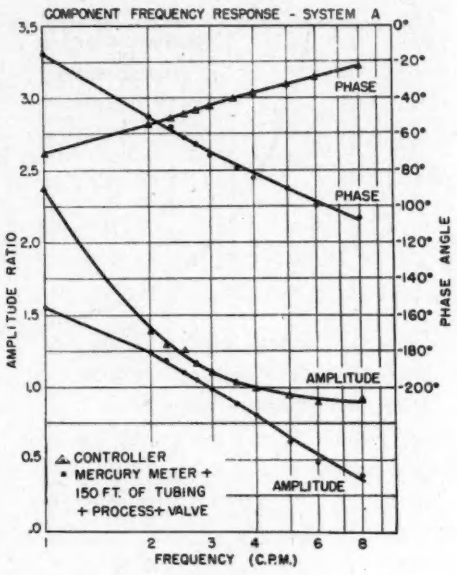

FIG. 8

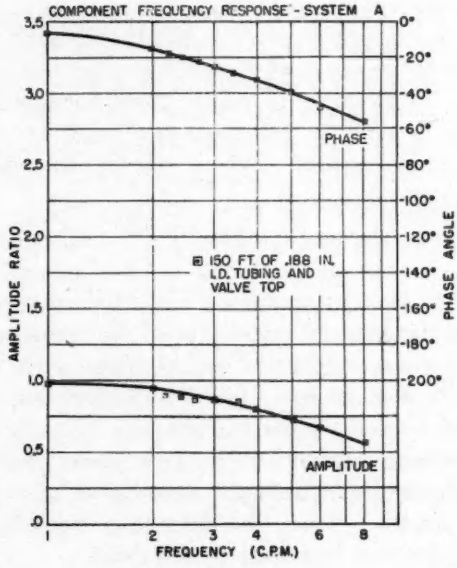

FIG. 9

The phase shift and amplitude data on the system component at different frequencies constitute the transfer function of the component. The individual transfer functions were combined using standard

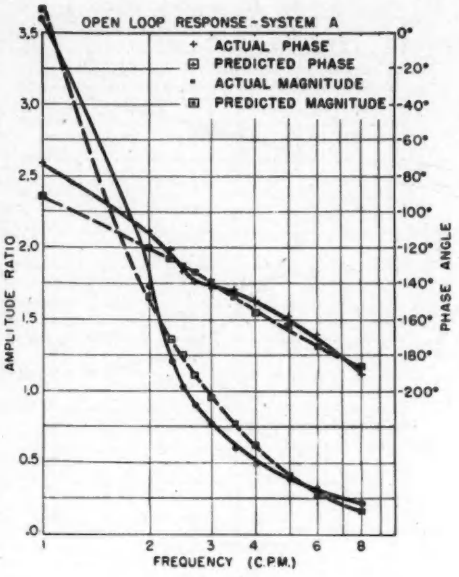

FIG. 10

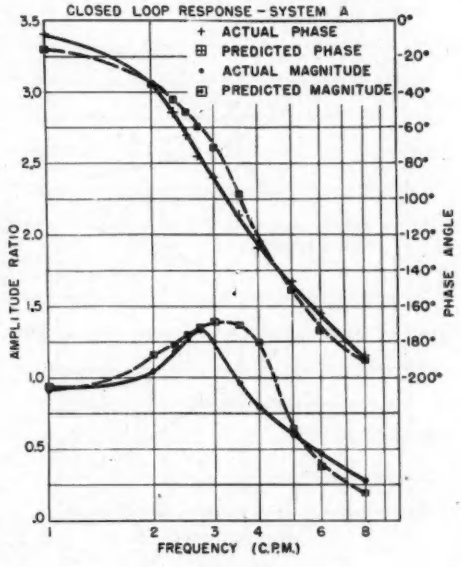

FIG. 11

vector methods to give the over-all transfer function of the system (response of the system to sinusoidally varying signals of different frequencies). The predicted transfer function was then compared with the measured system transfer function to show the degree to which prediction is possible.

Test Results and Interpretation

The frequency-response results on components of system A are shown in Figures 8 and 9.

TABLE II. SYSTEM A TRANSIENT RESPONSE

	Actual	Derived from measured closed-loop frequency response	Derived from predicted closed-loop frequency response
First overshoot	29% at 9.6 sec.	25% at 10.2 sec.	35% at 9 sec.
First undershoot	12% at 16.8 sec.	7% at 20.4 sec.	13% at 18 sec.
Second overshoot	Very slight	1.5%	2%

The system has been broken into three blocks for analysis. Figure 8 shows the diagrams for the controller and for a second block, comprised of the mercury meter plus 150 ft. of tubing plus the process plus the valve. Figure 9 shows the transfer function for a third block, comprised of 150 ft. of tubing and the valve-top volume. These individual transfer functions were combined by multiplying amplitude ratios and adding phase angles to derive the predicted open-loop transfer function, as shown in Figure 10.

The open-loop response corresponds to the frequency response which would be obtained if the process-variable line at the controller were disconnected and its signal recorded when the set point was cycled at various frequencies. The conversion from the open- to the closed-loop frequency response, and its inverse, is easily accomplished graphically or by charts, and will not be discussed here.

Figure 10 shows a comparison of the actual and predicted open-loop frequency responses. Note that by using the component curves, the source of undesirable magnitudes and phase shifts can be detected. Any unit which rapidly increases the negative phase angle of the open-loop system without a proportional decrease in amplitude ratio will contribute effective dead time to the system and decrease the system stability, thereby making control more difficult.

The prediction of the closed-loop response (derived from component checks) and the actual closed-loop response (as measured) are shown in Figure 11.

Note that the measured amplitude peak is 1.35, and occurs at a frequency of 2.7 cycles per min. Thus, from Figure 5, the damping ratio, ζ, is established as 0.4. The dynamic behavior of a second-order system having a damping ratio of 0.4 is shown in Figure 6. On the basis of this data, the transient

response of system A to a set point change was derived. A comparison of the derived and predicted results with the measured response curves is presented in Table II.

The methods used in analyzing the remaining systems are the same as those used for system A. Consequently, the curves are presented in the same order and comments are made on the closed-loop response only.

The effect of changing one component in a system is shown in system B (mercury meter with process mounted controller). The component frequency-response diagrams are shown in Figures 12 and 13. The measured and predicted frequency-response diagrams for the system B closed loop are shown in Figure 15; frequency-response diagrams for the open loop are shown in Figure 14. Note that by reducing the transmission lag, the negative phase angle (phase lag) is reduced, and in fact levels off at approximately $-140°$ above about 3 cycles per min. Thus, the resonant frequency has been increased from 2.7 to 3.3 cycles per min. It should also be noted that the system stability has been increased. The result of applying the simple approximation for transient response to this system is shown in Table III. The magnification of 1.57 is representative of a damping ratio of 0.35 and the resonant frequency is 3.3 cycles per min.

In system C, the mercury meter of system A has been replaced with a dry meter. The component frequency response is shown in Figure 16.

The actual and predicted open-loop responses of the system are shown in Figure 17.

The measured and predicted closed-loop frequency-response diagrams are shown in Figure 18.

Note that replacing the mercury meter with a dry meter has resulted in a decrease in the phase lag of the measuring system, thus raising the resonant frequency from 2.7 cycles per min. in system A to 11 cycles per min. in system C. This system was intentionally made less stable that the other cases in order to illustrate the utility of the methods with a minimum amount of system damping. The measured amplitude ratio is 2.43, giving a damping ratio of 0.21. The results of applying the approximation are shown in Table IV.

Note that in this case there was a considerable error in the prediction of resonance. This was due to the low damping used on the system. It also emphasizes the need for accurate measurements where

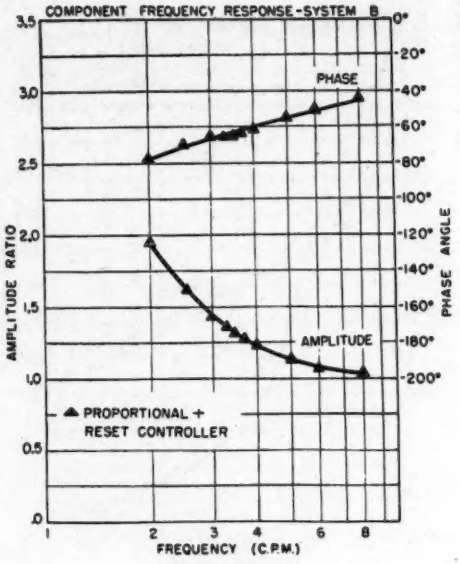

FIG. 12

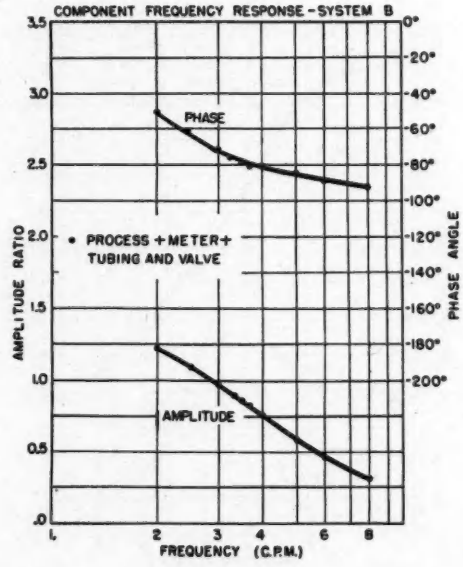

FIG. 13

several component transfer functions are to be combined.

An examination of system D illustrates the effect of removing transmission lag in a fast flow-control loop. The component frequency response is shown in Figure 19. The smaller phase lag shown in the open-loop frequency response diagram in Figure 20 indicates a much faster recovery from transients.

In this case the dynamic behavior of the system, with high gain settings on the controller and under

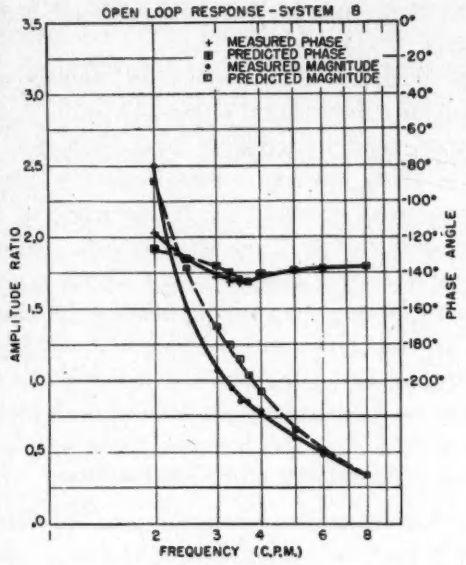

FIG. 14

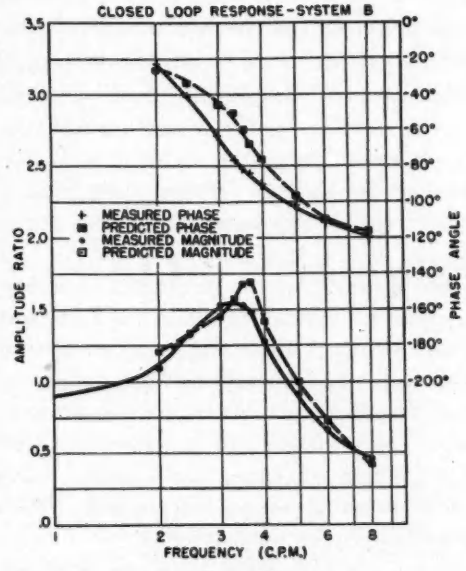

FIG. 15

TABLE III. SYSTEM B TRANSIENT RESPONSE

	Actual	Derived from measured closed-loop frequency response	Derived from predicted closed-loop frequency response
First overshoot	30% at 7.8 sec.	30% at 8.4 sec.	35% at 8 sec.
First undershoot	12% at 13.2 sec.	10% at 16.8 sec.	12% at 16 sec.
Second overshoot	Very slight	3%	5%

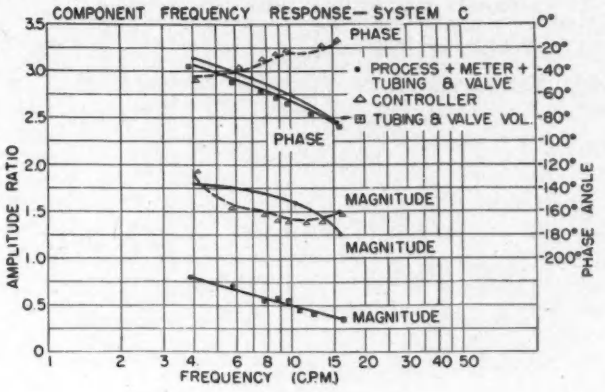

FIG. 16

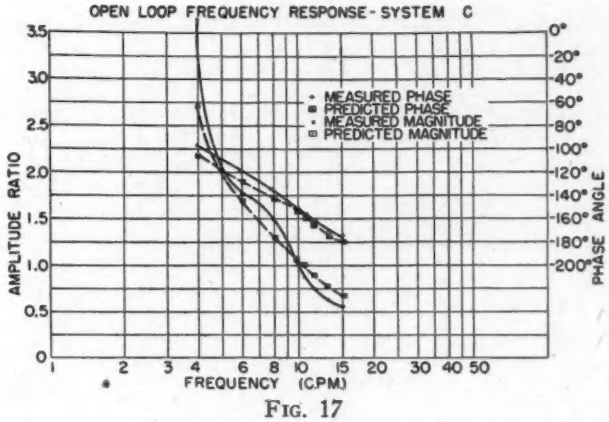

FIG. 17

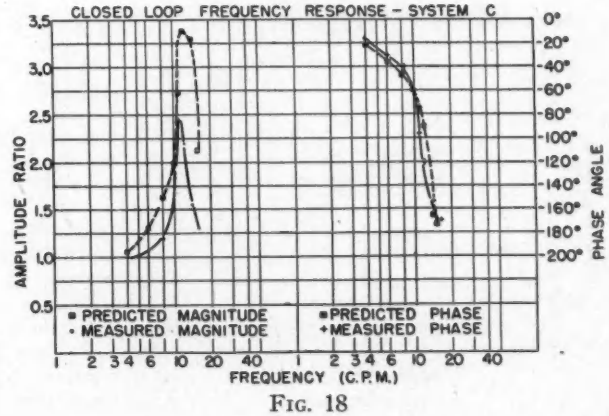

FIG. 18

TABLE IV. SYSTEM C TRANSIENT RESPONSE

	Actual	Derived from measured closed-loop frequency response
First overshoot	45% at 3 sec.	51% at 2.7 sec.
First undershoot	26% at 5.5 sec.	20% at 5.6 sec.
Second overshoot	14% at 8.2 sec.	12% at 7.8 sec.

FIG. 19

FIG. 20

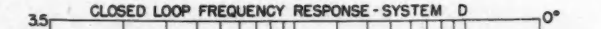

FIG. 21

conditions of sudden changes in set-point pressure, was influenced to a considerable degree by the non-linearities of the components within the control loop. It was found, however, that the linearity of the system could be improved by adjusting the controller settings for a slightly overdamped system response. The closed-loop frequency response is shown in Figure 21. Note that no amplitude peak occurred in the plot of the relation between amplitude ratio and frequency.

This illustrates a case where the simple methods of examining the frequency response in the region of resonance, used in the first three examples, break down. From the open-loop frequency response, however, some observations can be made as to the system performance. If the open-loop frequency-response curves of systems C and D are compared, a decrease of phase lag and attenuation for the same frequency range is noted in system D. A decrease in phase lag and attenuation is indicative of faster recovery to the control point following an upset.

Summary and Conclusions

The four examples discussed here indicate that the servo analysis methods can be applied to process-control problems to obtain useful and reasonably accurate predictions of performance. The application of graphical methods (based on a simple system) has been illustrated, and some means for the comparative evaluation of more complicated systems have been mentioned. Obviously, for maximum utility of frequency-response data, the information must be evaluated in the light of previous control and process experience. It supplements but does not replace experience.

The development of this technique is in its early stages. An examination of the blocks to be analyzed shows that some are under the jurisdiction of process designers and plant operators, while others are the responsibility of the instrument manufacturers. The success of the program will be dependent upon the extent to which all three participate. Naturally, there will be limitations of the method. These can be overcome only as they are met.

When the methods have been exploited we may reasonably expect them to perform many useful functions. Among these are:

(1) To permit prediction of system performance from tabulated information on the individual components of the system.

(2) To establish the necessary response characteristics which an instrument or process being designed must have in order to make the complete system into which it is installed operate as desired.

(3) To assist the designer in determining the source of undesirable effects and to permit mini-

mizing their effect, either by a change in process or instrumentation or by intelligent compromises.

(4) To permit comparison of the performance of various processes as well as other components where a number of choices are available.

(5) To provide a means of cataloging previous experience.

(6) As information is gained, valuable predictions as to "noise" effects on a process and how processes can be improved can be obtained directly from the transfer function. Naturally, practical experience is of tremendous importance for this type of work.

(7) Predictions of performance can be made, so that in the selection of equipment, performance may be discussed along with the other important factors, such as the economics, convenience, maintenance, servicing, etc.

It is not expected that all systems will prove as simple to analyze and test as the system chosen here. The authors, however, present this data in the hope that others may be encouraged to investigate and publish results on the use of the methods, thus furthering their use as an engineering tool for process work.

Acknowledgment

The authors wish to express their appreciation to E. C. Grogan for his assistance in assembling the test data.

Bibliography

1. Brown, G. S., and Campbell, D. P., Instrument Engineering—Its Growth and Promise in Process Control Problems, *Mech. Eng.* **72**, 124 (1950).
2. Zeigler, J. G., and Nichols, N. B., Optimum Settings for Automatic Controllers, *Trans. Am. Soc. Mech. Engrs.* **64**, 759 (1942); Process Lags in Automatic Control Circuits, *Ibid.* **65**, 433 (1943).

General References

Brown, G. S., and Campbell, D. P., "Principles of Servomechanisms," New York, John Wiley & Sons, Inc., 1948.

Chestnut, H., and Mayer, R. W., "Servomechanisms and Regulating Systems," Vol. I, New York, John Wiley & Sons, Inc., 1951.

Rutherford, C. I., The Practical Application of Frequency Response Analysis to Control Problems, *Proc. Inst. Mech. Engrs.* (*London*) **162**, No. 3, 334 (1950).

(*Manuscript received November 6, 1951.*)

The Principles of Textile Finishing*

Emery I. Valko

Polytechnic Institute of Brooklyn, Brooklyn, New York

Abstract

The historical relationship between the science and the technique of textile finishing is illustrated herein by a description of the principles of indigo dyeing. This ingenious technique was developed thousands of years ago, but it has been understood only recently. The rapid progress of polymer and colloid science has reversed the situation and enabled the *theory* of finishing to take the lead. A need has arisen for a new systematics of finishing. The topical and the energic characterizations have been suggested for this purpose—the first is based on consideration of the site of the finish in the textile (interyarn-intrayarn, interfiber-intrafiber); the second on consideration of the forces acting between finish and fiber. The significance of the spatial and energic factors is discussed in relation to some finishing processes.

Introduction

The industry of textile finishing is an old one; the science of textile finishing is a new one. Both are now in a state of rapid progress; almost every day new facts and new theories are recorded. A need has developed for a more complete systematics of textile finishing which would provide a framework for, and bring order into, the mass of scattered information on the subject. It should be useful to the

* Based on a paper delivered at the Second Canadian Textile Seminar, Queens University, Kingston, Ontario, Sept. 15–16, 1950.

uninitiated as an introduction and to the experienced as an aid in reviewing and evaluating progress.

"Chemical finishing" refers to all processes which aim at the improvement of textile materials by chemical means. Dyeing is perhaps the most important of these processes.

Originally, the term "chemical finishing" applied only to processes carried out after the yarn is woven or knitted into fabrics. According to this definition, the dyeing of raw stock or yarn and the mercerizing of yarn would be excluded, whereas the same operations with fabric would be included. Therefore, the broader definition given above is preferable.

Scientific Explanation of an Old Process

The problems and methods of the science of chemical finishing of textiles may be illustrated in terms of our present knowledge and theories [14] by a brief outline of a typical finishing process—dyeing cotton with indigo.

The crystalline particles of indigo, which is a water-insoluble compound, are brought into contact with an aqueous solution. By the addition of suitable water-soluble compounds (caustic soda and hydrosulfite), the pH of the solution is set at a value higher than 11 and its redox potential is reduced below − 500 mv. This redox potential is lower than the equilibrium potential of the oxidation-reduction system of indigo-indigo white, which is represented by the following equation:

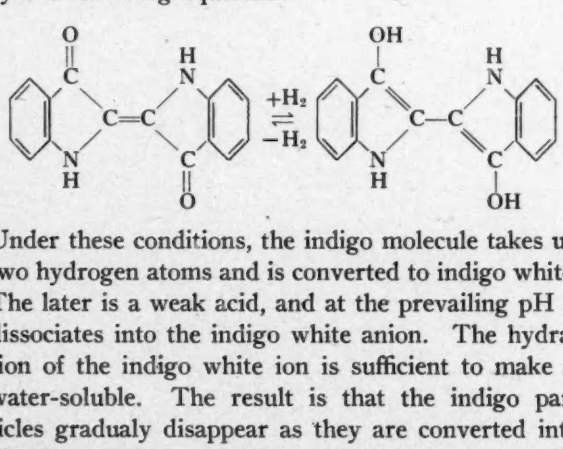

Under these conditions, the indigo molecule takes up two hydrogen atoms and is converted to indigo white. The later is a weak acid, and at the prevailing pH it dissociates into the indigo white anion. The hydration of the indigo white ion is sufficient to make it water-soluble. The result is that the indigo particles gradualy disappear as they are converted into dissolved indigo white ions. The hydration of the indigo white ions is not sufficient, however, to prevent their partial association into dimers or trimers. These aggregates are in equilibrium with the single indigo white ions, which represent a definite fraction of the total dye present in the solution.

The cotton fiber is then introduced into the solution. Disregarding the lumen and the occasional cracks and crevices, the cellulose molecules in the fiber are closely attached to each other. The distance between them is too short to permit the entrance of the dye ions. The indigo molecule is one of the smallest dye molecules, its longest linear extension being approximately 12 Å., but even smaller molecules than this are unable to penetrate the fiber. However, the organization of the cellulose molecules is not uniform throughout the whole mass of the fiber. The major portion of the fiber contains the cellulose molecules in a strict three-dimensional order, which we call the "crystalline state," whereas the remaining portion shows a lesser degree of order, and therefore is called "amorphous." This smaller, disorganized portion of the cotton fiber forms an interlocking network throughout the whole mass of the fiber. Water molecules and cellulose molecules have a strong attraction to each other because they can be bound together by hydrogen bonds of comparatively high energy content. Nevertheless, the mutual linking of the cellulose molecules in the crystalline region is too firm to be overcome by this attraction of the water to the cellulose. The mutual linking of the cellulose molecules in the amorphous portion is somewhat weaker. When the cotton fiber is brought into contact with the water, the attraction of the water molecules to the cellulose molecules results in swelling of the fiber as the water molecules enter the amorphous region and push the crystalline regions farther apart. Starting from the surface, the water penetrates through the whole mass, although avoiding the crystalline regions, until it forms a system of channels extending from surface to surface. The amorphous regions are thus converted into a kind of cellulose gel. At equilibrium, or saturation, when the cohesion of the cellulose at certain points balances the attraction of the water molecules, the cotton fiber contains about 25% water by weight.

The channels created in the cotton by the swelling along the path of the amorphous region are submicroscopic. Their average diameter is of the order of about 50 Å. Individual indigo white ions can enter these channels readily; carried deeper and deeper by diffusion, they penetrate the whole fiber, although leaving the crystalline regions intact.

Without specific forces acting between the cellulose and the dye, an equilibrium would be reached when the concentration of the dye in the cellulose gel

reaches the concentration of the dye in the surrounding dye bath. However, attractive forces are active between the two kinds of molecules—cellulose and dye. The structural formula of the indigo white molecule shows the presence of a chain of alternating single and double bonds. Such a system of conjugated double bonds possesses a common electronic cloud which is polarizable. The interaction between the hydroxyl groups of the cellulose and the electronic cloud of the dye stabilizes the hydrogen bond between the two. Since the conjugated chain of indigo white is short, the attractive forces between this compound and cellulose are comparatively weak, but are sufficient to cause a definite preferential adsorption (substantivity) by the cellulose.

The indigo white ions entering the submicroscopic channels of the fiber become partly attached to the cellulose by attractive forces. Only the fraction which remains free is available to further penetration. Therefore, the diffusion of the dye in the fiber is slower than in water. Since the dye is ionized, electrical forces between the charged fiber surface and the dye also reduce the speed of peneration. The cross section of the fiber shows the progress of the dye in the form of a ring gradually growing from the periphery toward the center. The rate of this growth can be estimated from three factors: the size of the dye molecule, the substantivity, and the electrical potential of the fiber. In the final equilibrium, the concentration of the dye in the fiber is several times higher than in the dye bath, causing a partial exhaustion, the magnitude of which is determined by the intensity of the attractive forces.

After a sufficient amount of indigo white is absorbed by the fiber, the fiber is removed from the bath and rinsed with water. The rinsing reduces the pH and increases the redox potential of the solution surrounding the fiber. As a consequence of this, the indigo white ions in the fiber are first converted into the undissociated indigo white acid and then, upon taking up oxygen, into indigo. The indigo molecules are not held firmly enough by the cellulose molecules; as they are released, they form crystalline particles in the fiber. These particles are too large to diffuse, and are therefore safely locked in the gel formed by the hydrated amorphous regions. Upon drying, the cellulose molecules of the amorphous region associate with each other, and the dye particles remain firmly embedded in the fiber. The process is completed.

Progress in the Application of Science to Finishing

Some of our major industries, such as those of radio, television, and automotive engines, are dominated by science inasmuch as their origin as well as most phases of their progress were based on available fundamental scientific knowledge. The role of fundamental science in the textile industry, and particularly in the textile-finishing industry, has until recently been limited largely to the explanation of observed phenomena and of methods used. Important discoveries, such as the mercerization of cotton, the manufacture of viscose rayon, and the development of crease-resisting finishes, were made on the basis of empirical observations rather than theoretical deductions. There are two reasons for this: First, the industry of clothing is one of the oldest, its origin dating back many thousands of years. Patient exercise of trial and error and the accumulation of chance discoveries and minute observations for generation after generation developed the craft of converting the fibers of animal and vegetable origin into useful and beautiful fabrics, and established the technique of textile finishing essentially as we know it today. The second reason is the extreme complexity of fibers and fiber-treating compounds from the chemical and physicochemical standpoint. The elucidation of these systems had to await the development of the science of polymers and of colloids.

In the dyeing of cotton with indigo, as described above, ingenious use is made of three phenomena: the reversible oxidation-reduction equilibrium of a complex organic compound, the reversible hydration of the cellulose molecules in the amorphous region, and the reversible adsorption by the cellulose of the molecules containing a chain of conjugated double bonds. Our knowledge of these phenomena was developed during the last 25 years, yet the process is at least 3,000–4,000 years old. Even today, there are few finishing processes which surpass the old indigo process in ingenuity.

The industry of textile finishing is still basically empirical; the main accomplishment of the theory until now is to explain those phenomena of which practical use has been made for a long time. However, it is wrong to assume that theory serves only to satisfy intellectual curiosity, and that industry can afford to neglect and disregard it.

Finishing today is a large-scale industrial operation which cannot be handled by a few artisans who are the possessors of accumulated experience handed down from generation to generation. Rather, it requires educated technologists who are able to deal with new problems as fast as they arise, which necessitates fundamental scientific knowledge.

The development of new fibers is evidence that textile science has finally caught up with textile technology. The chemist succeeded in linking together hundreds of small molecules, in a controlled manner, to build up the polymer molecule and molding these into fibers. In selecting the material for clothing, man is no longer restricted to fibers obtained from plants and animals; he is now faced with the task of seeking out the best fibers from the almost countless possibilities offered by chemical synthesis. The logical consequence is the development of a multitude of synthetic fibers which compete with and complement each other.

The new fibers present a great many difficult problems which require immediate attention. The low affinity of synthetic fibers for water is such a problem, since it causes static electricity and decreases the ability of the fiber to take up dyes. With the natural fibers, the development of finishing could have proceeded on the empirical basis for hundreds or thousands of years; with the new fibers, answers are needed tomorrow. It is evident that only the full utilization of existing fundamental knowledge can map the shortest routes. The task of the scientist is no longer to supply explanations for the methods discovered and exercised by the artisan, but to devise the methods and the controls.

While each new fiber has some innate weakness, which can be overcome by the use of an appropriate finish, each also has some superiority over the older fibers, which in turn creates a new effort to improve the old fibers. The results are an increasing awareness of the capacity of textile materials to meet special requirements through the use of suitable finishes, and a healthy competition invigorating the textile-finishing technique as a whole.

In order to accelerate the tempo of progress, the method of trial and error must be replaced by planned research. The science of textile finishing has become indispensible.

Classification of Finishes

Due to the empirical background of textile finishing, textbooks and monographs dealing with this subject have indicated until now only a rudimentary systematics. Two distinguishing categories have been used: the nature of the fiber and the purpose of the finish. The first classification, dividing the field into the technology of cotton, wool, silk, rayon, etc., becomes, with the increased use of new fibers, and especially their blends, increasingly impractical. It has also the disadvantage that, when made the basis of a survey, it necessitates the repetition of common principles and of methods used. The second classification is usually a mere listing of operations, although the finishes could be grouped according to purpose of finish—namely, improvement of the textile: (1) functionally, by increasing the protection against the elements (water-repellency) or by avoidance of hazardous effects (flame-resistance, repellency of pathogenic germs); (2) in durability (mothproofing, mildewproofing, abrasion-resistance); (3) esthetically (sheen, color, softness, drape, shape retention).

The first two classes of finishes are occasionally called "utilitarian," the third "luxury." However, the distinction between them has little justification. Since garments in general, whether loincloth or ermine, serve just as much for adornment as for protection, any finish which makes the garment look "new" for a longer time increases its useful life. Therefore, a luxury finish may add more to the durability of the garment than a utilitarian finish which, for instance, keeps it intact from the ravages of insects.

In many cases the finish has a multiple purpose. Urea-formaldehyde finish not only imparts crease-resistance and dimensional stability to rayon, but it also increases the durability of the fabric by increasing the wet strength.

Finally, a treatment of the technology of finishing based on the classification of finishes according to purpose, like that according to nature of the fiber, leads to repetition of principles and methods used.

In order to arrive at a theoretically more satisfactory systematics, we begin with the obvious that improvement of the textile material can be effected by addition of a substance (as in most of the known waterproofing treatments and in dyeing), by removal of a substance (scouring), or by change of the structure or organization of the textile material (mercerization of cotton).

Considering only the additive treatments, two questions arise immediately. The first question is concerned with the site of the introduction of the

new substance—namely, whether it is deposited in the individual fibers and filaments or on their surface, and in the yarns or between the yarns or on the surface of the fabric. This constitutes the topical, or spatial, characterization of the process. The second question is concerned with the nature of the molecular forces which enable the textile material to receive and retain the new substance. This constitutes the energic characterization.

Penetration of Finishing Materials

For the purpose of the topical characterization we list the successively subordinate structural elements of textiles: fabric, yarn, fiber, crystallite (micelle), and molecule. Depending upon whether the change occurs between or within these elements, distinction is made between interyarn and intrayarn, interfiber and intrafiber, intermicellar and intramicellar processes.

The dimensions of the spaces involved and the nature of the treating compounds frequently give an indication of the site of the change without requiring specific investigation. The dimensions vary considerably with the nature of the textile material. In typical textiles, the distance between the yarns is of the order of 10–100 μ (0.0004–0.004 in.), and the distance between the fibers of the order of 1 μ (0.00004 in.).

The nature of the intermicellar distances was discussed in the description of the mechanism of the indigo dyeing. These distances in the dry fibers are without significance for the theory of finishing processes; conversely, the intermicellar distances in the swollen fibers are of the greatest significance. The microscopic surface of textile fibers is of the order of 2,000 cm.^{2}/g. (1,000 sq. ft./lb.). The internal submicroscopic surface (the area of the wall of the gel-filled chanels) is about 1,000 times larger, amounting to 2,000,000 cm.^{2}/g. (1,000,000 sq. ft./lb.). In order to cover the microscopic surface of the fiber with a fatty acid in the form of a monolayer in which the alkyl groups are perpendicularly oriented to the surface, 0.04% of the fatty acid, based on the weight of the fiber, would suffice. The covering of the submicroscopic surface would require 40% fatty acid.

The submicroscopic pores in water-swollen cotton, rayon, and wool have an average diameter of the order of 0.005 μ (50 Å., or 0.0000002 in.). It is therefore obvious that only molecular or ionic solutions can penetrate the swollen fiber. Soaps and other surface-active agents as well as soluble dyes undergo in aqueous solution an association equilibrium in which the larger aggregates or micelles are capable of dissociating reversibly into the single ions and molecules. These substances also penetrate the fiber.

Some compounds have sufficient attraction for the molecules of the fiber to separate them from each other not only in the disorganized, but also in the crystalline, region. Frequently, but not in every case, they disssolve the fiber. Sodium hydroxide of mercerizing strength penetrates the crystallites of cotton, but dissolves only partially degraded regenerated cellulose. Cuprammonium hydroxide solutions are either solvents or swelling agents for cellulosic fibers, depending upon the concentration.

Cellulose acetate and some of the new fibers can be swollen by certain solvents which preferentially enter the disorganized regions, but in some cases enter the crystallites too. Like cotton swollen with water, when these fibers are swollen (*e.g.*, with phenols), their interior becomes accessible to molecules to which the fibers are impregnable in the unswollen state. Some of the dyeing processes are based on preswelling of the fibers with organic liquids. There are also dyes (*e.g.*, some of the acetate dyes) which have the capacity to enter the unswollen fibers; apparently, they themselves are swelling agents.

In the case of yarns and fabrics, nonswelling liquids penetrate between the fibers if they wet them out and if their viscosity is low enough to permit them to flow sufficiently during the application. In the latter case, hydrostatic pressure (squeezing) accelerates the penetration. Macromolecules in the form of liquids or solutions can be brought between the fibers, but not into the fibers; their dimensions are too large for diffusion into the submicroscopic pores. Emulsions and suspensions cannot penetrate fibers, and if they are too coarse, they cannot even penetrate yarns.

Improving the Textile

The technical significance of the topical classification reveals itself when it is desired to determine which site of reaction is best suited for obtaining a desired improvement of the textile, and whether it is possible to localize the process at the chosen site or not. Such an inquiry is in accordance with the ultimate goal of the science of textile finishing—namely, the correlation of the chemical and physical nature of the finish with its performance in the textile—but it is limited by the amount of pertinent information available. The performance of a fabric

obviously is determined by the mechanical and chemical properties of the individual fibers and filaments and the construction of the yarn and fabric. Finishes modify the mechanical and chemical properties of the fibers; in most cases they modify profoundly the surface properties of the fibers and, thus, they affect the cooperation of the fibers in their assemblies—namely, in the yarns and fabrics. A study of the fiber surface would shed light not only on the cohesive behavior of the fibers, but also on their adhesion to the finishing compounds as well as to the ingredients of soil and to water. Since such a study is in the initial stage, the proposed investigation is confined to the exploratory level.

An important prerequisite of the science of finishing is the translation of the psychological and sensory properties of the fabrics into quantitative terms. This is easier with visual properties such as color and sheen than with tactile properties such as softness or with such complex properties as drape and shape retention. During the last few years, definite progress has been made toward correlating the subjective evaluation of fabric behavior with objective, reproducible quantities [8]. However, this progress is too recent; quantitative data connecting the chemistry and physics of finishes with some of the luxury properties are too scanty to be utilized in the present inquiry.

Table I contains the preliminary results of a survey. Far from attempting to be complete, it serves only for illustrative purposes.

Coloring of the textile can be achieved by intrafiber (intermicellar and intramicellar) adsorption of molecularly dissolved dye. A monomolecular adsorption on the surface of the fiber would not produce color of sufficient depth. Pigment colors of, say, 0.1 to 1 μ diameter, when applied to the surface of the fiber or yarn, give sufficient absorption of light.

Soft finish, or increased pliability, is obtained by decreasing the friction between the individual filaments and fibers. When the yarns are bent, lubricated fibers slip along each other more easily. Treatment with the emulsion of a fat or oil will fulfill the requirements of interfiber lubrication. Water-soluble lubricants, such as nonionic and cationic agents, have a tendency to penetrate the fibers. There is, however, no basis for the assumption that intrafiber absorption of these compounds contributes to flexibility by internal platicization. It appears probable that the portion of the lubricant which enters the fiber is wasted. Under these circumstances, there appears to be no need for treating the fabric with the solution of the lubricant for a prolonged period. The effect of cationic softeners on the shade and lightfastness of direct colors seems, however, to indicate that a fairly deep penetration of the cationic agents into the fibers is unavoidable. It can hardly be assumed that the cationic agents influence appreciably the shade of the dye, unless they penetrate about as deeply as the dye does. The amazing fact is that as little as 0.02% by weight of the cationic agent markedly influences the frictional properties of the fiber, and, at the same time, we have to assume that an appreciable portion of this material is present in an ineffective form—namely, in the interior of fibers. Apparently, this type of compound does not have to form a complete monomolecular film on the surface of the fiber, but has only to cover a fraction of the surface in order to reduce fiber friction. We will return to this point in the discussion of the energic relationships involved (p. 221).

The purpose of the antislip finish is to increase friction between the yarns. Some of the agents used for this purpose, such as certain water-soluble resin compounds, are capable of penetrating the yarns and even the fibers. Resin emulsions and aqueous solutions of high polymers, which also serve as antislip finishes, are capable of penetrating the yarns. By appropriate application methods, the wasteful penetration, with its concomitant stiffening of the fabric, can be minimized.

TABLE I. SITE OF DEPOSITION IN FINISHING PROCESSES

Process	Desirable site	Attained site
Dyeing		
Molecular	Intrafiber	Intrafiber
Pigment	Interfiber or interyarn	Interfiber
Softening	Interfiber	Interfiber and intrafiber
Antislipping	Interyarn	Intrayarn
Water-repellence	Interfiber	Interfiber and intrafiber
Crease-resistance	Intermicellar	Intermicellar
Dimensional stabilization of rayon	Intermicellar	Intermicellar
Shrinkage control of wool		
Resin treatment	Interfiber	Interfiber (?)
Chlorination	Intrafiber	Intrafiber

Another treatment which is directed essentially toward modification of the surface of the individual fibers is the water-repellent finish. The requirement for such a finish is that it increase the contact angle of water on the fabric to a value above 90°. Paraffin emulsions are ideally suited for fulfilling this requirement, but they do not give a durable effect. Aqueous solutions of the type of stearoylamidomethyl pyridinium chloride (Velan or Zelan), discussed below, may penetrate into the individual fibers and, from the theoretical standpoint, may be largely wasted. The amount which actually need be applied in order to obtain a satisfactory result is 100 times greater than the amount which would be sufficient to cover the microscopic surface in the form of a monomolecular layer.

The wrinkle- or crease-resistance of rayon has attracted a great deal of attention in the last 20 years. This most widely used process is based on the intermicellar deposition of urea-formaldehyde resin [5]. It is now generally accepted that in order to obtain crease-resistance, the irreversible elongation of the fiber (plasticity) has to be reduced and, if possible, its reversible elongation (elasticity) increased. It is thought that cross-linking of the cellulose molecules in the amorphous regions brings about the desired change of mechanical properties. If this is true, then it is obvious that intermicellar location of the cross-linking reagent is required. It appears, however, that the process had an empirical origin, since the inventors assumed that the filling out of the intermicellar spaces with a resin would directly result in the desired effect. In any case, interfiber deposition of the resin causes stiffness of the yarn and fabric, by preventing slippage of the fibers, and therefore has to be avoided or minimized unless the finish aims at an increased body of the fabric.

Since swelling of the fibers causes dislocation of the yarns in the fabric, resulting in shrinkage, a treatment which reduces the swelling promotes the dimensional stability of rayon fabrics. Cross-linking of the cellulose molecules in the disorganized regions reduces the swelling. It is assumed that this is the function of formaldehyde, urea-formaldehyde, and glyoxal, all of which are capable of penetrating the intercrystalline spaces and are used for such a finish [2].

A variety of finishes have been proposed for reduction of the felting shrinkage of woolen fabrics. Since felting depends upon at least two factors—the scaliness, or differential friction effect (greater coefficient of friction from tip to root than in the opposite direction), and the elastic hysteresis of the fibers—modification of either of these two factors may alter the felting tendency. Consideration of some of the antifelting finishes indicates the necessity of augmenting the topical classification by the morphological distinction of scales and cortex, and probably also of epicuticle [6].* Some of the proposed antifelting processes aim at the interfiber deposition of resin in order to cover the scales; microscopic examination indicates that the methylated methylol melamine resin used for felting control is located essentially at the scale region [9]. Fiber-bonding with resin also reduces the shrinkage, but causes stiffness of the fiber fabric; therefore, the methods of application are directed towards minimizing the "spot-welding," but allowing the covering of the scales. Finishing processes aimed at the removal of the scales are necessarily based on intrafiber reactions, but these should preferably be limited to the periphery of the cross section in order to avoid excessive fiber damage.

Cohesion of Finishing Materials

In the energic classification of finishing processes, distinction is first made between the cohesion forces, which are responsible for the combination of molecules of the same kind in crystals or liquids; adhesion forces, which are responsible for the combination of molecules of different kinds, as in solution and in adsorption processes; and covalent bonds, which hold the atoms together in the molecules. Each of the finishing processes makes use of one or more of these molecular forces—breaking up some of the links, restoring or creating other links. Scouring, for instance, is accomplished by overcoming the adhesion forces between the soil and the fiber by the adhesion forces acting between the detergent and the fiber and between the detergent and the soil.

In order to make a finish that is based on the introduction of a new substance into the textile durable, a mechanically strong union between the two components, fiber and finish, is required. A mere juxtaposition of them would result in the finish sticking loosely in the form of droplets or particles to the sur-

* For a detailed consideration of some finishing processes of rayon, especialy of dyeing, the microscopic inhomogenity of the fiber cross section, due to the existence of a denser skin surrounding the core, has to be taken into account as a part of the topical relations [10, 11, 12].

face of the fibers, yarns, or fabrics. The finish substance would gradually be shaken off, with resulting loss of the effect. A mechanically stronger union is achieved if the finish envelops the fiber or the yarn in the form of a continuous phase, or if the fiber as a continuous phase surrounds the finish. Such a situation can be created only if the cohesion of the fiber or the finish or both are first destroyed and then restored. (See Table II.)

TABLE II. ENERGIC BASIS OF THE UNION BETWEEN TEXTILE AND FINISH

1. Restoring, increasing, or creating cohesion of fiber (spun-dyeing, spun-dulling)
2. Restoring, increasing, or creating cohesion of finish (precipitation, coupling, oxidation, polymerization, polycondensation, coagulation, evaporation of solvent, etc.)
3. Utilizing attraction forces (adhesion) between fiber and finish (substantivity, ion-exchange)
4. Chemical reaction between fiber and finish (formation of acetals, urethans, etc., copolymerization)

It is apparent that a limited interdependence exists between the topical and the energic character of the finish, since a finish secured by means of restored fiber cohesion can only be located inside the fibers.

Cohesion of the fiber can be reduced by application of solvents or, in some cases, by heat. Spun-dyeing and spun-dulling consist of the addition of colored or white pigments to the dissolved or molten mass (dope) which is extruded to form the man-made fiber. Removal of the solvent or cooling restores or establishes the cohesion of the fiber, with resulting trapping of the pigment. Actually, finishing in these cases is part of the fiber manufacturing process; complete elimination of the cohesion of an already formed fiber to allow the entering of pigments is not feasible economically.

The application of this principle is therefore limited to man-made fibers. Its advantages are, among others, unsurpassed uniformity and washfastness. However, since it places certain phases of finishing in the hands of the fiber manufacturer, it encounters serious limitations due to the present structure of the converting industry. Nevertheless, because of its technical advantages, it probably will be applied to an increasing extent not only to dulling and dyeing processes, but also to other finishing processes.

Partial reduction of fiber cohesion by swelling, in order to permit the entrance of dissolved material, is characteristic for the majority of the wet finishes. In practically every case, the method of partial, reversible reduction and restoration of the cohesion of the fiber is combined with the method of temporary reduction or increase of the cohesion of the finish. The simplest example is the precipitation of a water-insoluble compound in the fiber by metathesis (successive treatment with solutions of $BaCl_2$ and Na_2SO_4 for delustering, and with solutions of aluminum acetate and sodium stearate for water-repellency). A large variety of reactions are utilized for this purpose in the dyeing industry. Reference should be made to the oxidation of leuco compounds, as described in the discussion of indigo dyeing, to the coupling of naphthols with diazo compounds, and to the aftertreatment of water-soluble dyes with complex-forming metal salts and with high-molecular-weight organic cations (dye-fixing agents).

An example of the increase of the cohesion of intrafiber-deposited finish is the polymerization and polycondensation of monomers. The outstanding illustration is the introduction of monomeric urea-formaldehyde as a so-called precondensate (monomethylol and dimethylol urea) into the submicroscopic pores of rayon and its condensation to macromolecular resin under the influence of an acid catalyst and heat. The dyeing industry has been polymerizing aniline salt to form aniline black for a long time. In this case, the polymerization produces the color itself, another example of the multifunctional methods of the industry.

Mechanical trapping by increased cohesion does not mean, in all cases, a complete protection of intrafiber-deposited pigments. Particles of vat and developed azo dyes can sometimes be removed by prolonged severe treatment with hot solutions of soap or other detergents; probably as a result of the slight, but definite, solubilizing action of the surface-active agent on the dye, a gradual migration of the dye particles to the fiber surface takes place.

If the finish should form the continuous phase around the fiber or yarn, restoration or increase of the cohesion of the finish is the only method available. The irreversible coagulation of emulsions such as synthetic or natural latices serves in this way. High polymers are applied also in dissolved form, and their cohesion is restored by evaporation of the solvent. Rubber is applied in organic solvents, starch or carboxymethyl cellulose in water. The cohesion of the deposited film is frequently further increased by polymerization or by other chemical means. Rubber is vulcanized on the fiber; alkali-soluble cellulose is

precipitated by removal of the alkali. Monomers can be applied in solvents which do not swell the fibers, and polymerized after evaporation of the solvents, the application of drying oils for the preparation of oilcloth being the classic example.

All of these processes are also used for fastening solid particles to the surface of fibers, yarns, or fabrics when the latter are embedded in the liquid "binder" that is capable of increasing the cohesion. This is the basis of the pigment-printing processes. Pigment printing was widely practised many years ago, eventually slipped into almost complete oblivion, and in the last few years emerged again as one of the most important methods of textile coloring. Albumen was one of the binders used in older times, and its denaturation by heat served for the irreversible increase of the cohesion; this is another example of the ingenuity exhibited in the empirical development of textile-finishing methods.

Another method of increasing the cohesion of the finish is used in the coating of textiles with plastisols. A plastisol is a dispersion of a resin in a plasticizer. After spreading the semiliquid mass on the surface of the fabric, it is converted into a tough, homogeneous film as the resin dissolves in the plasticizer on heating.

Adhesion—that is, the action of attractive forces between the finish and the fiber—is the basis of almost all conventional dyeing methods. It is usually applied in combination with the reversibly reduced cohesion of the fiber. The latter alone would not offer a practical method for the following reasons: First, the finish or dye could be removed easily merely by reopening the submicroscopic pores—*e.g.*, by swelling—although this could be remedied by increasing the cohesion of the dye as described above. Secondly, without attractive forces, the concentration of the dye or finish in the fiber would always remain below that in the finishing bath, and it would be further greatly reduced by rinsing. Exhaustion of the bath, of course, makes it possible to carry out the treatment under more economical conditions, because comparatively dilute treating solutions can be used and, after one treatment, discarded without appreciable loss.

There are only a few noncoloring finishes which make use of the substantivity. Some of the mothproofing agents and the cationic softeners are examples. Optical bleaches or brighteners—*i.e.*, substantive organic compounds which give a bluish fluorescence—are truly on the borderline between being dyes and noncoloring finishes.

We may speculate on the possibility that the firm anchorage of the cationic finish by means of ion-exchange (in the absence of aqueous solution this linkage is as strong as a covalent bond) is responsible for its superior efficiency when compared with softeners based on fats, oils, or nonionic and anionic surfactants that are attached to the fiber surface by weak van der Waals' forces. Cationic lubrication of fibers, from this point of view, is analogous to boundary lubrication of metals, whereas the other types of fiber softeners are more analogous to the hydrodynamic lubrication of metal surfaces.

The fourth and last method of the energic classification of finishing processes is the establishment of a covalent bond between the fiber substance and the finish. This is, of course, the firmest link, at least against mechanical treatments and solvents, and can be broken only by specific reagents to which the chemical combination is susceptible. Unfortunately, the possibilities of this method are limited: first, the reactivity of the macromolecules of the fiber is relatively low; and, secondly, the fiber strength is extremely sensitive toward treatments which cause degradation of the macromolecules. Formaldehyde and its derivatives play an outstanding role in textile chemistry because they are capable of entering into reactions with fibers under conditions which avoid extensive degradation. Recent patents mention isocyanates (forming urethans with hydroxylated compounds) and cyclic imines, among other substances, which react with fiber molecules under mild conditions. Alkylation has been suggested for the treatment of wool, especially after its reactivity has been increased by reduction [7]; and partial acylation and alkylation for the treatment of cotton.

One of the most advanced finishing treatments, which is based on an ostensively fundamental approach and which utilizes chemical combination between molecules of the fiber and the finish, is the water-repellent treatment with compounds of the type of stearoylamidomethyl pyridinium chloride [1]. We can distinguish three portions in this molecule according to their respective roles in the process. Since the combination of the cellulose molecule with the stearoyl radical is aimed to impart the required contact angle of the fiber surface with water, the stearoyl radical (*I*) can be considered the *effective* group. In order to make the molecule

capable of chemical reaction under mild conditions, it contains the amidomethyl radical (*II*), which has to form a semiacetal with the hydroxyl group of the cellulose. The amidomethyl radical is the *reactive* group. Finally, in order to establish the required intimate contact with the fiber, the reagent is solubilized in water due to the presence of the pyridinium radical (*III*), which is the *solubilizing* group.

Baking in the predried fiber causes the molecule to split off pyridine hydrochloride, whereas the stearoylamidomethyl group should attach itself to the cellulose molecule. There is some indication that in the industrial application the major fraction of the compound present does not enter the intended chemical reaction, and the stearoylamidomethyl group is used up largely in the formation of the waxy *bis* (stearoylamido) methane [3, 4]. Notwithstanding this, the principle of the process has proved its value as a working hypothesis and has stimulated the development of other durable finishes. Efforts to apply the same or similar principles for the establishment of covalent linkages between dyes and fibers have not progressed much beyond the laboratory and patent stage.

The production of completely synthetic fibers opens up another important avenue for finishing. Minor amounts of reactive compounds can be built in the polymer molecule prior to spinning of the fibers in order to provide the "hooks" onto which the molecules of the dye and finish can be attached afterwards [13]. Although at the present time this principle is not used in the commercial production of fibers, its potentialities are great enough to secure it an important role in future developments.

Literature Cited

1. Baldwin, A. W., and Walker, E. E., Brit. Patent 475,170 (1937) (assigned to Imperial Chemical Industries, Ltd.).
2. Cameron, W. G., and Morton, T. H., *J. Soc. Dyers Colourists* **64**, 329 (1948).
3. Davis, T. W., *J. Soc. Dyers Colourists* **63**, 260 (1947).
4. Evans, J. G., in "Fibre Science" (edited by J. M. Preston), Manchester, The Textile Institute, 1949, p. 248.
5. Foulds, R. P., Marsh, J. T., and Wood, F. C., Brit. Patents 291,473 and 291,474 (1928) (assigned to Tootal, Broadhurst Lee Co., Ltd.).
6. Gralén, N., *J. Soc. Dyers Colourists* **66**, 465 (1950).
7. Harris, M., Mizell, L. R., and Fourt, L., *Ind. Eng. Chem.* **34**, 833 (1942).
8. Hoffman, R. M., and Beste, L. F., TEXTILE RESEARCH JOURNAL **21**, 66 (1951).
9. Maresh, C., and Royer, G. L., TEXTILE RESEARCH JOURNAL **19**, 449 (1949).
10. Morehead, F. F., and Sisson, W. A., TEXTILE RESEARCH JOURNAL **15**, 443 (1945).
11. Preston, J. M., *J. Soc. Chem. Ind.* **50**, T199 (1931).
12. Preston, J. M., and Tsien, P. C., *J. Soc. Dyers Colourists* **62**, 368 (1946).
13. Valko, E. I., *Am. Dyestuff Reptr.* **31**, P210 (1942).
14. Valko, E. I., Physical Chemistry of Dyeing, in "Colloid Chemistry" (edited by J. Alexander), Vol. VI, New York, Reinhold Publishing Corp., 1946, p. 594.

(Manuscript received September 18, 1951.)

Correction

In the article "Heat-Resistance of Partially Acetylated Cotton Fabrics," by Edith Honold, Janice M. Poynot, and Alva F. Cucullu, which appeared in the January, 1952, issue of TEXTILE RESEARCH JOURNAL, there is an error in the data of Table II, page 28. The control value of the elongation at break for the acetylated fabric A-1 should read *"0.229 ± 0.011"* instead of *"0.299 ± 0.011."*